Combating Infectious Diseases:
Marine Natural Products Targeting HIV and Pathogenic Bacteria

by

Lyanne M. Gómez-Rodríguez

A dissertation submitted in partial fulfillment
of the requirements for the degree of
Doctor of Philosophy
(Chemical Biology)
in the University of Michigan
2019

Doctoral Committee:

Professor David H. Sherman, Chair
Professor Kathleen Collins
Professor Anna Mapp
Professor Alison Narayan

Lyanne M. Gómez-Rodríguez

lyannegr@umich.edu

ORCID ID: 0000-0002-7455-6509

© Lyanne M. Gómez-Rodríguez 2019

Dedication

To George R. R. Martin for reminding me that *what is dead may never die*

Acknowledgements

Finishing graduate school took a gigantic team effort in my case. Few people know how bad things got for me; the amount of times I wished to quit far excited the times I was hopeful I would finish. With all the anxiety gained and my mental health demise during this process, I am not entirely sure if I should be thanking those that led me to choose this mentally draining path. Perhaps a better approach for my sanity would be to acknowledge the people that urged me to become a "better version" of myself. Either way, I will get to call myself Dr. Gómez-Rodríguez thanks to the effort, love and dedication of many individuals that have directly or unknowingly impacted my life.

First and foremost I have to thank my mentor Dr. David Sherman for accepting me into his lab and providing me with the necessary tools to become a successful Ph.D. student. I am lucky to have worked under such an exemplary scientist and understanding human being. His office was always open for discussing my progress, the failures and even the current political climate. He urged me to continue through the more rough times of graduate school and had an optimistic view of my future when I couldn't see beyond what was directly in front of me. My committee members have also played a crucial role in making sure I stayed on track and providing constructive criticism. Dr. Anna Mapp and Alison Narayan reminded me each time that they were here to help me succeed and made sure I was getting appropriate mentoring in all areas pertaining to graduate school. I specially have to thank Dr. Kathleen Collins for allowing me to be part of such a rewarding collaboration and permitting me to attend her lab group meetings, where I gained crucial knowledge on the immunology side of my project.

Although it is easy to let the bad obscure the good, I had many fun moments in lab and outside thanks to some awesome coworkers, particularly Jennifer Schmidt, Andrew Robertson, Rosa Vazquez, Andrew Lowell, Robbie Hohlman, Amy Fraley and Maria Adrover-Castellano. A special thank you goes to my dear friend Dr. Ashootosh Tripathi. Not a single part of this would have been possible without his help, mentoring and guidance. Three weeks into my rotation in

the Sherman lab, he began molding me to become an independent scientist by leaving for India and having me practically rotate on my own. Oddly enough, this type of hands-off approach ultimately lead me to choose this lab. Ashu had to put up with my mood swings, allowed me cry in his office on multiple occasions and talked me out of leaving graduate school at least three a year. I will forever be grateful and indebted to him for his efforts, words of wisdom and teaching me his vast natural products knowledge.

Even though my family members and I are polar opposites, and did not understand what I was doing half the time, all their efforts through my graduate career, and my life in general, have been noted and appreciated although I have not been the best at expressing it. I have to thank my mom for listening to my mental breakdowns, even though she usually had no idea what to say or how to comfort me, and sending me so many care packages throughout the years. Also thanks to my dad and my grandma who have been my biggest cheerleaders during this time and always reminded me how proud they were.

My friends played an important role in keeping me focused, energized and lending me a shoulder to lean on. Ricardo Vazquez and Desiree Garcia-Torres helped me find my way through my first years and probably had the biggest impact on my life. Attabey Rodríguez-Benitez gave me the best pep talks before committee meetings, inspired me to start running and held my hand through awkward doctor appointments. I have to give special thanks to Valerie Irizarry, who I can always rely on to laugh at my jokes and was always available for necessary sugar breaks. Candilianne Serrano-Zayas and Bryant Rivera were there for me while I went through one of the most challenging and difficult times I ever had to go through. Your presence and very needed hugs did not go unnoticed. I specially want to thank my best friend Loruhama Delgado-Rivera for opening her home to me and providing me with an escape every time I needed one and for picking up that phone just to hear me vent for hours on end.

I met Omari Baruti on my first day as a graduate student. I don't think we talked at all for the first month although we sat next to each other everyday. Five years later I don't know how I'll live without having him across the hall to seek comfort, ask for advice or just annoy when I got bored. He was another big "Lyanne will finish graduate school" advocate and will probably be the person I miss the most out of this entire journey. With such a drive and dedication, I know without a doubt not even the sky will stop him. To Ashley Velez, my roommate, best friend, personal trainer, therapist, travel partner and countless other titles: thank you for putting up with

me. You saw me at my lowest and my highest, celebrated my successes as if they were your own and talked me down from more panic attacks that you probably noticed. Your continuing peaceful nature and positive outlook on the world can be contagious and I hope I never have to know what life feels like without you in it. Daniel, you came into my life at the end of this chapter and are helping me build an exciting new one. Thanks for teaching me how strongly I am able to feel, for filling my days with so much happiness, and specially thank you for feeding me and keeping me caffeinated as I worked on finishing this.

Table of Contents

Dedication ii

Acknowledgments iii

List of Figures ix

Abstract x

Chapter 1: Background and Introduction 1

1.1 Therapeutic Uses of Natural Products 1

1.1.1 Natural Products Throughout History 1

1.1.2 Drug Discovery Exploration and Development 2

1.2 Current Scope of Natural Products Drug Development 2

1.2.1 Scaffold Diversity 2

1.2.2 Drug Resistance 3

1.3 Natural Products Biosynthetic Pathways 4

1.3.1 Polyketide Synthases 4

1.3.2 Non-Ribosomal Peptide Synthetases 6

1.3.3 PKS-NRPS Hybrids and Tailoring Enzymez 6

1.4 Summary and Dissertation Outline 7

1.5 References 8

Chapter 2: Adipostatins E-J, New Potent Antimicrobials Identified as Inhibitors of Coenzyme-A Biosynthesis 12

2.1 Introduction 12

2.1.1 Urgent Need for New Antibiotics 12

2.1.2 Coenzyme A as a Drugable Target 13

2.1.3 Phosphopantothenoylcysteine Synthetase 13

2.2 Results and Discussion 15

2.2.1 High-Throughput Screening for Inhibitors of Coenzyme A

Biosynthesis Derived from Natural Product Extracts **15**

2.2.2 Isolation and Structural Elucidation of the Adipostatins (6-7, 10-15) **16**

2.2.3 Assessment of the Biological Activity of Adipostatins Against Purified PPCS Enzyme and Microbial Cultures **18**

2.3 Conclusion **20**

2.4 Supplemental Information (SI) **22**

2.5 Materials and Methods **59**

2.5.1 General Experimental Procedures **59**

2.5.2 Biological Material **59**

2.5.3 Culture Maintenance and Fermentation **60**

2.5.4 Isolation and Purification of Adipostain E-J (10-15) **60**

2.5.5 Gene Cloning, Expression, and Purification of Streptococcus pneumoniae PPCS **60**

2.5.6 Natural Product Extract Library **61**

2.5.7 Assay Development and High-Throughput Screening **61**

2.5.8 Confirmation and Counterscreen Assay **62**

2.5.9 Dose-Response Assays Against Purified Enzymes **62**

2.5.10 Dose-Response Assays Against Microbial Cell Cultures **63**

2.5.11 16S rDNA PCR Amplification, Cloning and Sequencing **64**

2.6 References **64**

Chapter 3: Isolation, Characterization and Structural Elucidation of HIV-1 Nef Inhibitors **68**

3.1 Introduction **68**

3.1.1 Viral Proliferation **68**

3.1.2 HIV is a Global Threat **68**

3.1.3 Current Available Treatments **69**

3.1.4 HIV-1 Nef as a Druggable Target **70**

3.2 Results and Discussion **73**

3.2.1 High-Throughput Screening **73**

3.2.2 Isolation and Structural Elucidation of Active Natural Products **74**

3.2.3 Biological Testing **76**

3.3 Conclusion **79**

3.4 Supplemental Information (SI) **80**

3.5 Materials and Methods **87**

3.5.1 General Experimental Procedures **87**

3.5.2 Biological Material **87**

3.5.3 Culture Maintenance and Fermentation **88**

3.5.4 Isolation and Purification of Bafilomycin A_1, B_1 and C_1 **88**

3.5.5 Natural Product Extract Library **89**

3.5.6 Assay Development and High-Throughput Screening **89**

3.5.7 Lysosome Acidity Tracking **89**

3.6 References **90**

Chapter 4: Discussion and Future Directions **95**

4.1 Thesis Overview **95**

4.2 HIV-1 Nef Inhibitors Future Directions **96**

4.2.1 Derivatization of Bafilomycins and Concanamycin A **96**

4.2.2 Elucidation of ConA Nef Inhibition Mechanism **99**

4.3 Contributions **101**

4.4 References **101**

List of Figures

Figure 1.1 Natural Products as a source for medicine 3
Figure 1.2 General PKS module scheme 5
Figure 1.3 General NRPS module scheme 7
Figure 2.1 Schematic depicting pantothenate uptake and transformation into CoA through the CoA biosynthetic pathway 13
Figure 2.2 Reactions catalyzed by phosphopantothenoylcysteine synthetase 14
Figure 2.3 Triage of hits obtained during HTS of PPCS against the microbial natural product extracts library 15
Figure 2.4 Planar structure of adipostatins (A-B, E-J) 18
Figure 2.5 Adipostatins in vitro bioactivity 20
Figure 3.1 CDC HIV-1 infection statistics 69
Figure 3.2 Areas targeted by ART during HIV-1 replication 70
Figure 3.3 Mechanism of MHC-I degradation by HIV-1 Nef 72
Figure 3.4 Published Nef inhibitors 73
Figure 3.5 Flowchart for the identification of Nef inhibiting strains 74
Figure 3.6 LC-MS/MS generated molecular network of 34893-N3I 75
Figure 3.7 Plecomacrolides known to posses V-ATPase inhibitory activity 76
Figure 3.8 Plecomacrolides activity profile for MHC-I cell surface restoration 77
Figure 3.9 ConA is able to restore HLA-A2 expression and increases killing by CTLs 78
Figure 3.10 Lysosome acidification analysis through LysoTracker 79
Figure 4.1 Potential fumarate analogues to study fumaryl transferase substrate flexibility 97
Figure 4.2 Baf-A_1 production in S. lohii peaks around day six 98
Figure 4.3 Proposed derivatization sites for Baf-A_1 and ConA 99
Figure 4.4 Use of labeled ConA for the identification of target proteins 100

Abstract

Natural product metabolites have proven time and time again to be efficient therapeutics against a wide range of targets and possess great potential for structural diversity in pharmaceutical discovery. These diffusible metabolites mainly produced by plants, fungi and bacteria have the tendency to be toxic as they are sometimes secreted to avoid or warn predators. Those originating from microbes are particularly attractive because of their inherent structural characteristics, the ability to be grown in large-scale cultures and the potential to manipulate or engineer their biosynthetic pathways to produce a wide range of structural analogs. The work presented herein will focus on the search for secondary metabolites from marine microbial extracts present in the Center for Chemical Genomics at the Life Sciences Institute for treatment and eradication of life-threatening diseases, such as the Human Immunodeficiency Virus (HIV) and pathogenic bacterial infections.

The first chapter will expose phosphopantothenoylcysteine synthetase (PPCS) as a druggable target for new antimicrobial development. This enzyme is responsible for installing a cysteamine group within phosphopantetheine, a key structural element in biological acyl transfer reactions found embedded within coenzyme A (CoA). In this study, we adapted a biochemical assay specific for bacterial PPCS to screen for inhibitors of CoA biosynthesis against a library of marine microbial derived natural product extracts (NPEs). Analysis of the NPE derived from *Streptomyces blancoensis* led to the isolation of novel antibiotics (**10-12**, and **14**) from the adipostatin class of molecules. The most potent molecule (**10**) displayed *in vitro* activity with IC_{50}= 0.93 μM, against *S. pneumoniae* PPCS. The whole cell antimicrobial assay against isolated molecules demonstrated their ability to penetrate bacterial cells and inhibit clinically relevant pathogenic strains. This establishes the validity of PPCS as a pertinent drug target, and the value of NPEs to provide new antibiotics.

For the second project we focused on using natural products to target the HIV-1 Nef accessory protein for inhibition. This protein has a leading role in evading recognition by cytotoxic T lymphocytes (CTLs) and spreading the virus efficiently through the host cell.

Specifically, this protein mediates the mislocalization and subsequent degradation of the antigen-presenting major histocompatibility complex I (MHC-I). Targeting Nef could potentially reverse its effects on infected cells and reduce the viral load significantly. A high-throughput cell-based screen was developed in collaboration with Dr. Collins lab (UM-Medical School) to identify inhibitors of Nef-mediated MHC-I downregulation by infecting cells expressing HLA-A2, a common allele of MHC-I, with an adenoviral vector potently expressing Nef. From the 11 strains determined to posses Nef inhibitory activity, we identified the plecomacrolide family of natural products as the active component in at least two of the strains. Specifically, bafilomycins and concanamycin A potently restored surface expression of the MHC-I molecules in human primary cells at pM to nM concentrations.

Chapter 1
Background and Introduction

1.1 Therapeutic Uses of Natural Products

1.1.1 Natural Products Throughout History

It is a well-recorded fact that humans have been taking advantage of the potency in plants and fungi to benefit our health for thousands of years. As early as the 30th century BC we have documented herbal medical records from the Sumerians.[1-2] Later on, Egyptians made use of honey, fruits and plant extracts to create topical ointments, oils for curing constipation and mouthwashes to combat common colds.[3-5] The incorporation of plants and soils into medical practice gained popularity throughout Asian cultures during the 2nd century BC,[1, 6] and kept spreading during the 15-16th centuries to civilizations like the Greeks and Romans.[4] Philosophers and scientists like the Greek Theophrastus and Roman Pliny the Elder compiled information on their known uses of plant therapeutics, their application and proper storage. Unbeknownst to them at the time, the healing properties from these life-changing treatments rise from secondary metabolites, also termed natural products (NPs), mainly produced by plants, fungi, cyanobacteria and bacteria. The NPs are organic compounds not required for the organisms main survival, given they have no involvement in their development, but provide protection against competing species when these are released to the environment.[7-8]

During the early 1800s, an important turn in natural products exploration occurred when Friedrich Sertürner isolated an analgesic from opium plants.[9] As the Greco-Roman plant medicine had a prominent influence over the Western world, the newly discovered drug was named morphine after the Greek God of dreams, Morpheus, as it made patients drowsy. The discovery of the opioid class of drugs and their success at treating acute and chronic pain increased the curiosity towards plant medicine and inspired many scientists to seek novel compounds, leading to discoveries such as codeine and nicotine.[4, 10] With these great findings

new issues concerning NPs production time and quality arose. These challenges caused the scientific drug discovery efforts to shift towards chemical synthesis, which gave way to the first synthetic natural product salicylic acid in 1853.[11] Inarguably, the most important development in the field was the later discovery in 1928 by Alexander Fleming of the fungal derived penicillin antibiotic.[12] This antibiotic was introduced in 1942 to treat bacterial infections[13] and it is still widely used to this day, although it has encountered drug resistance by different types of bacteria. The improvement on human health that came with these findings built the foundations for microbial focused drug discovery and fostered the pharmaceutical industry that is known today.

1.1.2 Drug Discovery Exploration and Development

As the pharmaceutical industry grew and more microbial-focused research programs were developed, the natural products field bloomed into its so-called "golden age" through the early 1900s.[14] The search for biologically relevant molecules that could act as anti-fungal, anti-bacterial, anti-cancer and a wide variety of other diseases yielded the discovery of tetracycline, gentamicin and streptomycin (Fig 1.1).[15] At this time many NP discovery programs shifted their efforts towards developing microbial fermentation methods and technologies with the goal to probe the wide range of secondary metabolites produced by bacteria. Several decades later, two cholesterol biosynthesis inhibitors forming the statins class of molecules were discovered, compactin and mevinolin, thanks to their anti-fungal activities.[16-17] Due to their success when included into the patient's daily routine, as well as the positive impact in the pharmaceutical business, many of the research in the field was redirected towards the search for additional statin molecules and their production.

1.2 Current Scope of Natural Products

1.2.1 Scaffold Diversity

With so many NPs discovery groups identifying different biologically relevant targets to inhibit, a wide range of novel scaffolds were unearthed as expected. This rich source for diversity emerged from millions of years of exposure to biotic and abiotic stresses caused by both environmental factors and unnatural occurrences.[18] Thanks to this, secondary metabolites posses several therapeutic properties, which have lead NPs to be effective in most clinical medicine areas. By 2013 over a third of the novel Food and Drug Administration (FDA)

approved entities were NP or NP derivatives.[19] Microbes in particular produce intriguing diffusible metabolites when reaching stationary phase that have the potential to be toxic against neighboring species, as part of the continuous war for resources.[20] Their inherent structural characteristics, ability to be produced from cultured bacteria in large-scale and the potential to manipulate or engineer their biosynthetic pathways to produce a range of structural analogs make bacterial NPs particularly attractive for medicinal research areas. With how extensive they have been studied, it is no surprise a great deal of drugs marketed nowadays are comprised of bacterial NP or its derivatives.[21]

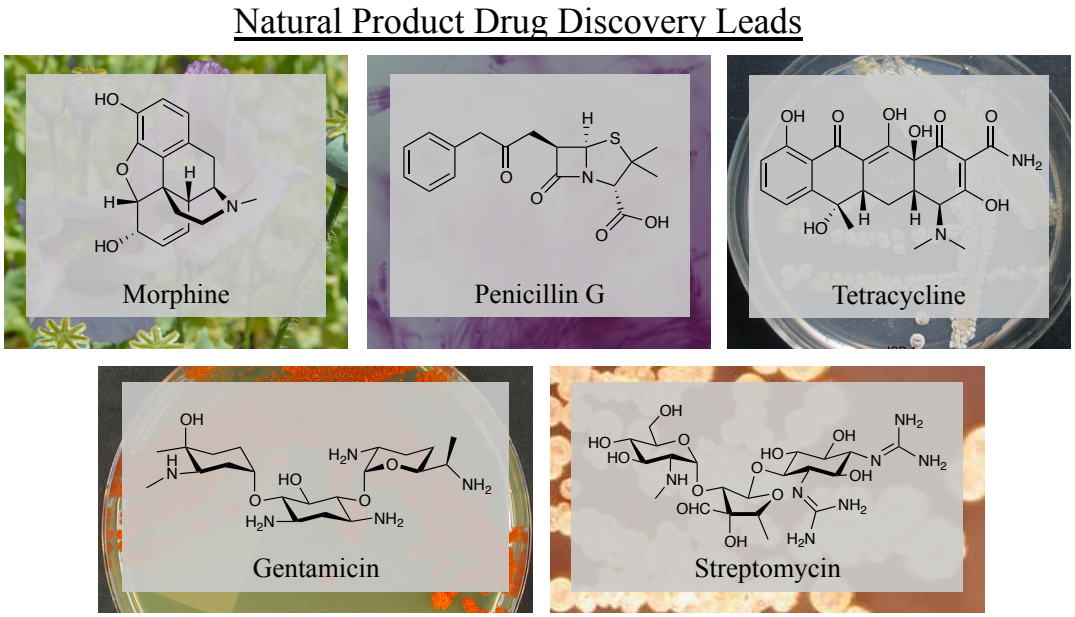


Figure 1.1. *Natural Products as a source for medicine.* These examples of clinically relevant secondary metabolites are derived from plants, fungi or bacteria and show the wide range of scaffold diversity that can be exploited for therapeutic purposes.

1.2.2 Drug Resistance

The popularity and success of NP drug discovery continued to apply pressure on companies to present new drugs to the market at higher rates and quantities. In spite of their success in clinical trials and with the many limitations surrounding production costs, difficulties with isolation, time consumption and arduous labor, there was a decline in pharmaceutical NP research.[22-23] Efforts were mostly shifted to combinatorial synthesis and high-throughput screening campaigns that created large, small molecule libraries.[24-25] Regrettably, this decline in

NP drug discovery seamed to have a correlation with a plunge in the introduction of lead compounds, and subsequent drug approval by the FDA.[26-27]

This loss in drug discovery is frightening given that an estimated 2 million patients in the US alone are exposed to infections that cannot be effectively eradicated by the current available treatments.[28] Most classes of drugs currently used were discovered before the 1970s and only a small amount of novel scaffolds have been introduced thereafter.[29] Since then researchers have developed techniques, such as synthetic modifications and synergistic approaches, to increase potency on the drugs available, but bacteria have been faster at acquiring resistance to the new antibiotic generations than scientists have been able to strategize.[30-31] Equally alarming, the public health is at further risk of drug resistance from many cancers and viruses towards their chemotherapeutics and antiviral treatments. It is of the utmost importance for researchers to continue the search for novel chemical scaffolds as well as new biologically relevant areas to target for inhibition. With the sheer amplitude of undiscovered marine microbes in the globe and the enormous chemical diversity shown to date, bacteria represent a possible route towards uncovering potential bioactive molecules.

1.3 Natural Products Biosynthesis

Historically, most NPs that have shown promising biological activities belong to the sub-classes of polyketides (PKs), like geldanamycin and erythromycin,[32-33] or non-ribosomal peptides (NRPs), such as actinomycin and vancomycin.[34-35] Their biosynthetic machinery consists of multimodular catalytic domains, all arranged in an orderly fashion. The reactions within each module yield molecules with elaborate stereospecificity and regiospecificity.[36] Fusion PKs-NRPs molecules are also present in nature and possess their own unique structural characteristics.

1.3.1 Polyketide Synthases

Biosynthetic pathways involved in the production of polyketides, called polyketide synthases (PKS), are classified into three categories.[37-38] Type I is composed of large modular proteins gathered as an assembly line where each module contains various domains with their specific roles.[39] Synthesis of the secondary metabolites is divided into three main stages: loading, elongation and release. The process begins with the loading of a two carbon acetyl-CoA molecule, or a derivative, into the loading site. In general, a PKS module will contain a

ketosynthase (KS), acyltransferase (AT) and a acyl carrier protein (ACP), with possible additional domains that can provide further modifications to the molecules by converting the new keto group to a hydroxyl, double bond or single bond (Fig 1.2).[40] For elongation to occur, the AT domain will select a specific acyl-CoA derivative, usually malonyl-CoA and its derivatives, and load it into its ACP domain. Successively, the KS domain mediates the carbon-carbon bond formation by taking the polyketide chain from the previous ACP through non-covalent docking interactions, and catalyzing the decarboxylation of the new malonyl derivative.[41-42] This resulting nucleophile will then react with the growing chain through a Claisen condensation, leaving the current ACP with the elongated polyketide chain. The process will repeat through the assembly line-like pathway with a vast number of domain combinations and malonyl derivative extender units available to create diverse structural backbones. Finally, the TE domain will hydrolyze the finished molecule from the last ACP domain, freeing it from the megasynthase.

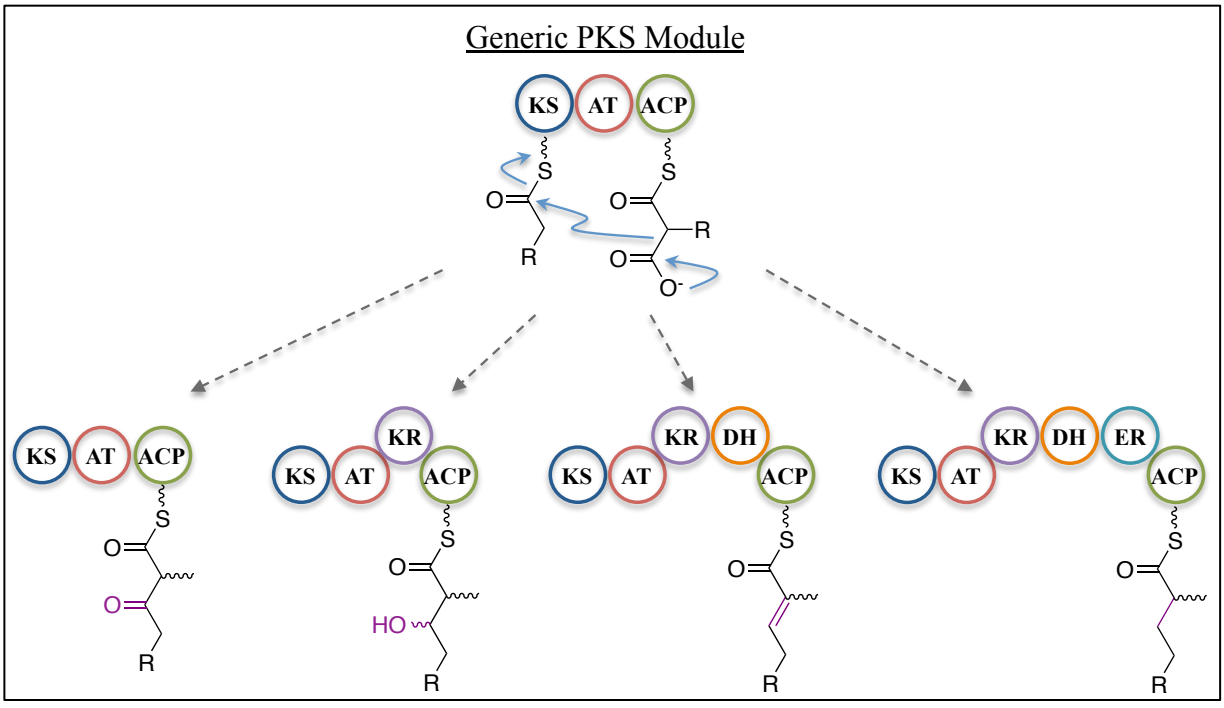


Figure 1.2. *General PKS module scheme*. After selection of the extender unit by the AT domain and subsequent loading into the ACP domain, decarboxylation followed by a Claisen condensation are catalyzed by the KS domain. Additional domains can be present to perform keto reduction (KR), dehydration (DH) and double bond reduction (ER).

1.3.2 Non-Ribosomal Peptide Synthetases

Similar to PKs, NRPs are made through distinct modular enzymes part of a large assembly line called non-ribosomal peptide synthetase (NRPS). As the name suggests, the building blocks or units used to assemble the molecules are amino acids or their derivatives, as opposed to the acyl derivatives used for PKS. The assembly of these ribosome independent peptides follows a similar fashion in that it contains a starting and a release module with a number of elongation modules in between. Each of the modules requires an adenylation domain (A), condensation domain (C) and a peptidyl carrier protein (PCP) for it to function (Fig 1.3).[43-45] The starting unit is activated by the A domain through a trans-esterification with ATP. In turn, the PCP domain requires proper assembly with the addition of the prosthetic 4'-phosphopantetheinyl moiety to a serine residue, which will result in a free thiol group. The aminoacyl-adenylate will react with the thiol, a process catalyzed by the A domain, to create a covalent bond between the PCP domain and the amino acid. During the elongation process, the C domain will catalyze the interaction between the amino group of the current amino acid and the activated thioester group from the previous to create a peptide bond. Additional domains that further diversify the growing chain can also be present within the elongation modules. One of the most common is the epimerization domain (E), which inverts the stereochemistry of the amino acid from L to the uncommon D configuration. Other modifying domains catalyze methylation of the amino group (NMT) and cyclization into thiazoline or oxazoline rings (Cy) in amino acids with nucleophilic side chains. Further oxidations of the rings into thiazoles or oxazoles, as well as reductions into thiazolidines or oxazolidines, can be achieved by additional oxidation and reduction domains. Like PKS, a thioesterase domain will hydrolyze the final peptide molecule from the synthetase to form a macrocycle, although sometimes a reductive release is possible in the presence of a reductase domain and results in a linear peptide with either an alcohol or aldehyde at its terminal.[46]

1.3.3 PKS-NRPS Hybrids and Tailoring Enzymes

Given the many similarities between both PKS and NRPS, it is possible to have pathways with characteristics of both classes of NPs.[47] The hybrid systems use modules of both PKS and NRPS for its production line in either sequence. These combinations further expand the array of secondary metabolite core scaffolds the microbes are able to create, which can later be exploited

by scientists. Finally, both PKs and NRPs, as well as fusion molecules, are further modified after release by enzymatic tailoring. Some of these modifications are made by halogenases, cyclases, oxidoreductases, methyltransferases and glycosyltransferases.[48] With the abundance of functional groups that can be introduced into the secondary metabolites thanks to tailoring enzymes, a lot of the properties can be manipulated through their application via combinatorial biosynthesis, e.g. higher solubility, increased bioactivity, lower toxicity.

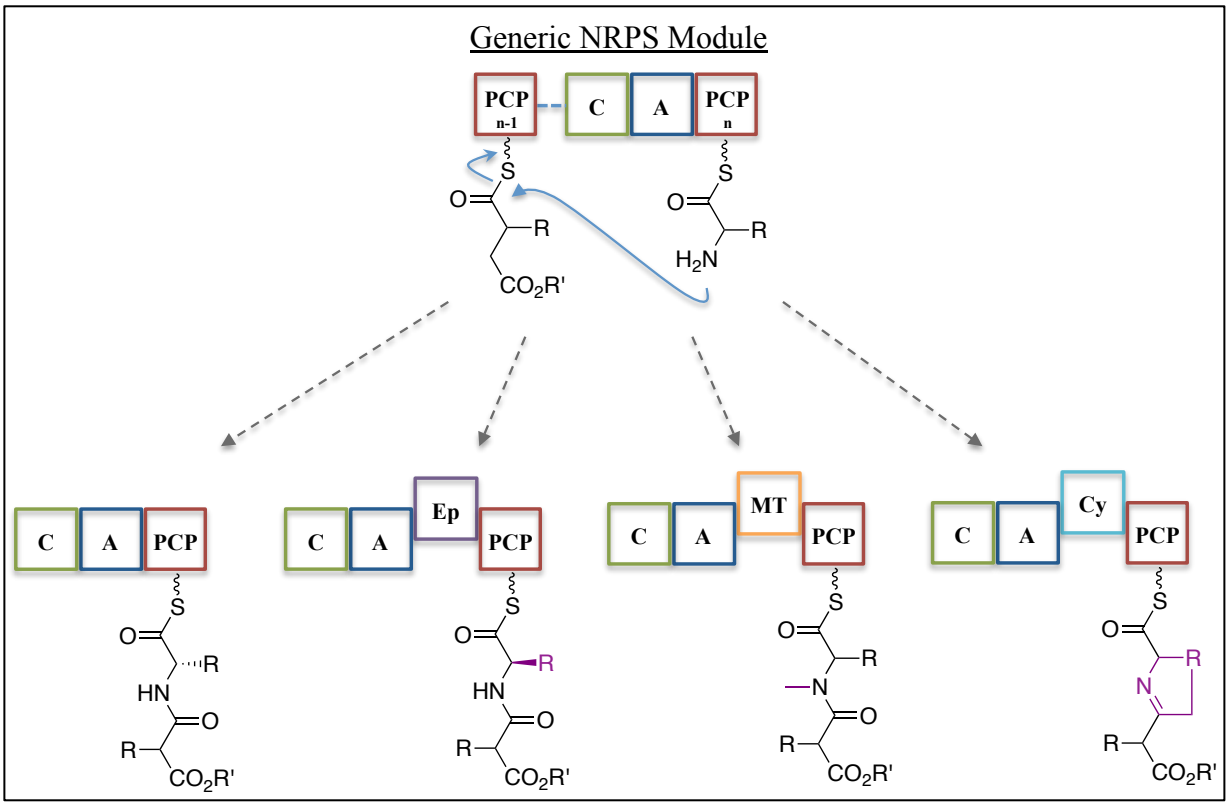


Figure 1.3. *General NRPS module scheme*. After selection of amino acids by the A domain and loading into PCP domain, peptide bond formation is aided by the C domain. Additional domains can be present and are responsible for epimerization (Ep), amino group methylation (MT) and cyclation of nucleophilic side chains with the amino group (Cy).

1.4 Summary and Dissertation Outline

Although unidentified at the time, natural products have been used throughout the ages as therapeutics during simple tasks such as covering wounds with plants or prescribing herbal drinks for sores and aches.[2-3] Since then, scientists have uncovered the wide array of secondary metabolites produced by plants, fungi and microbes alike, with unique structural functionalities

thanks to the numerous possible combinations in their biosynthetic pathways. The growing public health concerns pertaining severe infections and diseases make searching for novel areas to target a focus for scientists. With the vast expanse of current drugs on the market that originated from NPs, and the many distinctive scaffolds surely waiting to be discovered, NPs represent an important and promising area for the discovery of future therapeutics.

This dissertation will feature two independent projects that center on using NP extracts produced by marine microbes to identify potential inhibitors of biologically relevant targets. The first project shown in chapter 2 will explore using a member of the Coenzyme A (CoA) biosynthesis called phosphopantothenoylcysteine (PPCS) as a drug target for developing new antimicrobials.[49-50] To achieve this we adapted a biochemical assay specific for bacterial PPCS to screen for inhibitors of CoA biosynthesis against a library of marine microbial derived natural product extracts (NPEs).

The following chapter will present the Nef protein as a target for HIV-1 eradication from host cells. This accessory protein encoded by HIV is a key player in the immunoevasion of the virus from the cytotoxic T lymphocytes (CTLs).[51-53] We believe targeting the Nef protein for inhibition could potentially reduce the infected cells viral load significantly. A high-throughput screen was developed in collaboration with Dr. Kathleen Collins lab (UM-Medical School) that tests the wide variety of marine microbes present in the Center for Chemical Genomics (CCG) at the Life Sciences Institute. We aimed to identify a new class of Nef inhibitors that could potentially aid in future developments of antiretroviral therapy. A summary of this dissertation and a look into the future directions for this project will be exposed in the fourth and final chapter.

1.5 References

1. Cragg, G. M.; Newman, D. J. Biodiversity: a continuing source of novel drug leads. *Pure Appl Chem* **2005,** *77*, 7-24.
2. Bernardini, S.; Tiezzi, A.; Laghezza Masci, V.; Ovidi, E. Natural products for human health: an historical overview of the drug discovery approaches. *Nat Prod Res* **2018,** *32*, 1926-1950.
3. Borchardt, J. K. The beginnings of drug therapy: ancient mesopotamian medicine. *Drug News Perspect* **2002,** *15*, 187-192.
4. Sneader, W. *Drug discovery: a history.* John Wiley & Sons, Ltd: Chichester, 2005.
5. Cragg, G. M.; Newman, D. J. Natural products: a continuing source of novel drug leads. *Biochim Biophys Acta* **2013,** *1830*, 3670-3695.

6. Unschuld, P. U. *Nan-ching the classic of difficult issues*. University of California Press: Berkeley and Los Angeles, CA, 1986.
7. Dewick, P. M. *Medicinal natural products: a biosynthetic approach*. John Wiley & Sons: West Sussex, 2009; Vol. 3rd ed.
8. Colegate, S. M.; Molyneux, R. J. In *Bioactive natural products: detection, isolation and structure determination*, CRC Press: Boca Raton, Fl, 2008; pp 421–437.
9. Dias, D. A.; Urban, S.; Roessner, U. A historical overview of natural products in drug discovery. *Metabolites* **2012,** *2*, 303-336.
10. Hosztafi, S. The discovery of alkaloids. *Pharmazie* **1997,** *52*, 546–550.
11. Kaiser, H. Von der Pflanze zur Chemie - Die Frühgeschichte der "Rheumamittel". [From the Plant to Chemistry - The Early History of the "Rheumamittel"]. *Z Rheumatol* **2008,** *67*, 252–262.
12. Tan, S. Y.; Tatsumura, Y. Alexander Fleming (1881–1955): Discoverer of penicillin. *Singapore Med J* **2015,** *56*, 366-367.
13. Torok, E.; Moran, E.; Cooke, F. *Oxford Handbook of Infectious Diseases and Microbiology*. 2 ed.; Oxford University Press: Oxford, UK, 2009.
14. Wainwright, M. *Miracle Cure: The Story of Penicillin and the Golden Age of Antibiotics*. Blackwell Scientific: Oxford, UK, 1990.
15. Baker, D. D.; Chu, M.; Oza, U.; Rajgarhia, V. The value of natural products to future pharmaceutical discovery. *Nat Prod Rep* **2007,** *24*, 1225–1244.
16. Brown, G.; Smale, T. C.; King, T. J.; Hasenkamp, R.; Thompson, R. H. Crystal and molecular structure of compactin, a new antifungal metabolite from Penicillium brevicompactum. *J Chem Soc Perkin Trans* **1976,** *1*, 1165-1170.
17. Endo, A.; Kuroda, M.; Tanzawa, K. Competitive inhibition of 3-hydroxy-3-methylglutaryl coenzyme a reductase by ML-236A and ML-236B fungal metabolites, having hypocholesterolemic activity. *FEBS Lett* **1976,** *72*, 323.
18. Sarker, S. D.; Latif, Z.; Gray, A. I. *Methods in biotechnology: natural product isolation*. Human Press Inc.: Totowa, NJ, 2006; Vol. 2nd ed.
19. Patridge, E.; Gareiss, P.; Kinch, M. S.; Hoyer, D. An analysis of FDA-approved drugs: natural products and their derivatives. *Drug. Discov. Today* **2015,** *0*, 1-4.
20. Stachowicz, J. J.; Lindquist, N. Hydroid defenses against predators: the importance of secondary metabolites versus nematocysts. *Oecol.* **2000,** *124*, 280-288.
21. Bérdy, J. Thoughts and facts about antibiotics: Where we are now and where we are heading. *J. Antibiot.* **2012,** *65*, 385-395.
22. Bhatnagar, I.; Se-Kwon, K. Marine antitumor drugs: status, shortfalls and strategies. *Mar Drugs* **2010,** *8*, 2702-2720.
23. Lamottke, K.; Ripoll, C.; Walczak, R. The roots of innovation. *EBR* **2011,** *15*, 52-56.
24. Koehn, F. E.; Carter, G. T. The evolving role of natural products in drug discovery. *Nat Rev Drug Discov* **2005,** *4*, 206-220.
25. Roggo, S. Natural Products in Drug Discovery. *CHIMIA* **2007,** *61*, 312.
26. Kinch, M. S.; Patridge, E.; Plummer, M.; Hoyer, D. An analysis of FDA-approved drugs for infectious disease: antibacterial agents. *Drug Discov Today* **2014,** *19*, 1283-1287.
27. Patridge, E.; Gareiss, P.; Kinch, M. S.; Hoyer, D. An analysis of FDA-approved drugs: natural products and their derivatives. *Drug Discov Today* **2016,** *21*, 204-207.
28. Centers for Disease Control and Prevention, O. o. I. D. Antibiotic resistance threats in the United States. http://www.cdc.gov/drugresistance/threat-report-2013 (accessed July 20).

29. Lee Ventola, C. The Antibiotic Resistance Crisis Part 1: Causes and Threats. *Pharm Ther* **2015,** *40*, 277-283.
30. Wright, P. M.; Seiple, I. B.; Myers, A. G. The Evolving Role of Chemical Synthesis in Antibacterial Drug Discovery. *Angew Chem Int Ed Engl* **2014,** *53*, 8840-8869.
31. Wambaugh, M. A.; Shakya, V. P. S.; Lewis, A. J.; Mulvey, M. A.; Brown, J. C. S. High-throughput identification and rational design of synergistic small-molecule pairs for combating and bypassing antibiotic resistance. *PLoS Biol* **2017,** *15*, 1-33.
32. Whitesell, L.; Shifrin, S. D.; Schwab, G.; Neckers, L. M. Benzoquinonoid ansamycins possess selective tumoricidal activity unrelated to src kinase inhibition. *Cancer Res* **1992,** *52*, 1721-1728.
33. McGuire, J. M.; Bunch, R. L.; Anderson, R. C.; Boaz, H. E.; Flynn, E. H.; Powell, H. M.; Smith, J. W. Ilotycin, a new antibiotic. *Schweiz Med Wochenschr* **1952,** *82*, 1064-1065.
34. Geraci, J. E.; Heilman, F. R.; Nichols, D. R.; Wellman, E. W.; Ross, G. T. Some laboratory and clinical experiences with a new antibiotic, vancomycin. *Antibiot Annu* **1957**, 90-106.
35. Hertweck, C. The Biosynthetic Logic of Polyketide Diversity. *Angew Chem Int Edit* **2009,** *48*, 4688-4716.
36. Horsman, M. E.; Hari, T. P.; Boddy, C. N. Polyketide synthase and non-ribosomal peptide synthetase thioesterase selectivity: logic gate or a victim of fate? . *Nat Prod Rep* **2016,** *33*, 183-202.
37. Hopwood, D. A. Genetic Contributions to Understanding Polyketide Synthases. *Chem Rev* **1997,** *97*, 2465−2497.
38. Staunton, J.; Weissman, K. J. Polyketide biosynthesis: a millennium review. *Nat. Prod. Rep.* **2001,** *18*, 380-416.
39. Weissman, K. J. Uncovering the structures of modular polyketide synthases. *Nat Prod Rep* **2015,** *32*, 436-453.
40. Weissman, K. J. The structural biology of biosynthetic megaenzymes. *Nat Chem Biol* **2015,** *11*, 660-670.
41. Lambalot, R. H.; Gehring, A. M.; Flugel, R. S.; Zuber, P.; LaCelle, M.; Marahiel, M. A.; Reid, R.; Khosla, C.; Walsh, C. T. A new enzyme superfamily - the phosphopantetheinyl transferases. *Chem Biol* **1996,** *3*, 923-936.
42. Walsh, C. T.; Gehring, A. M.; Weinreb, P. H.; Quadri, L. E.; Flugel, R. S. Post-translational modification of polyketide and nonribosomal peptide synthases. *Curr Opin Chem Biol* **1997,** *1*, 309-315.
43. Walsh, C. T. Insights into the chemical logic and enzymatic machinery of NRPS assembly lines. *Nat Prod Rep* **2016,** *33*, 127-135.
44. Schwarzer, D.; Finking, R.; Marahiel, M. A. Nonribosomal peptides: from genes to products. *Nat Prod Rep* **2003,** *20*, 275-287.
45. Cane, D. E.; Walsh, C. T. The parallel and convergent universes of polyketide synthases and nonribosomal peptide synthetases. *Chem Biol* **1991,** *6*, 19-25.
46. Du, L.; Lou, L. PKS and NRPS release mechanisms. *Nat Prod Rep* **2010,** *27*, 255-278.
47. Du, L.; Sanchez, C.; Shen, B. Hybrid peptide-polyketide natural products: biosynthesis and prospects toward engineering novel molecules. *Metab Eng* **2001,** *3*, 78-95.
48. Olano, C.; Mendez, C.; Salas, J. A. Post-PKS tailoring steps in natural product-producing actinomycetes from the perspective of combinatorial biosynthesis. *Nat Prod Rep* **2010,** *27*, 571-616.

49. Kupke, T. Molecular Characterization of the 4′-Phosphopantothenoylcysteine Synthetase Domain of Bacterial Dfp Flavoproteins. *J. Biol. Chem.* **2002,** *277* (39), 36137-36145.
50. Strauss, E.; Kinsland, C.; Ge, Y.; McLafferty, F. W.; Begley, T. P. Phosphopantothenoylcysteine synthetase from Escherichia coli. Identification and characterization of the last unidentified coenzyme A biosynthetic enzyme in bacteria. *J. Biol. Chem.* **2001,** *276* (17), 13513-13516.
51. Kammula, E. C.; Mötter, J.; Gorgels, A.; Jonas, E.; Hoffmann, S.; Willbold, D. Brain Transcriptome-Wide Screen for HIV-1 Nef Protein Interaction Partners Reveals Various Membrane-Associated Proteins. *PLoS One* **2012,** *7*, 1-12.
52. Bresnahan, P. A.; Yonemoto, W.; Ferrell, S.; Williams-Herman, D.; Geleziunas, R.; Greene, W. C. A dileucine motif in HIV-1 Nef acts as an internalization signal for CD4 downregulation and binds the AP-1 clathrin adaptor. *Curr. Biol.* **1998,** *8*, 1235-1238.
53. Swann, S. A.; Williams, M.; Story, C. M.; Bobbitt, K. R.; Fleis, R.; Collins, K. L. HIV-1 Nef blocks transport of MHC class I molecules to the cell surface via a PI 3-kinase-dependent pathway. *Virology* **2001,** *282*, 267-277.

Chapter 2

Adipostatins E-J, New Potent Antimicrobials Identified as Inhibitors of Coenzyme-A Biosynthesis

2.1 Introduction

2.1.1 Urgent Need for New Antibiotics

Since the surfacing of antibiotics, the quality of life has improved immensely by the successful treatment of fatal bacterial infections. Sadly, their triumph also led to the misuse of these drugs and gave rise to mutated resistant bacteria capable of combating antibiotics and proliferating in the host after treatment.[1-2] The emergence and rapid spread of antibiotic resistance presents a multifaceted challenge to health management through serious pathogenic infections. Currently, the extent of these multidrug resistance pathogens is epitomized by 'ESKAPE' organisms (*Enterococcus* spp., *Staphylococcus aureus*, *Klebsiella* spp., *Acinetobacter baumannii*, *Pseudomonas aeruginosa* and *Enterobacter* spp.).[3]

Methicillin resistant *Staphylococcus aureus* (MRSA) is known for causing skin and soft tissue infections, such as abscesses and furuncles, and even pneumonia in more extreme cases. With two in 100 people being MRSA carriers, a big segment comprised of medical personnel, this antimicrobial resistant version of *S. aureus* is a serious health threat.[4] Alarmingly, MRSA resists treatment from currently available β-lactam antibiotics and some strains have also shown resistance to other common antibiotics, such as tetracycline and erythromycin.[5-7] Other commonly encountered antimicrobial resistant bacteria are the vancomycin resistant *Enterococci* (VRE), *E. faecalis* and *E. faecium*. Although they do not usually cause complications while living in human intestines, they can sometimes cause bloodstream and urinary tract infections.

The genesis of the current antibiotic crisis can be directly attributed to the lack of discovery platforms for novel antimicrobials.[8] Efforts that began in the past few decades by enhancing the established core scaffolds by synthetic modifications have continued, but only one

new antibiotic class (daptomycin) was introduced between 1962-2015.[9-10] Therefore, a reliable platform to combat antibiotic resistance needs to be developed through novel target based approaches for the discovery of new chemical entities.[8, 11]

2.1.2 Coenzyme A as a Drugable Target

Coenzyme A (CoA) biosynthesis in particular may represent an effective antimicrobial target due to the substantial hurdles it presents to bacterial antibiotic resistance (Fig 2.1).[12] CoA is an indispensible enzyme cofactor for all living organisms involved in metabolic reactions such as fatty acid metabolism and the Krebs cycle, as well as secondary metabolic reactions. It has been estimated that between 7-13% of all enzymes use CoA to achieve their activity.[12-13] In many cases deprivation of CoA has lead to cell stasis or improper cell development, while knockouts of CoA biosynthetic genes have shown to have lethal repercussions.[12, 14] Given its importance and universal use, CoA has long been sought by researchers as a target for its regulation and biosynthesis.

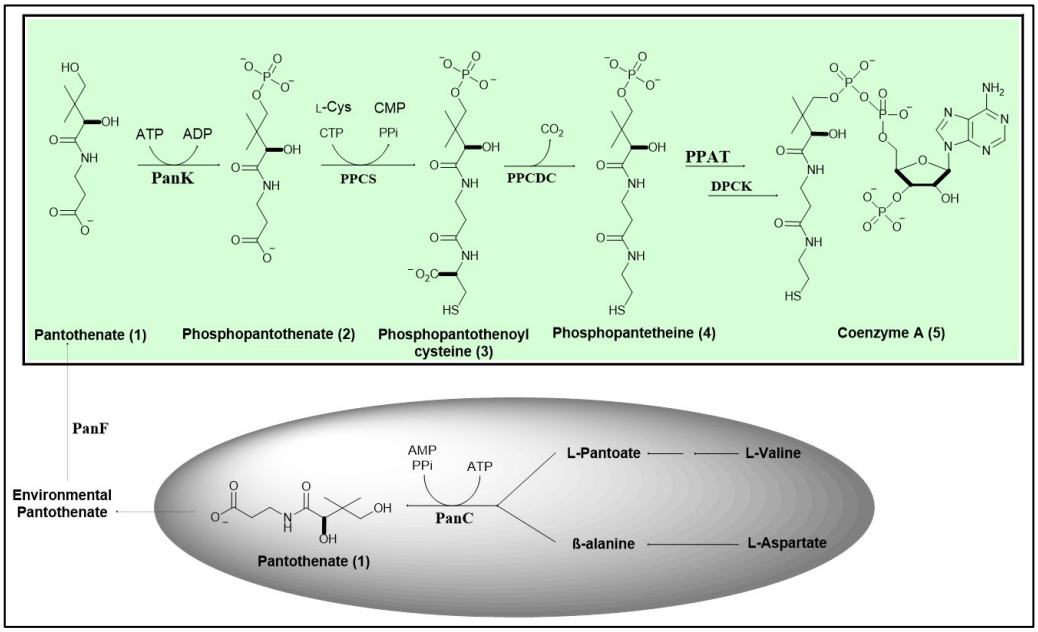


Figure 2.1. *Schematic depicting pantothenate uptake and transformation into CoA through the CoA biosynthetic pathway.* Most organisms rely on the uptake of exogenous pantothenate and virtually all organisms have pantothenate uptake capabilities.

2.1.3 Phosphopantothenoylcysteine Synthetase

CoA biosynthesis occurs as part of a five-step process; phosphopantothenoylcysteine synthetase (PPCS) is involved in the second step by catalyzing the installation of a cysteine

moiety to 4'-phosphopantothenate (**2**) (Fig 2.1-2.2).[15-16] PPCS can be broadly classified into three groups: Type I PPCSs, primarily found in bacteria and archaea, are manifested in nature as the C-terminal domain of a bifunctional protein fusion in conjunction with phosphopantothenoylcysteine decarboxylase (PPCDC) and require CTP to function.[15-16] Type II PPCSs, expressed as monofunctional enzymes, utilize either ATP or CTP and can be found mainly in eukaryotes.[17-18] Type III PPCSs, also expressed monofunctionally, have been shown to be CTP specific and are found in a smaller subset of bacteria.[18] Although the peculiar nucleotide selectivity could be an attractive target for the design of bacterial inhibitors validated by a series of intermediate-mimicking inhibitors,[18] no novel chemical structures have been identified.

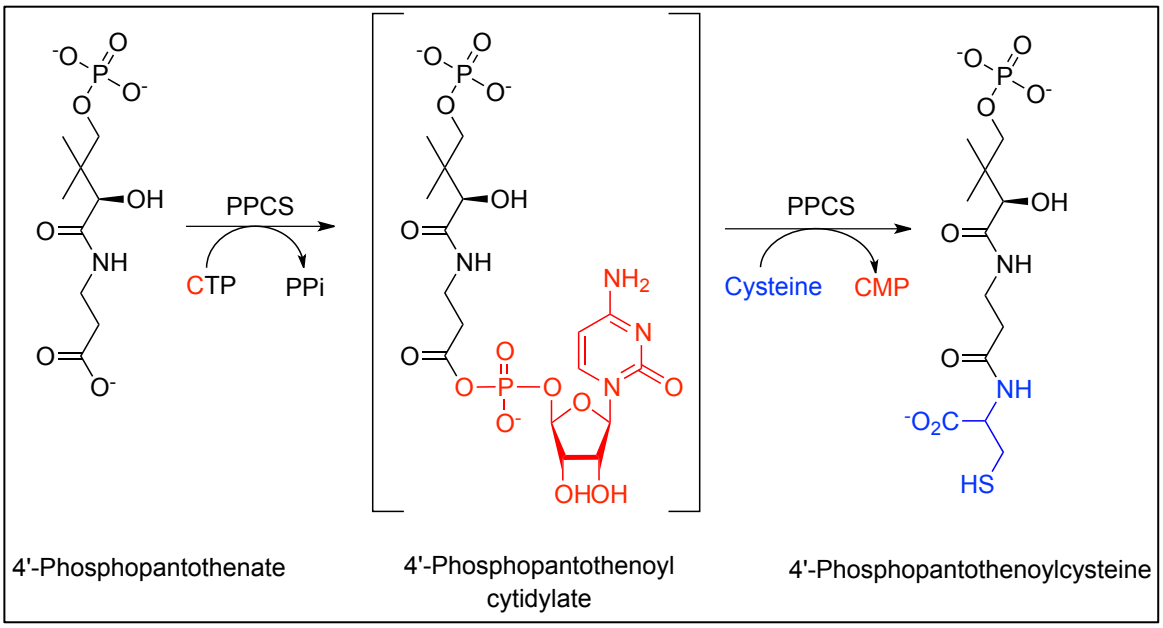


Figure 2.2. *Reactions catalyzed by phosphopantothenoylcysteine synthetase*. The current proposed two-step mechanism consists of the creation of a 4'-phosphopantothenoyl cytidylate intermediate after nucleophilic attack on the CTP by the carboxylic acid, followed by an attack from the cysteine amino group onto the cytidylate.[19]

In our ongoing quest to discover new structural classes of antibiotics,[11, 20-22] we developed an *in vitro* high throughput assay against bacterial PPCS to investigate our unique NPE library in the search for new microbial inhibitors.[23] Herein, we describe the discovery of six new congeners belonging to the adipostatin class of metabolites, isolated and characterized through a HTS campaign. We have also established the efficacy of newly discovered molecules through an *in vitro* study against a panel of 11 clinically relevant pathogenic microbes.

2.2 Results and Discussion

2.2.1 High-Throughput Screening for Inhibitors of Coenzyme A Biosynthesis Derived from Natural Product Extracts

Motivated by the urgent requirement of new structural class of antibiotics, we selected a marine microbial derived NPE library housed at the CCG to identify inhibitors of bacterial PPCS in collaboration with Dr. Jiangwei Yao from Dr. Dotson's lab. According to a recent study, natural products account for the majority of currently marketed drugs[10] and the marine environment represents a potentially unexplored source of novel chemical entities.[24] We optimized the malachite green reporter based enzymatic HTS assay specific to *S. pneumoniae* PPCS,[25] and conducted a high throughput campaign against a library of 11,000 marine microbial-derived NPEs (Fig 2.3; Fig SI-2.2). The malachite based HTS assay and the inorganic pyrophosphatase based counterscreen when selected against the threshold of $\geq$ 90% and $\leq$ 10% respectively, yielded active extracts from 22 strains (Fig 2.3). The lowest concentration of PPCS used for the HTS assay was 12.5 nM, which produced a response fit for screening (SI-2.1). Low enzyme concentrations were preferred to capitalize on the opportunity for detecting extracts that contain low abundance bioactive constituents.

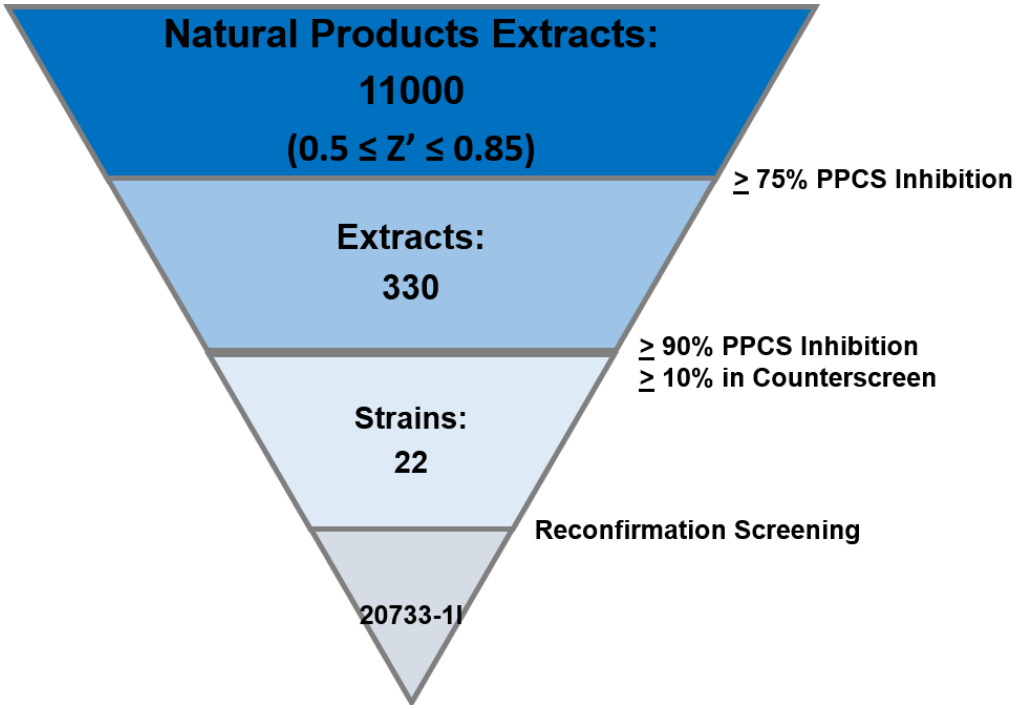


Figure 2.3. *Triage of hits obtained during HTS of PPCS against the microbial natural product extracts library.*

Among the active extracts, *Streptomyces blancoensis* (strain 20733-1; Fig SI-2.1-2.6) was of particular interest owing to the observed Hill slope of 2.6 with an IC_{50} value of 0.03 mg/mL (Fig SI-5). The strain was originally isolated from marine sediments collected in San Miguel, Costa Rica (-9° 33' 29", 85° 06' 40") in the Cabo Blanco Nature Reserve.

*2.2.2 Isolation and Structural Elucidation of the Adipostatins (**6-7, 10-15**)*

A recurring bioactivity guided preparative C18 fractionation (Fig SI-2.7) and ensuing RP-C18 HPLC purification (Fig SI-2.8) yielded two known adipostatins A-B (**6-7**) and six new congeners, adipostatins E-J (**10-15**) with structures likely derived from a type I PKS pathway.

The HR-APCI-MS data and the analysis of 1D and 2D NMR data confirmed the identity of **6** and **7** to be adipostatins A and B; previously reported as glycerol-3-phosphate dehydrogenase inhibitors.[26] Furthermore, **6** and **7** in addition to two more congeners adipostatins C-D (**8-9**) have been recently reported to possess anti-parasitic activity,[27] however **8** and **9** were not observed in our study. Adipostatin E (**10**) was purified as light yellow amorphous solid possessing the molecular formula of $C_{22}H_{38}O_2$ based on $[M+H]^+$ ion peak *m/z* 335.2899 (Figure SI-2.9). The ^1H and ^{13}C NMR data, recorded in CD_3OD, indicated the polyketidic nature of **10** with the tell tale presence of ^1H NMR peak at δ 1.31 suggesting an aliphatic chain consisting primarily of methylene groups. The presence of triplet at δ_H 0.86 (δ_C 11.2) suggested a terminal methyl group, which in turn showed a COSY relay with δ_H 1.32 (δ_C 30.1) methylene connected to the tertiary carbon (δ_C 40.3) through δ_H 1.18. Further analysis of the ^1H and gCOSY spectrum suggested two more methyl doublets at δ_H 0.88 and 0.89 connected to δ_H 1.52 (δ_C 27.3), completing the terminal dimethyl moiety (Fig SI-9-14).

Furthermore, the ^{13}C and HSQC NMR spectra revealed the presence of at least three quaternary carbons at δ_C 145.3 (an aromatic carbon) and δ_C 159.2 (two aromatic carbons). Moreover, the COSY correlations between two equivalent aromatic protons with signals at δ_H 6.08, 6.12 along with their gHMBCAD correlation with carbons at δ_C 100.9, 107.9, 145.3 and 159.2 unambiguously demonstrated the presence of a resorcinol moiety (Table I; Figure SI-2.9-2.14). The rest of the molecule consisted of a methylene aliphatic chain en suite to complete the planar structure of **10** (Fig 2.4).

The adipostatin E (**10**) carries a single stereocenter at carbon-17; which owing to its structural complexity was analyzed using *J*-based configuration analysis (JBCA) for proposing relative configuration.[28] We calculated $^3J_{H\text{-}H}$ values using a combination of phase sensitive double

quantum filtered (PS-DQF-COSY) and homonuclear 2D*J* (HOMO2D*J*) spectroscopy (Fig SI-2.15-2.16). The chemical shifts obtained at the C18-C17 axis suggested a large coupling constant at $^{3}J_{H18\text{-}H17} \approx 6.1$ Hz inferring their anti orientation and therefore, providing only two possible conformations. However, upon analyzing ROESY data (Fig SI-2.17) closely, it became evident that the defined difference of proton chemical shifts at $\delta_{H\text{-}19}$ and $\delta_{H\text{-}20}$ does not provide robust evidence to suggest a plausible conformation.

Adipostatin F (**11**) was isolated by RP-HPLC from the same C18 fraction containing compound **10**. The HR-APCI-MS of the molecule provided the same molecular formula $C_{22}H_{38}O_2$ as **10** based on similar $[M+H]^+$ ion peak *m/z* 335.2920 indicating **10** and **11** to be regioisomers (Fig SI-18). As expected, the extensive 1D and 2D NMR spectra showed comparable chemical shifts with a similar carbon backbone except towards the terminal end. The presence of merged doublets at δ_H 0.88-0.90 with distinct carbon shifts (δ_C 22.6, 22.61 and 16.4, respectively) together with COSY relay from δ_H 0.88 to δ_H 0.90 through δ_H 1.35 and δ_H 1.30, respectively suggested the tri-methyl containing terminal moiety completing the planar structure of **11** (Table I; Fig 2.4; Fig SI-2.19-2.21).

Furthermore, HR-APCI-MS analysis of **12** and **13** yielded the $[M+H]^+$ ions at *m/z* 349.3090 and 349.3087, respectively (Fig SI-2.20, 2.26), indicative of their structural relationship as positional isomers established through the same predicted molecular formula of $C_{23}H_{40}O_2$. The extensive 1D and 2D NMR spectra revealed equivalent chemical shifts compared to the carbon skeleton of **10** and **11** with the only apparent difference appearing as an additional CH_2 component (Fig SI-2.21-2.29). Further characterization revealed a clear difference at the terminus of the aliphatic chain; where the presence of a clear doublet at δ_H 0.90 (δ_c 23.1) in **12** and a triplet at δ_H 0.88 (δ_C 22.7) in **13** established them to be adipostatins G (**12**) and H (**13**), respectively (Table I; Fig 2.4).

The same C18 fraction also led to the isolation of **14** and **15** with HR-APCI-MS providing the molecular formula of $C_{24}H_{42}O_2$ and $C_{26}H_{46}O_2$ based on $[M+H]^+$ ion peak at *m/z* 363.3180 and *m/z* 391.2852, respectively (Fig SI-2.30, 2.34). The in-depth analysis and comparison of ^{1}H, HSQCAD and gCOSY spectra obtained for **14**, clearly indicated the extension in aliphatic framework with terminal branching into a di-methyl unit for completing the structure of adipostatin I (**14**). Similarly, the NMR spectra acquired for compound **15** suggested further elongation of the aliphatic chain by two CH_2 units ending with a terminal triplet at δ_H 0.92 (δ_C

22.9) affirming the structure of adipostatin J (**15**) (Table I; Fig 2.4; Fig SI-2.31-2.37). Although both **13** and **15** had been recently putatively identified in a metabolic profiling study of wheat,[29] their spectral data and the antimicrobial activity are not available.

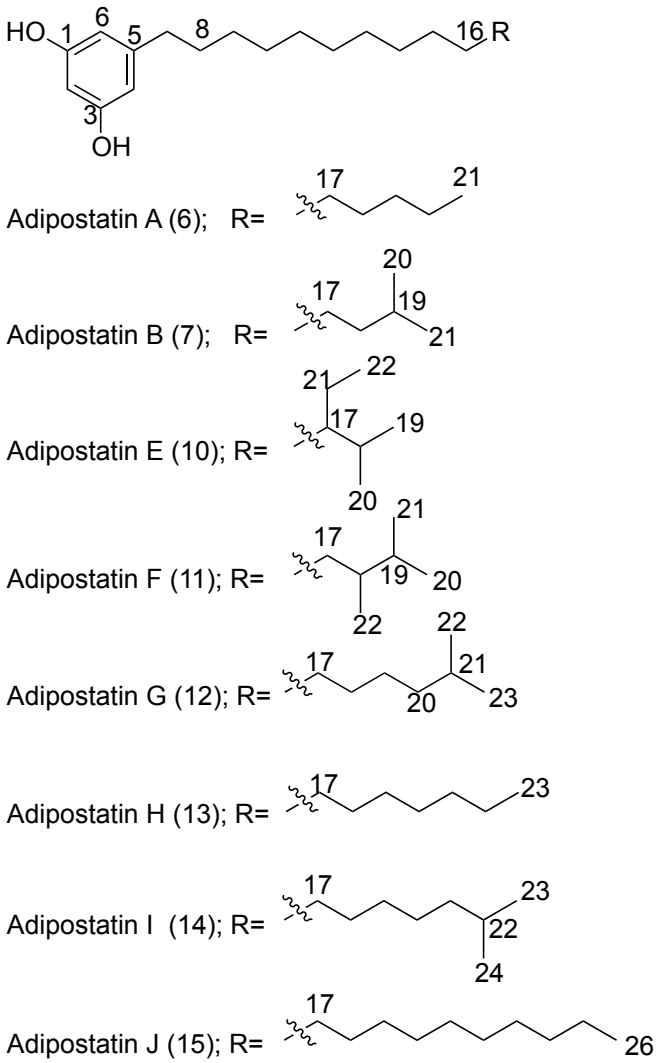


Figure 2.4. *Planar structure of adipostatins (A-B, E-J).* All were elucidated using extensive 1D and 2D NMR spectroscopy.

2.2.3 Assessment of the Biological Activity of Adipostatins against Purified PPCS Enzyme and Microbial Cultures

The malachite green based bioassay was next employed to assess the dose response of known adipostatins A, B, H and J (**6-7, 13** and **15**) and new congeners adipostatins E-G and I (**10-12** and **14**) against purified *S. pneumoniae* PPCS. The *in vitro* enzymatic assay revealed an

intriguing trend where **6-7**, **13** and **15** were observed to possess minimal inhibitory activity against the phosphopantothenoylcysteine synthetase tested up to a concentration of 300 μM. However, adipostatins E-G and I (**10-12**, **14**) exhibited significant *in vitro* inhibition against PPCS with IC_{50} values of 0.93 μM, 7.1 μM, 4.3 μM and 6.62 μM, respectively (Fig 2.5). The differential *in vitro* activity of molecules seems to suggest a structure activity relationship, where a critical chain length is required for bioactivity that increases with simple functional group branching at the chain terminus (Table SI-2.1). Unfortunately, yield of isolated molecules were not enough to compute thorough MIC values in current setup.

Coenzyme A biosynthesis plays a vital role in the growth and survival of pathogenic microbes. Therefore, we envisaged a live microbial culture study to demonstrate that the new adipostatin natural products can penetrate clinically relevant bacteria in order to access the enzyme target, a recognized asset of secondary metabolites over some synthetic chemical scaffolds.[30] The *in vivo* study included all the isolated adipostatins against a panel of eleven pathogenic microbial isolates (SI-1; Table SI-1). All the pathogens selected for bioassay were grown to mid log phase ($0.4 < OD_{600} < 0.6$) and 48 μL of culture was inoculated in 384 well plates pre-spotted with positive controls (kanamycin, vancomycin) and adipostatins A-B & E-J over the concentration range of 200 μg/mL to 0.8 ng/mL (Fig 2.5; Fig SI-2.39; SI 2.1; Table SI-2.1). The *in vivo* assay unambiguously established adipostatin E (**10**) to be the most potent molecule within the class with an IC_{50} value against *E. faecalis, B. subtilis, L. monocytogenes, B. anthracis* and *S. pneumoniae* observed to be 9.23 μM, 3.44 μM, 5.98 μM, 15.6 μM, and 10.1 μM, respectively (Fig 2.5; Fig SI-2.38; Table SI-2.1). Interestingly, none of the adipostatins were observed to possess noticeable inhibition against Gram-negative microbes (*viz., E. coli, S. enterica* and *S. flexneri*; Fig SI-2.39; Fig SI-2.38; Table SI-2.1). This might indicate that the molecule could also be affecting peptidoglycan synthesis and fatty acid synthesis through inhibition of CoA biosynthesis and, therefore, are more potent towards Gram-positive bacteria. Furthermore, adipostatins A-B (**6-7**), which were earlier observed to possess modest PPCS inhibitory activity *in vitro* (Table SI-1), showed modest *in vivo* antimicrobial activity with IC_{50} values at least 10 orders of magnitude higher compared to **10** (Table SI-2.1). This observation indicates an additional cellular target, which could be glycerol-3-phosphate dehydrogenase given their earlier reported inhibitory mechanism.[26] In the future, further chemical diversification through synthesis or biosynthetic pathway engineering could enable extensive analysis of the

selectivity (Gram-positive only) and the preliminary SAR for further optimizing the antibiotic activity of adipostatins.

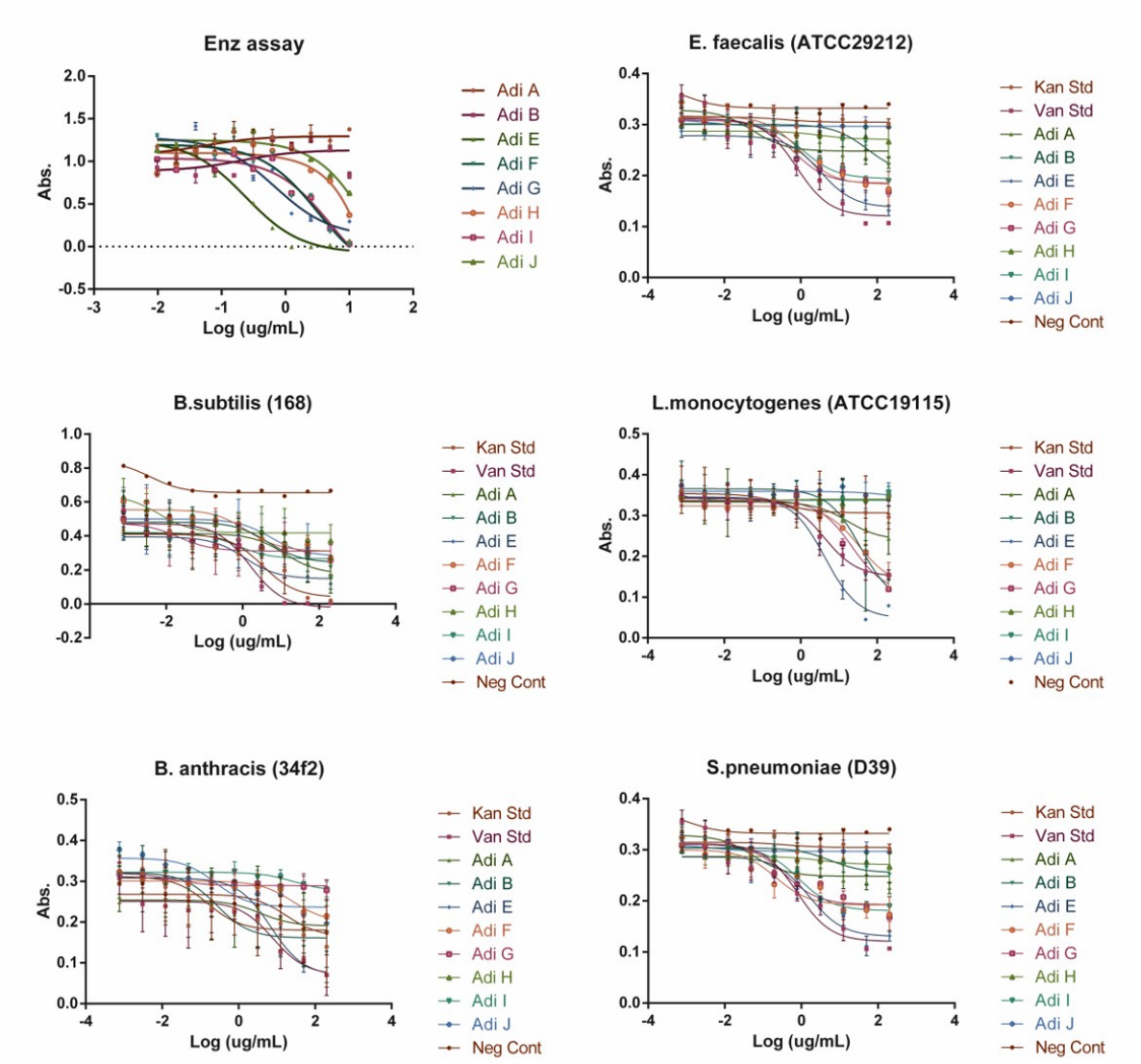


Figure 2.5. *Adipostatins in vitro bioactivity.* Results from malachite green bioassay against purified S. pneumoniae PPCS enzyme and anti-microbial assay against five Gram-positive pathogens. Experiments done in biological triplicates.

2.3 Conclusion

The compounds reported herein represent the first known natural product inhibitors of PPCS isolated from a marine microbial-derived NPE library. Adipostatins A (**6**), B (**7**) were earlier reported to possess glycerol-3-phosphate dehydrogenase and anti-parasitic activity, but intriguingly both **6** and **7** did not exhibit any appreciable PPCS inhibitory activity. Interestingly,

same is the case with adipostatin H (**13**) and J (**15**) which have been previously described to be isolated from *Cameroonian propolis* and cereal bran, respectively.[31-32] This class of molecules has been traditionally isolated with varying biological activity profiles, and recent studies have also shown their participation in physiological and metabolic regulations. For example, alkyl-resorcinols produced by cereal plants were reported to decrease grazing by livestock due to its supposed antifeedant properties.[33] Moreover, there are multiple reports where the ability of resorcinol lipids to bind with phospholipid proteins are described at great length indicating their potential to effectively interact with protein drug targets.[33]

Earlier reports have validated PPCS as an effective drug target,[18, 34-35] one of which describes the fungal metabolite CJ-15,801 acting as an antimetabolite of pantothenic acid, and processed by the PanK enzyme. The subsequent product is then accepted by *E. coli* PPCS as a tight binding inhibitor that impedes CoA biosynthesis (Figure 2.1).[34-36] In contrast, the current study establishes direct competitive inhibition of PPCS with respect to CTP and is devoid of antimetabolite activity due to the unique structural characteristics of **10**-**15** compared to reported counterparts.[34-37] Therefore, our study further supports the therapeutic utility of PPCS and demonstrates its potential for uncovering natural product chemical diversity *viz.,* adipostatins E-J (**10**-**15**). Furthermore, the differential *in vitro* activity suggests an apparent structure activity relationship relating to aliphatic chain length and terminal branching. This information provides important insights for future (bio)synthetic manipulation to improve both potency and target selectivity.

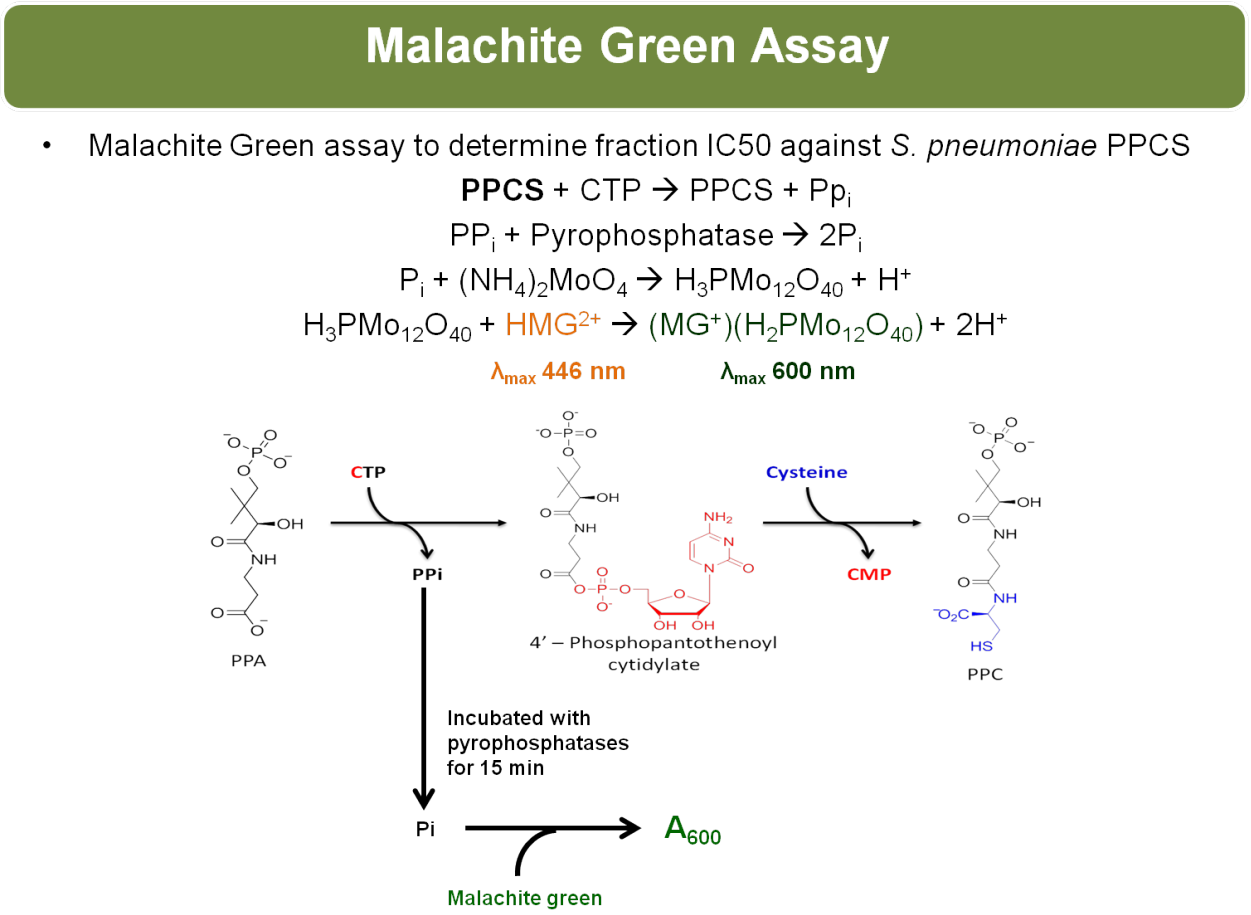
We have also illustrated that the adipostatins possess an innate ability to transfer through bacterial barriers and inhibit growth of cultures, including *E. faecalis, B. subtilis, L. monocytogenes,* and *B. anthracis*. This characteristic is notable as most of the previously reported CoA biosynthesis inhibitors have shown limited action against varied microbes, and thus affirms the potential value of **10**-**15** as well as the validity of PPCS as an antibacterial target.[34, 36, 38] The inability of adipostatins to function as antibiotics against Gram-negative bacteria establishes their potential to be classified as precision antibiotics, which may have advantages in limiting collateral effects on the human gut microbiome. Given the simultaneous decline in antibiotic drug discovery and a weak pipeline of clinical candidates along with increasing multidrug resistant bacteria, the adipostatins may represent a promising natural product lead scaffold to be exploited against significant Gram-positive human pathogens.

2.4 Supplemental Information (SI)

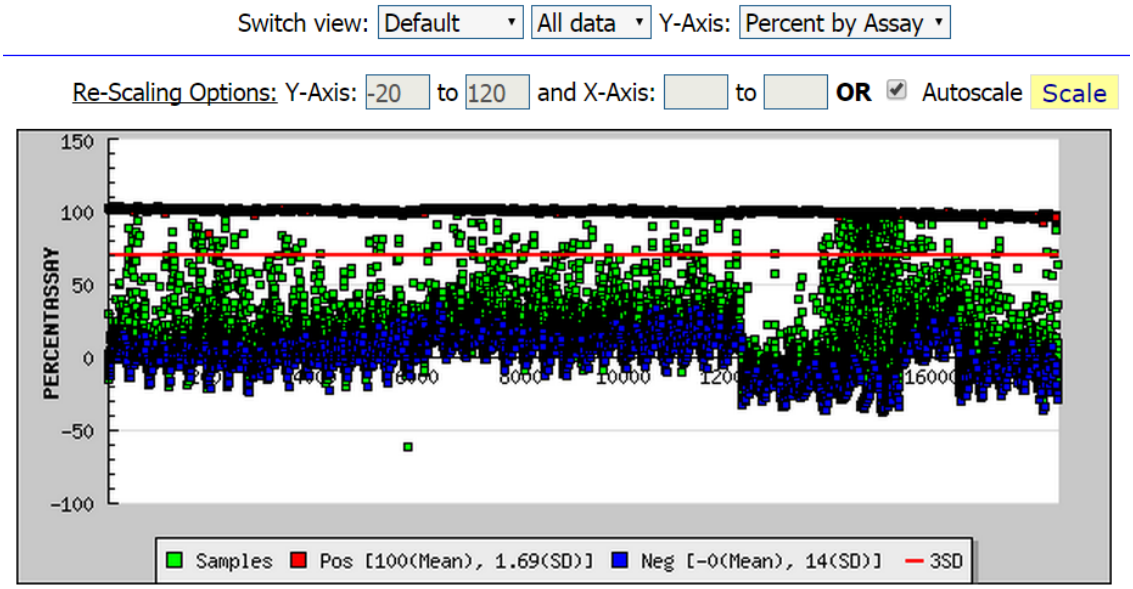
2.4.1. Phylogenetic Analysis

Phylogenetic analyses were conducted in GENEIOUS R6. Geneious version 8.1 created by Biomatters. Available from http://www.geneious.com/ [3] The evolutionary history was inferred using the Neighbor-Joining method. The bootstrap consensus tree inferred from 1000 replicates was taken to represent the evolutionary history of the taxa analyzed.

2.4.2. Development of an PPCS enzymatic assay for screening, the malachite green assay tailored to PPC synthetase.

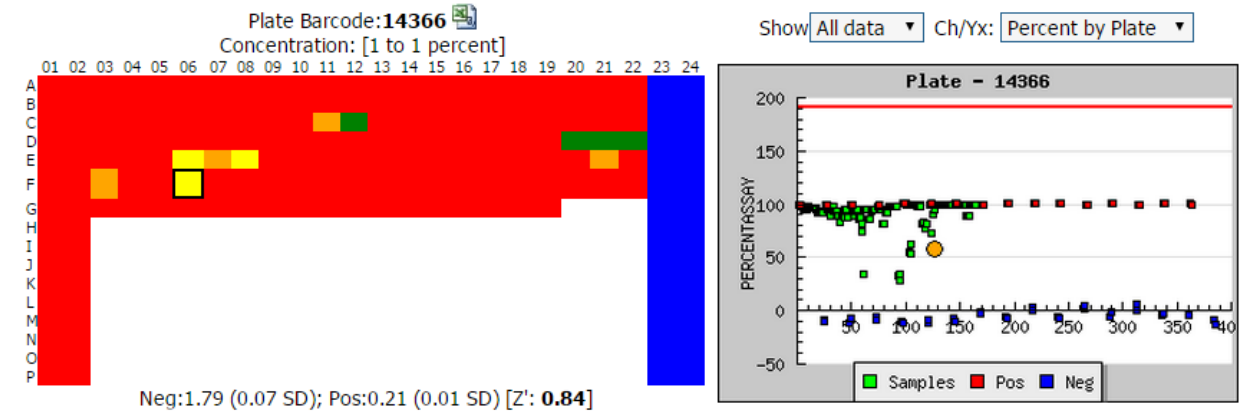


2.4.3. High throughput screening assay view against 11, 000 NPEs. Assay conducted by Dr. Jiangwei Yao (Dotson Lab).

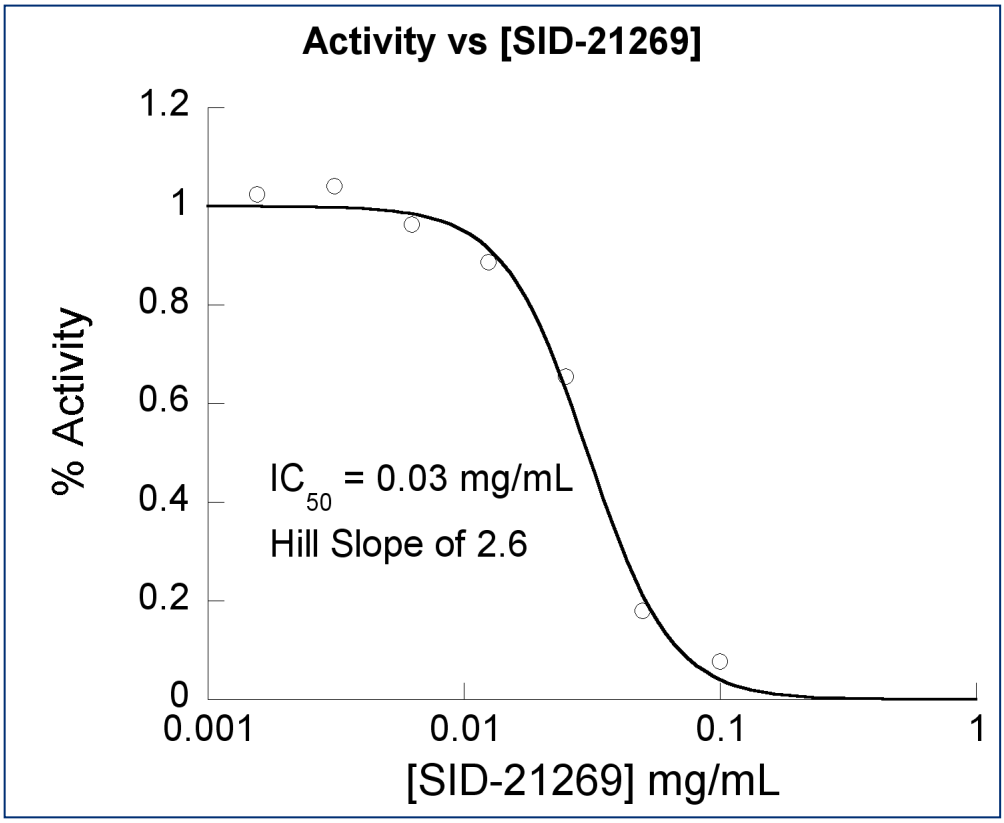


2.4.4 High throughput screening plate view of the plate containing selected active strain (20733-1) [Shown by orange dot on Plate 14366].

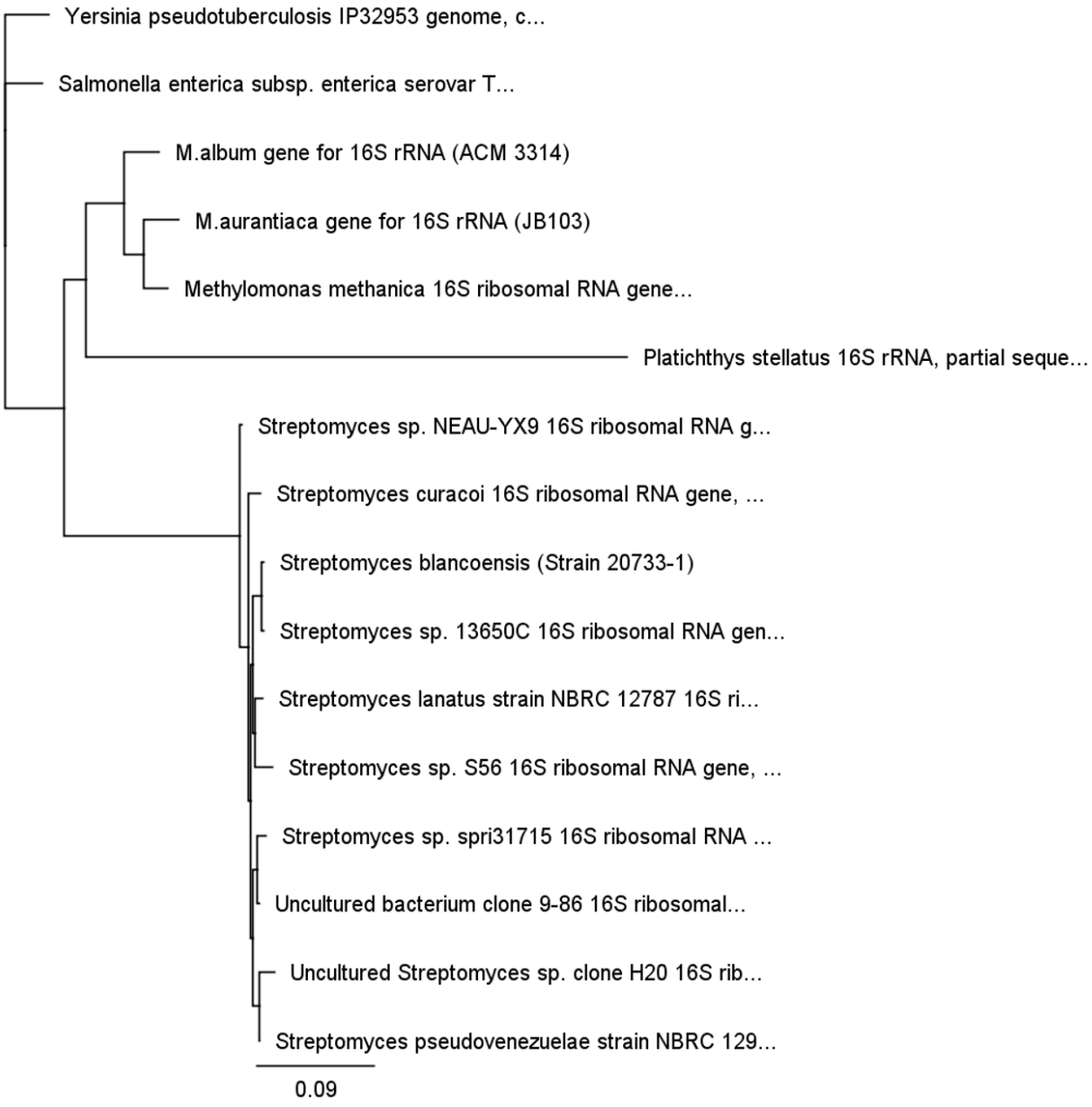
TARGETNAME	INVESTIGATOR	ASSAYDATE	PLATEID	EXTPLATEID	SOURCE_LIBRARY
PPCS [Campaign View]	GarryDotson	2009-08-13	14694	RP-14694	Retest_Plates-Original



2.4.5. Determination of IC50 and Hill slope of SID-21269 (strain 20733-1). Data were fit via a standard sigmoidal dose response curve.

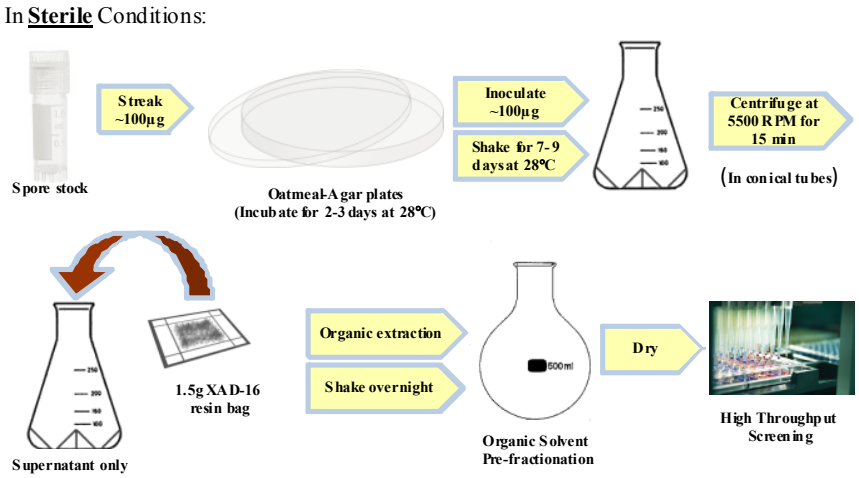


2.4.6. Phylogenetic analysis of the 16S rDNA gene sequences of adipostatins producing-Streptomyces sp. 20733-1.

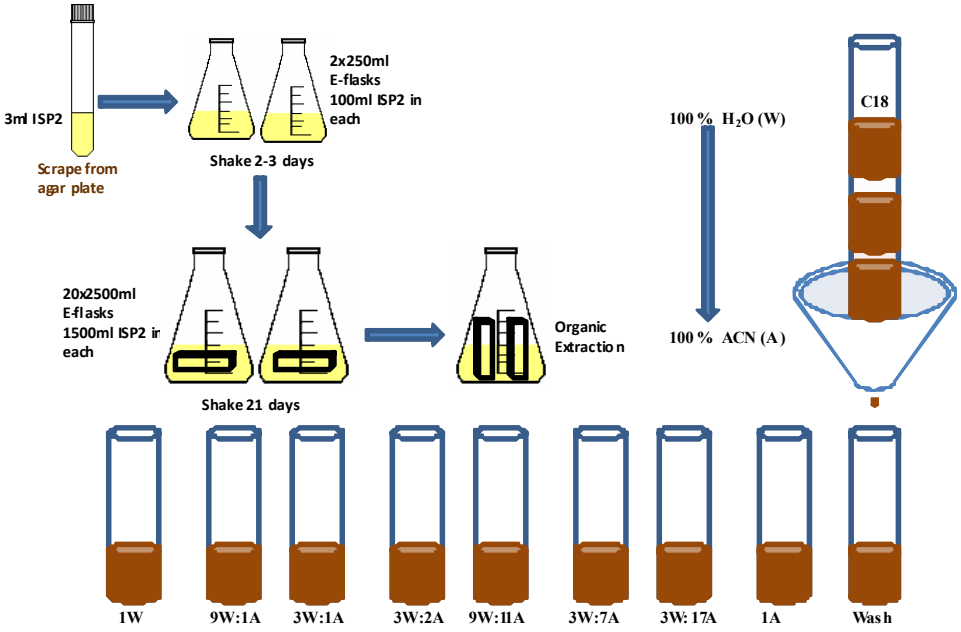


2.4.7. Small and large scale extraction schemes, respectively.

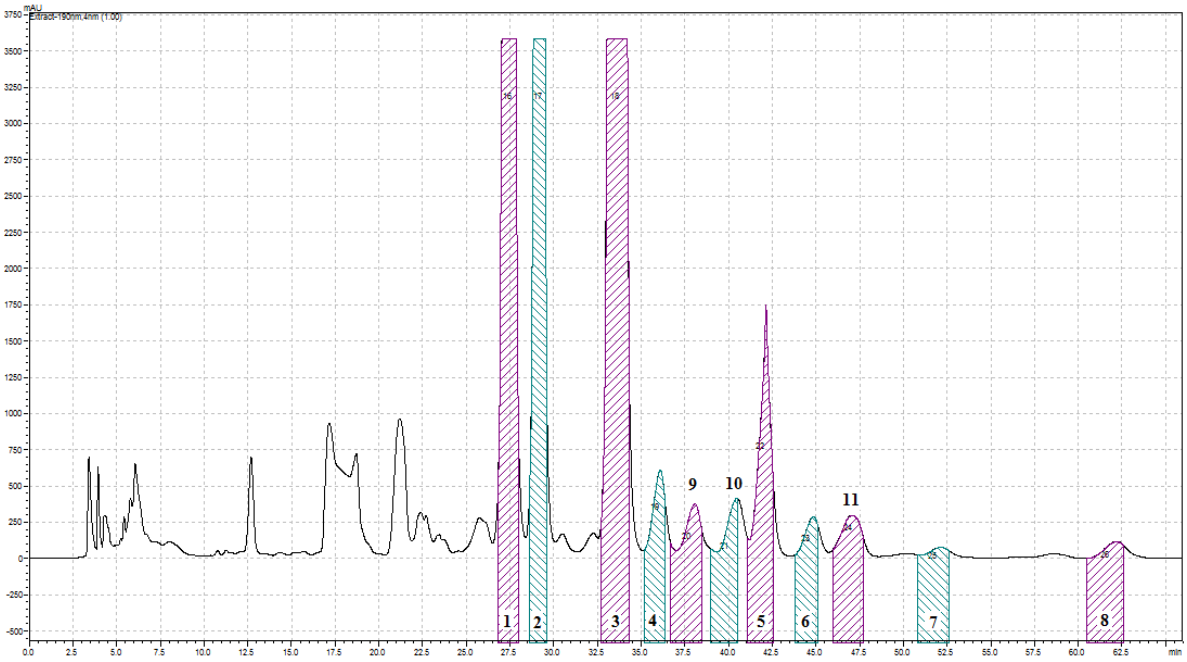
Small Scale Extraction Scheme

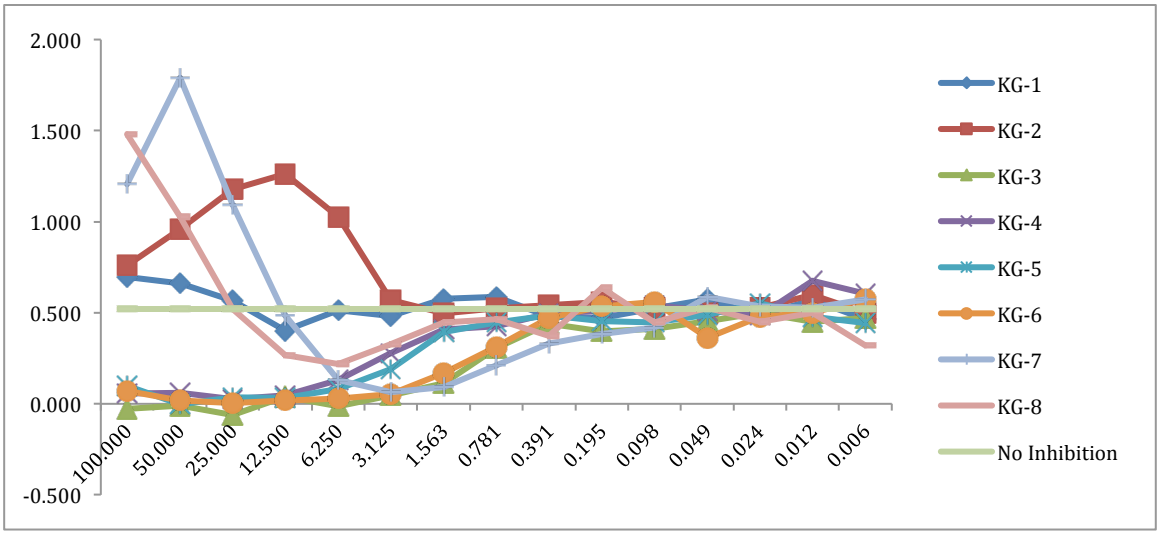


Large Scale Extraction Scheme



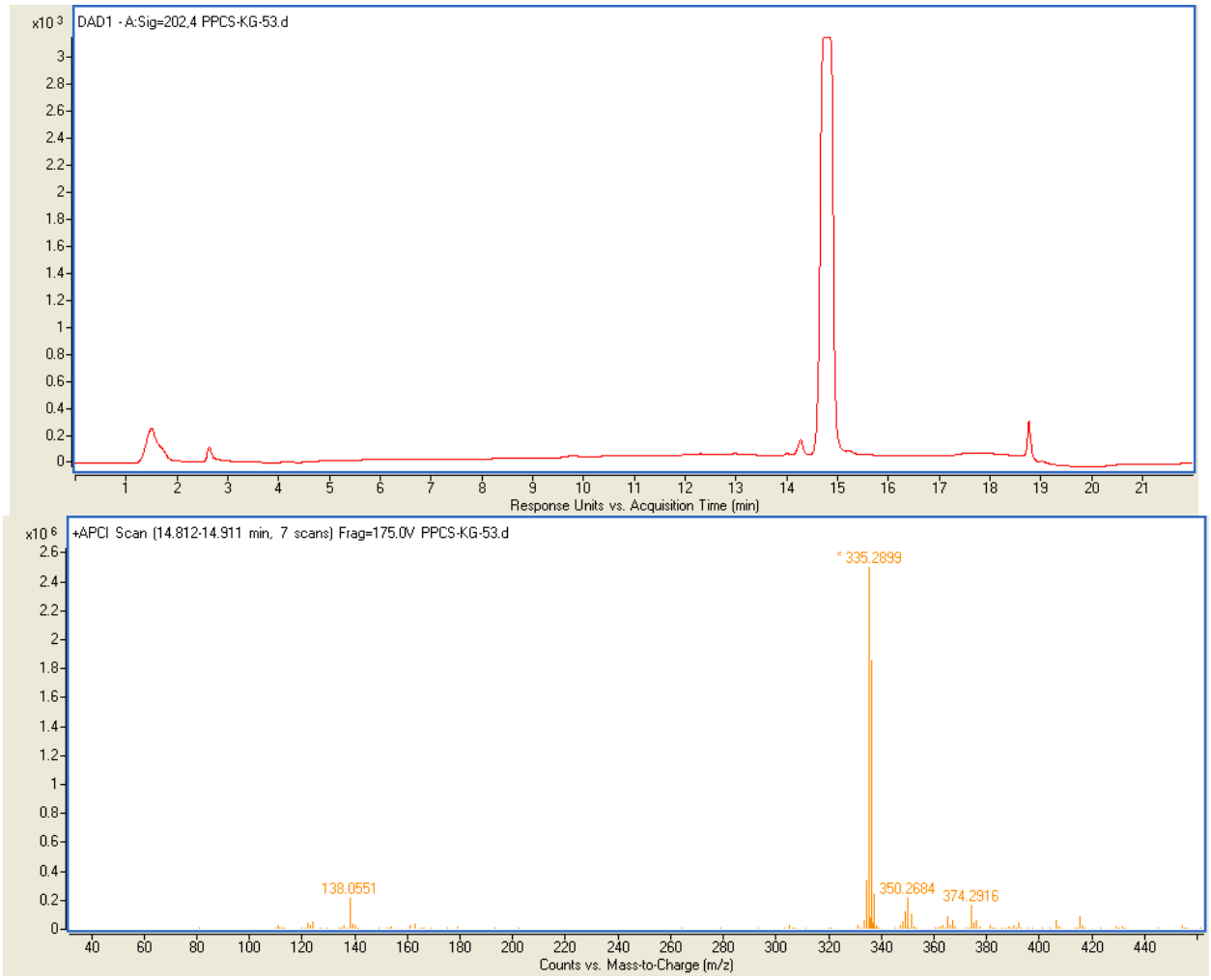
2.4.8. Bioassay guided HPLC purification of adipostatins A-B, E-J. Assays conducted by Dr. Kyle Heslip (Dotson Lab).



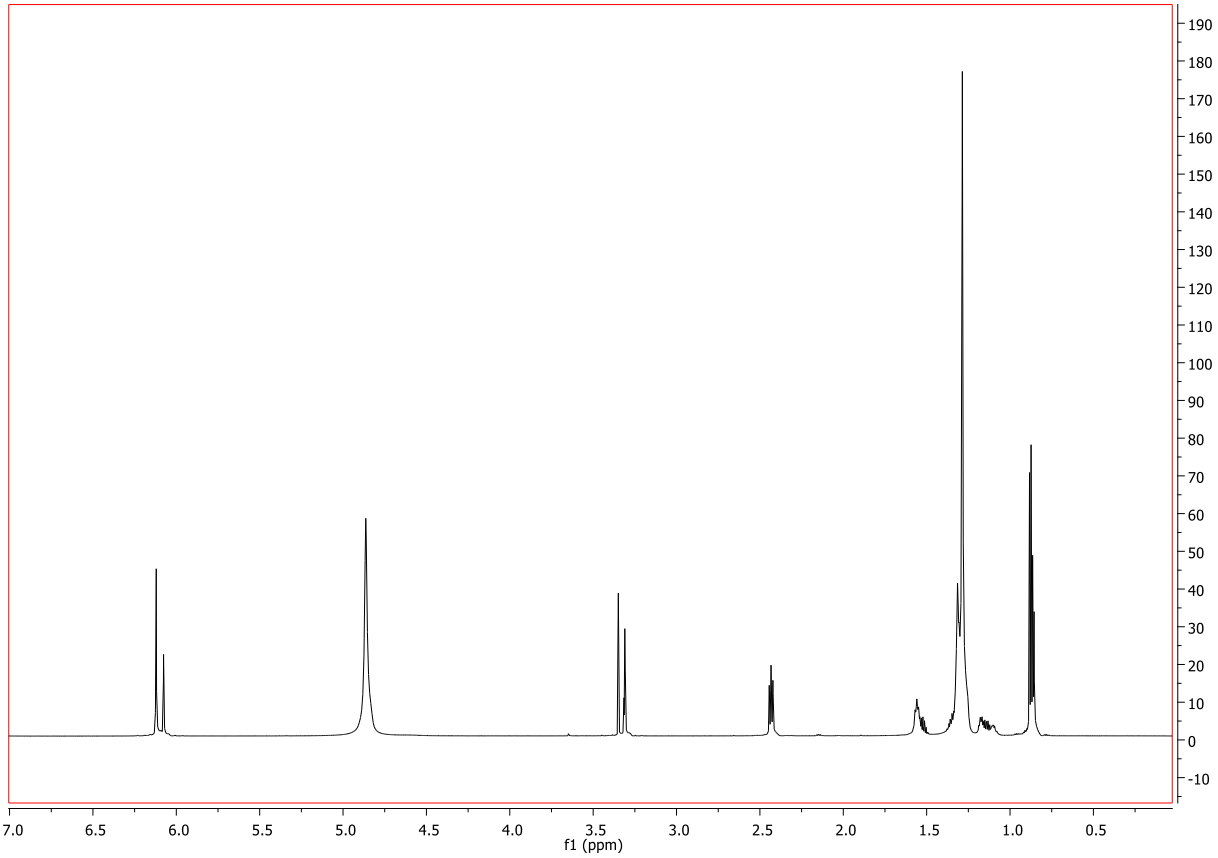


*2.4.9. HR-APCI-MS chromatogram of adipostatins E (**10**).*

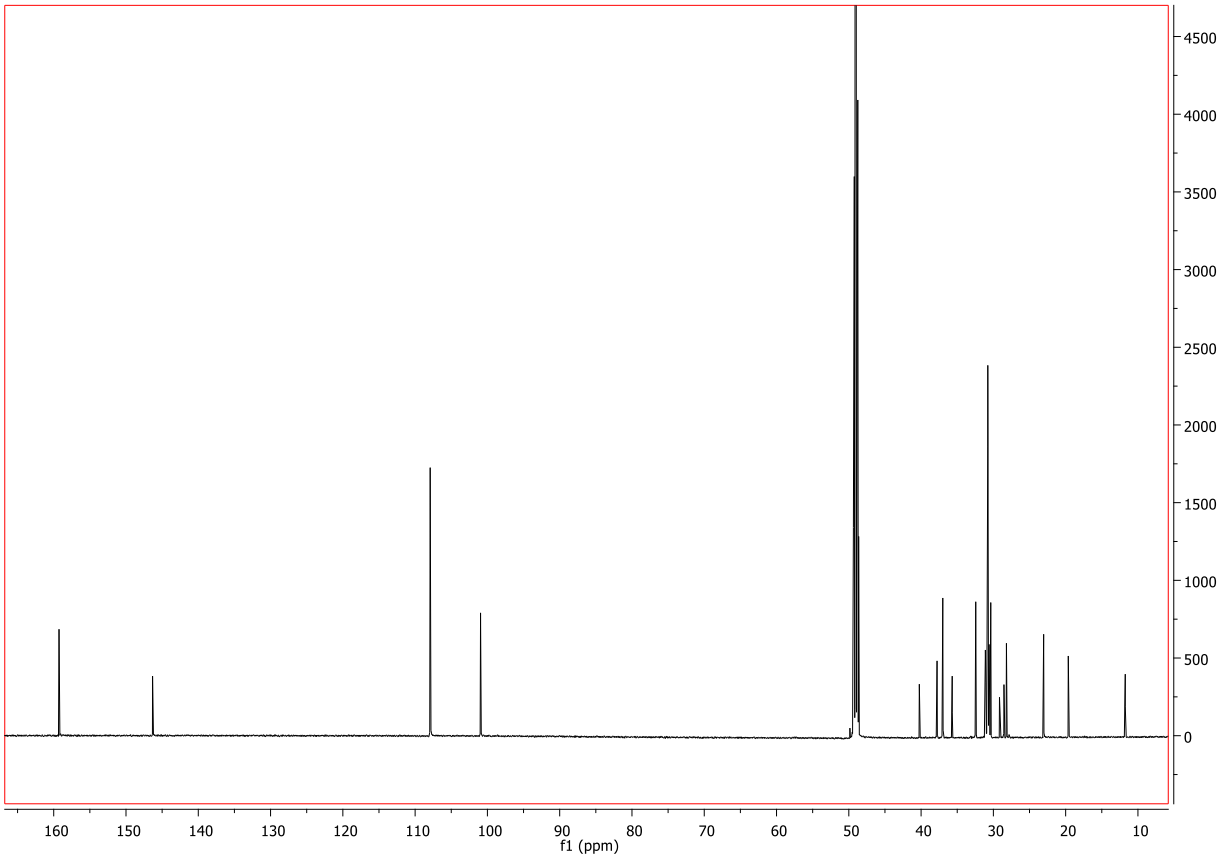
SMILES: OC1=CC(O)=CC(CCCCCCCCCCC(CC)C(C)C)=C1



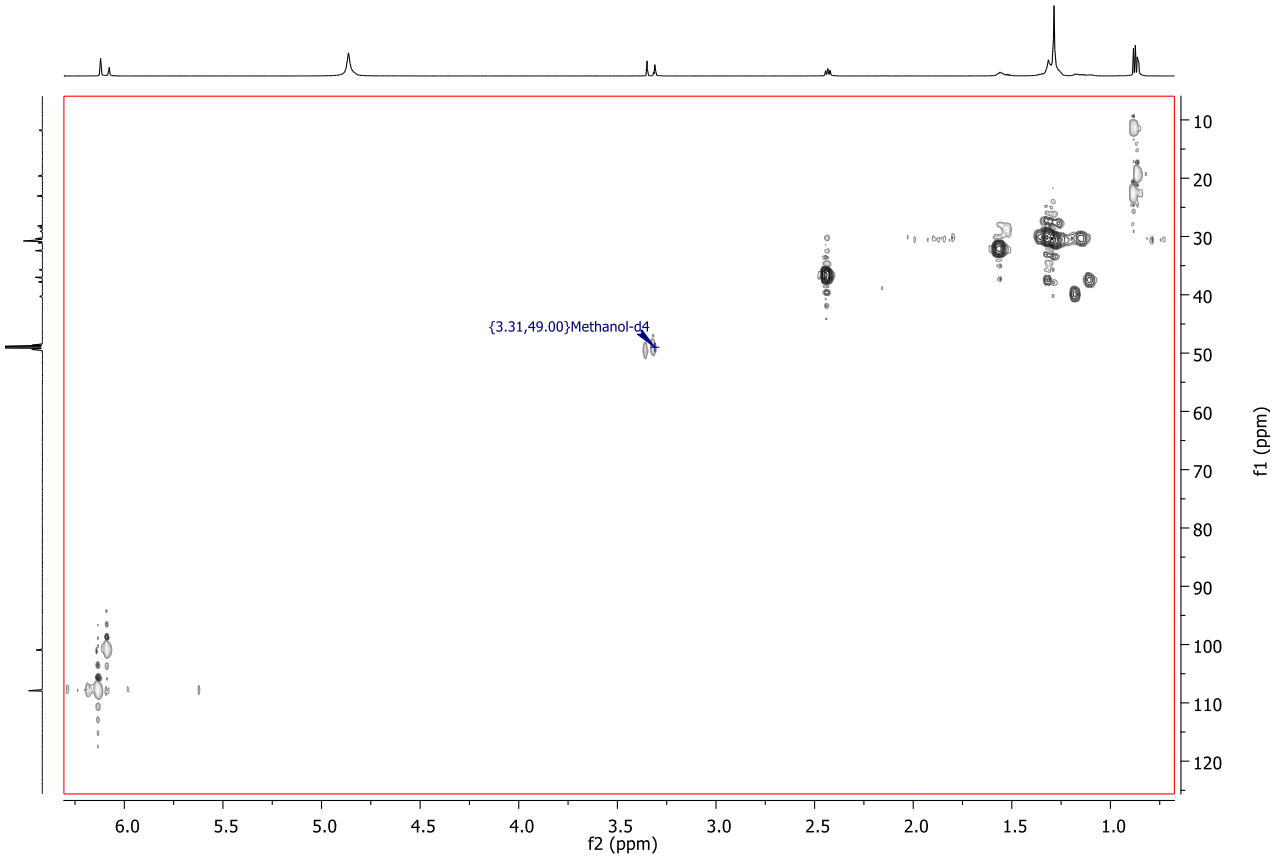
*2.4.10. ^{1}H NMR (600 MHz, CD3OD) spectrum of adipostatin E (**10**).*



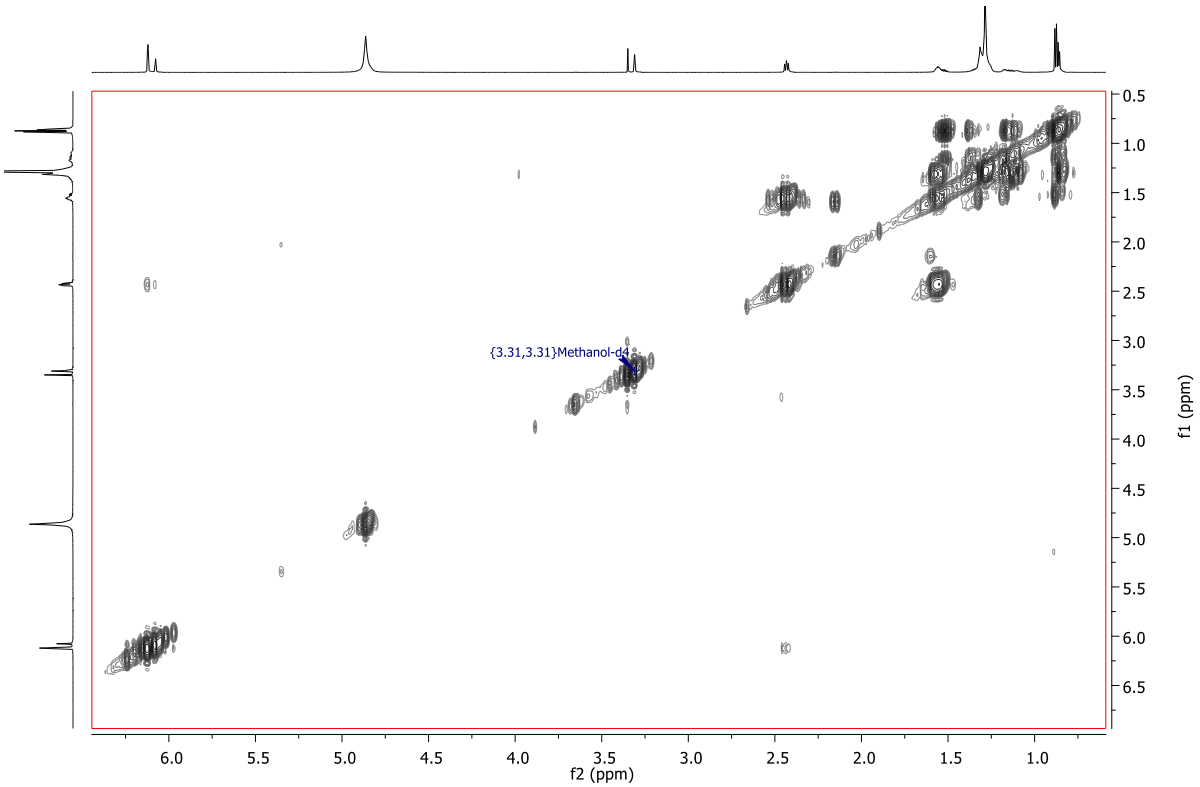
*2.4.11. ^{13}C NMR (600 MHz, CD3OD) spectrum of adipostatin E (**10**).*



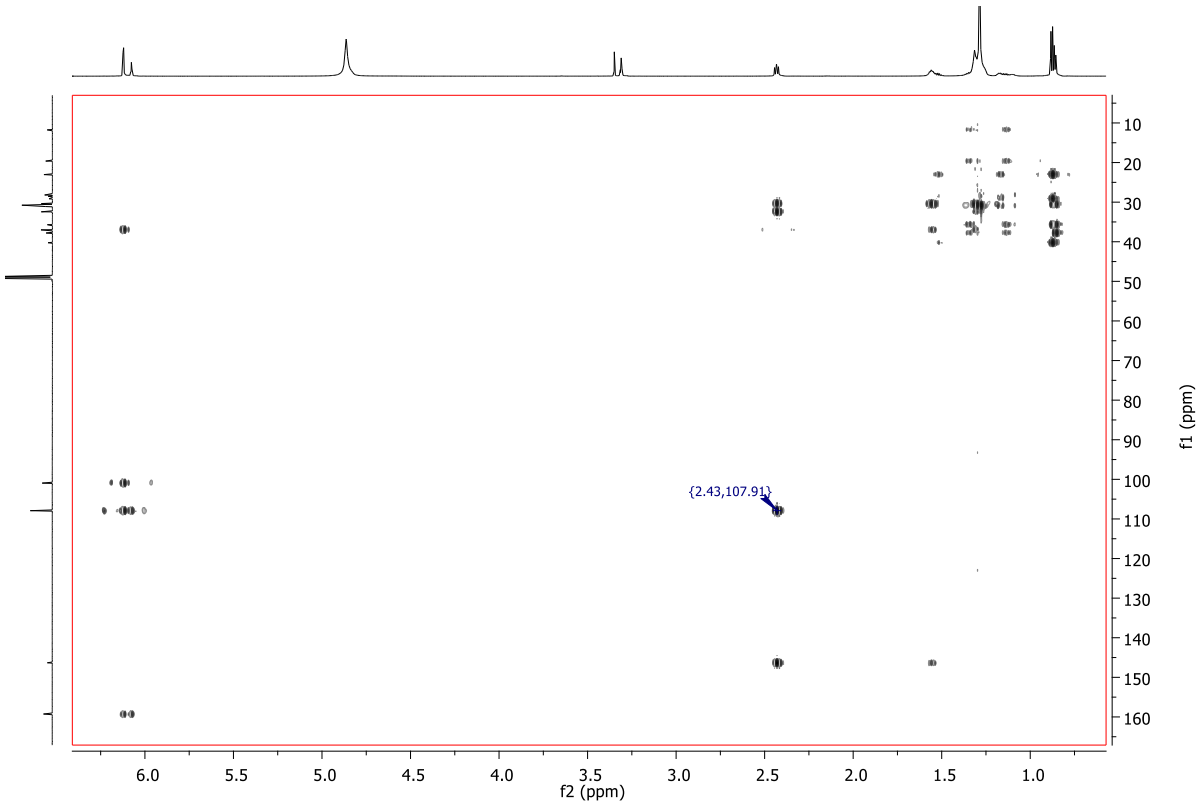
*2.4.12. gHSQCAD NMR (600 MHz, CD3OD) spectrum of adipostatin E (**10**).*



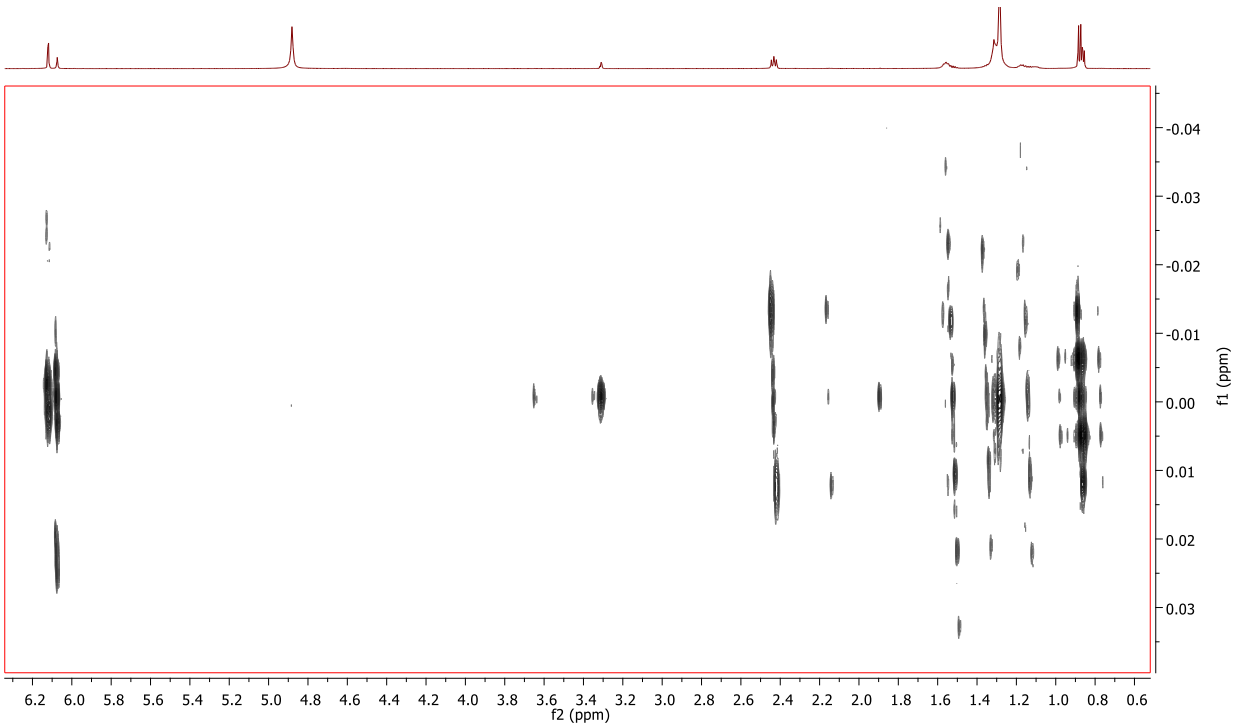
*2.4.13. gCOSY NMR (600 MHz, CD3OD) spectrum of adipostatin E (**10**).*



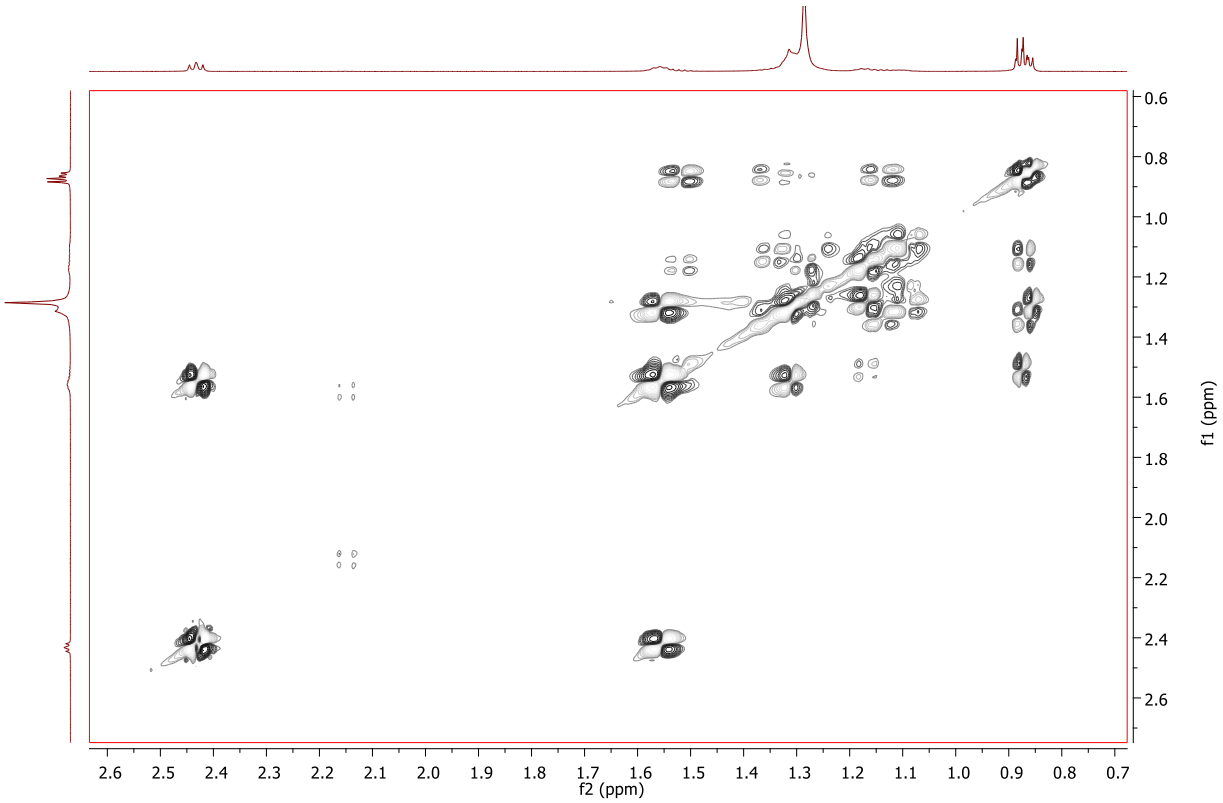
*2.4.14. gHMBCAD NMR (600 MHz, CD3OD) spectrum of adipostatin E (**10**).*



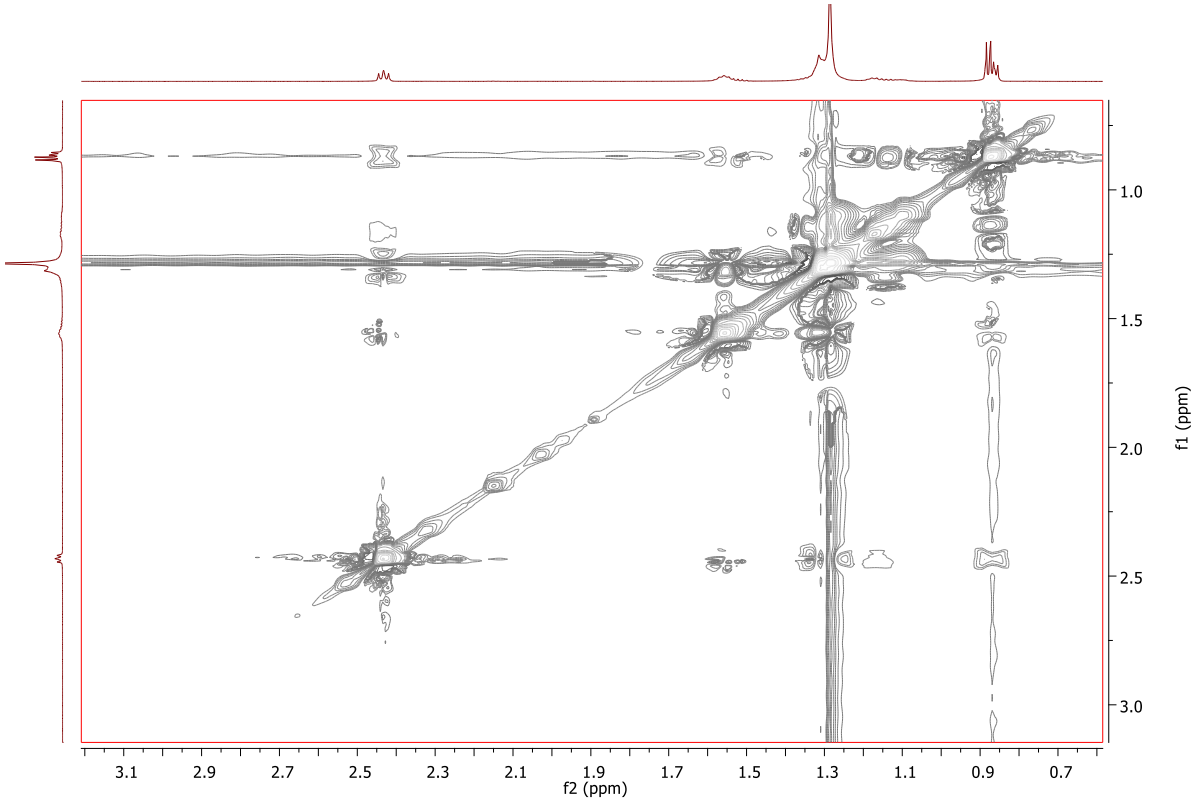
*2.4.15. HOMO2DJ NMR (600 MHz, CD3OD) spectrum of adipostatin E (**10**).*



*2.4.16. dqfCOSY NMR (600 MHz, CD3OD) spectrum of adipostatin E (**10**).*

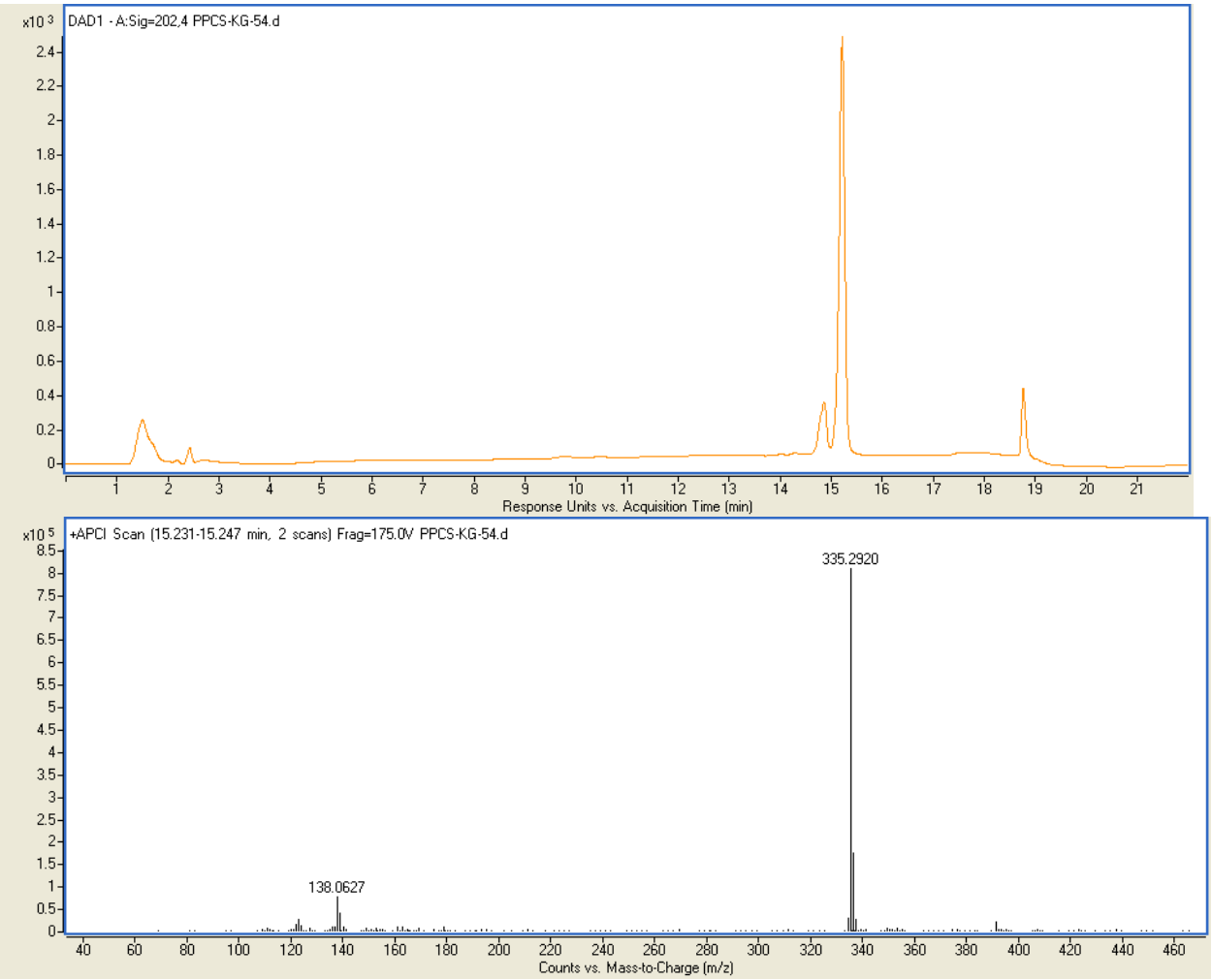


*2.4.17. ROESY NMR (600 MHz, CD3OD) spectrum of adipostatin E (**10**).*

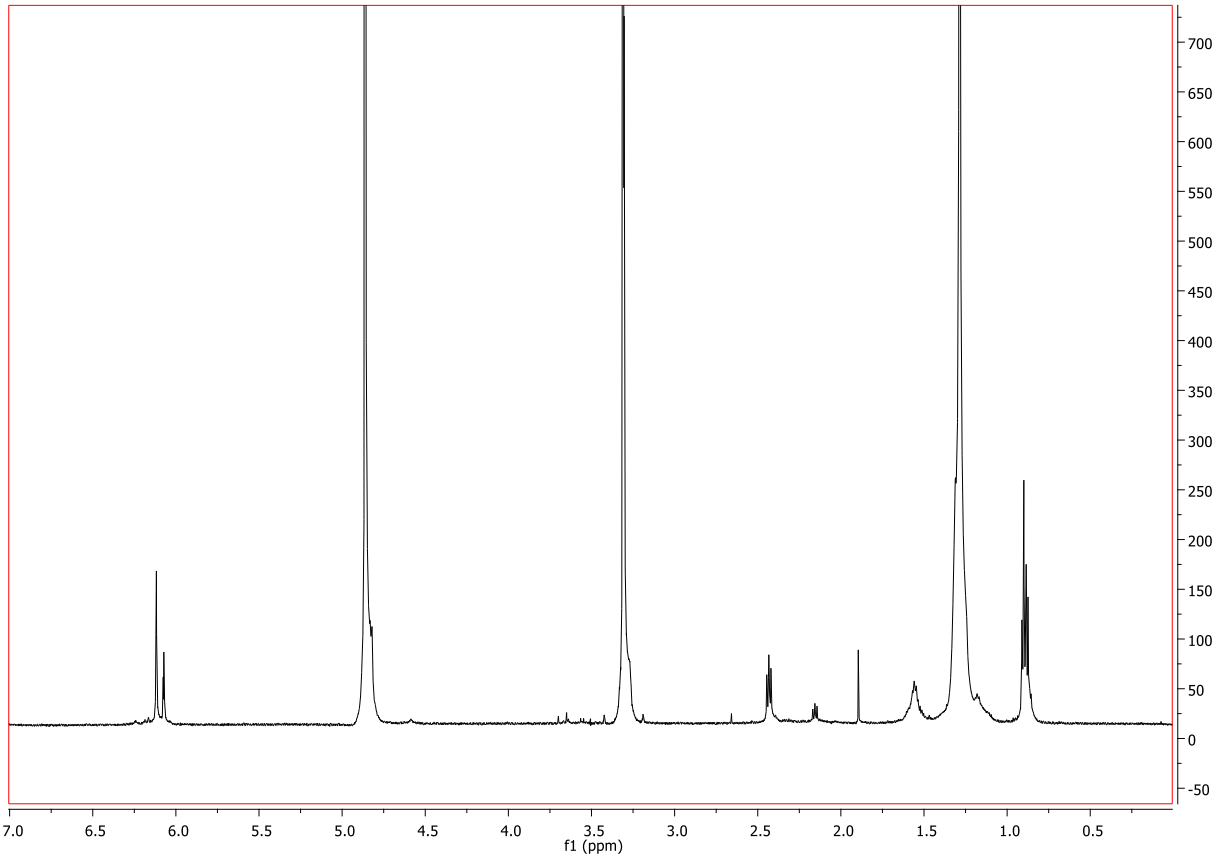


*2.4.18. HR-APCI-MS chromatogram of adipostatins F (**11**).*

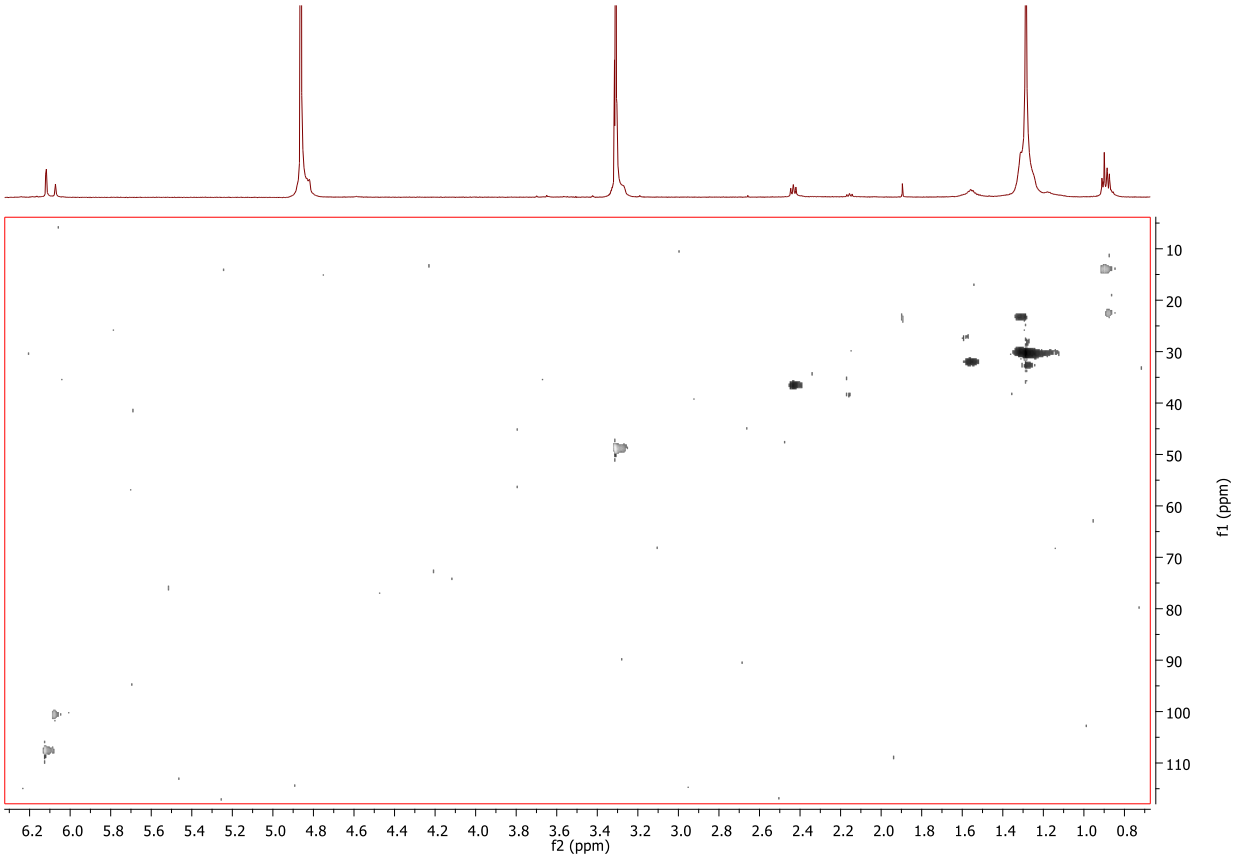
SMILES: OC1=CC(O)=CC(CCCCCCCCCCCC(C)C(C)C)=C1



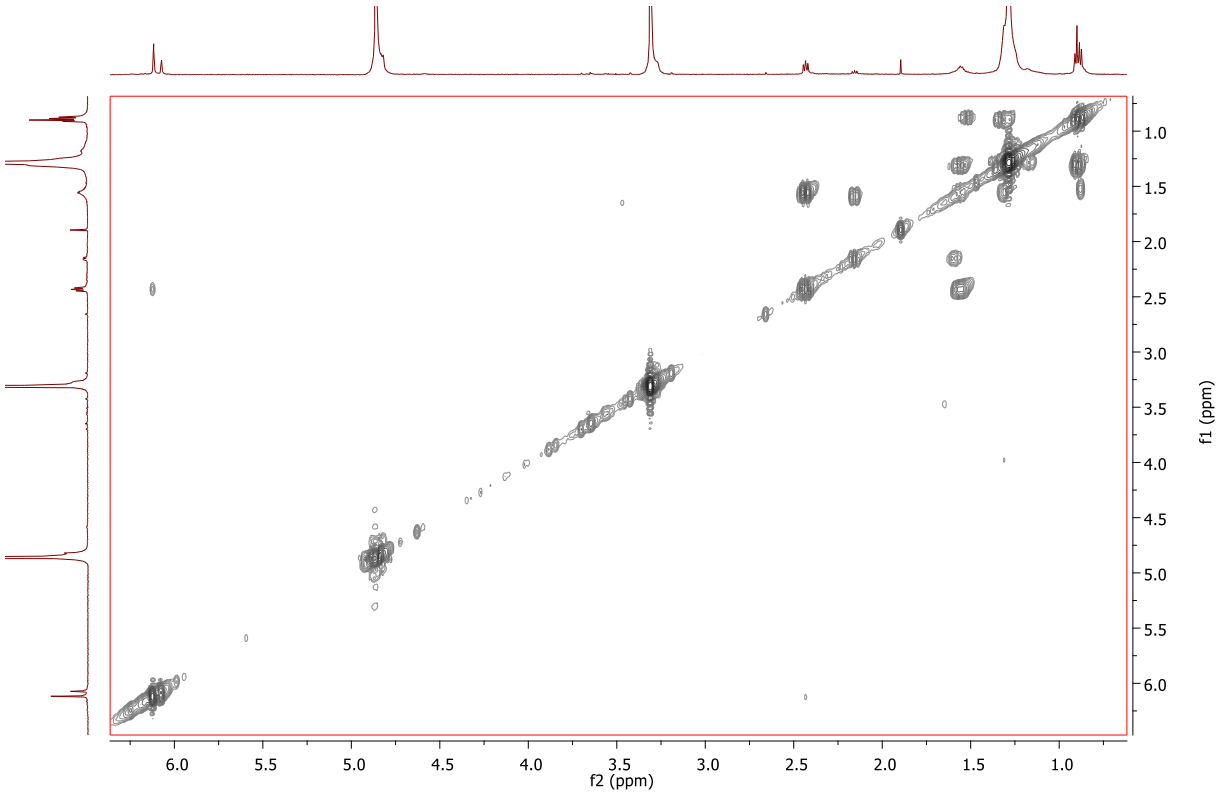
*2.4.19. ^{1}H NMR (600 MHz, CD3OD) spectrum of adipostatin F (**11**).*



*2.4.20. gHSQCAD NMR (600 MHz, CD3OD) spectrum of adipostatin F (**11**).*

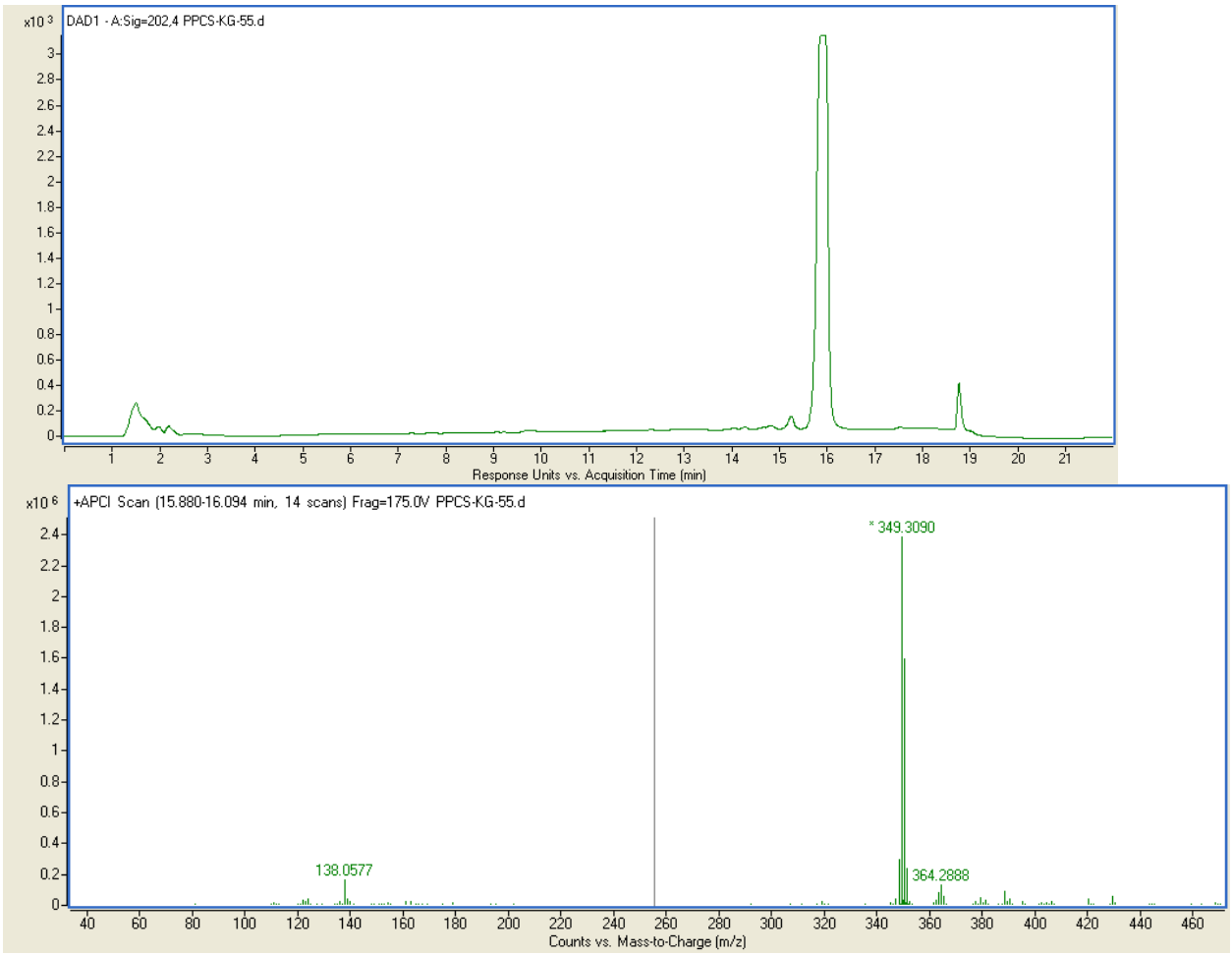


*2.4.21. gCOSY NMR (600 MHz, CD3OD) spectrum of adipostatin F (**11**).*

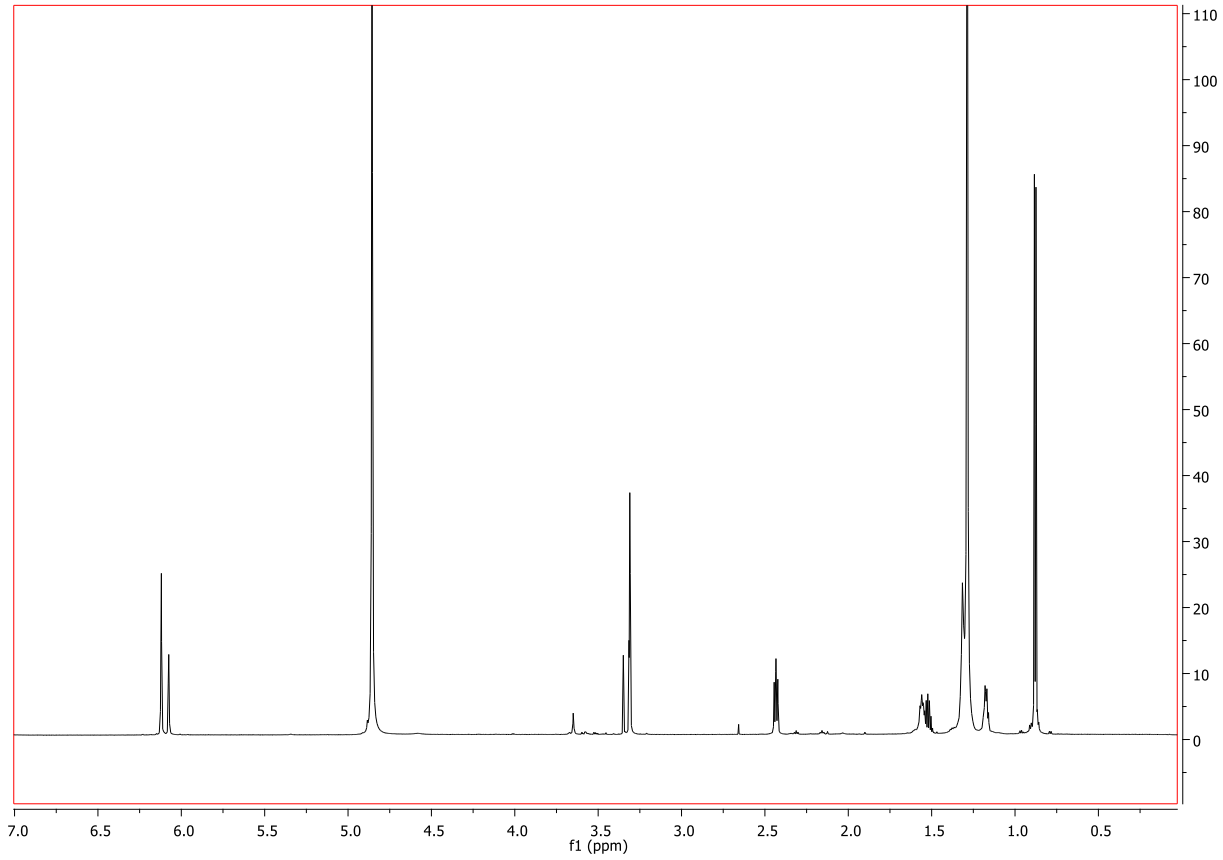


*2.4.22. HR-APCI-MS chromatogram of adipostatins G (**12**).*

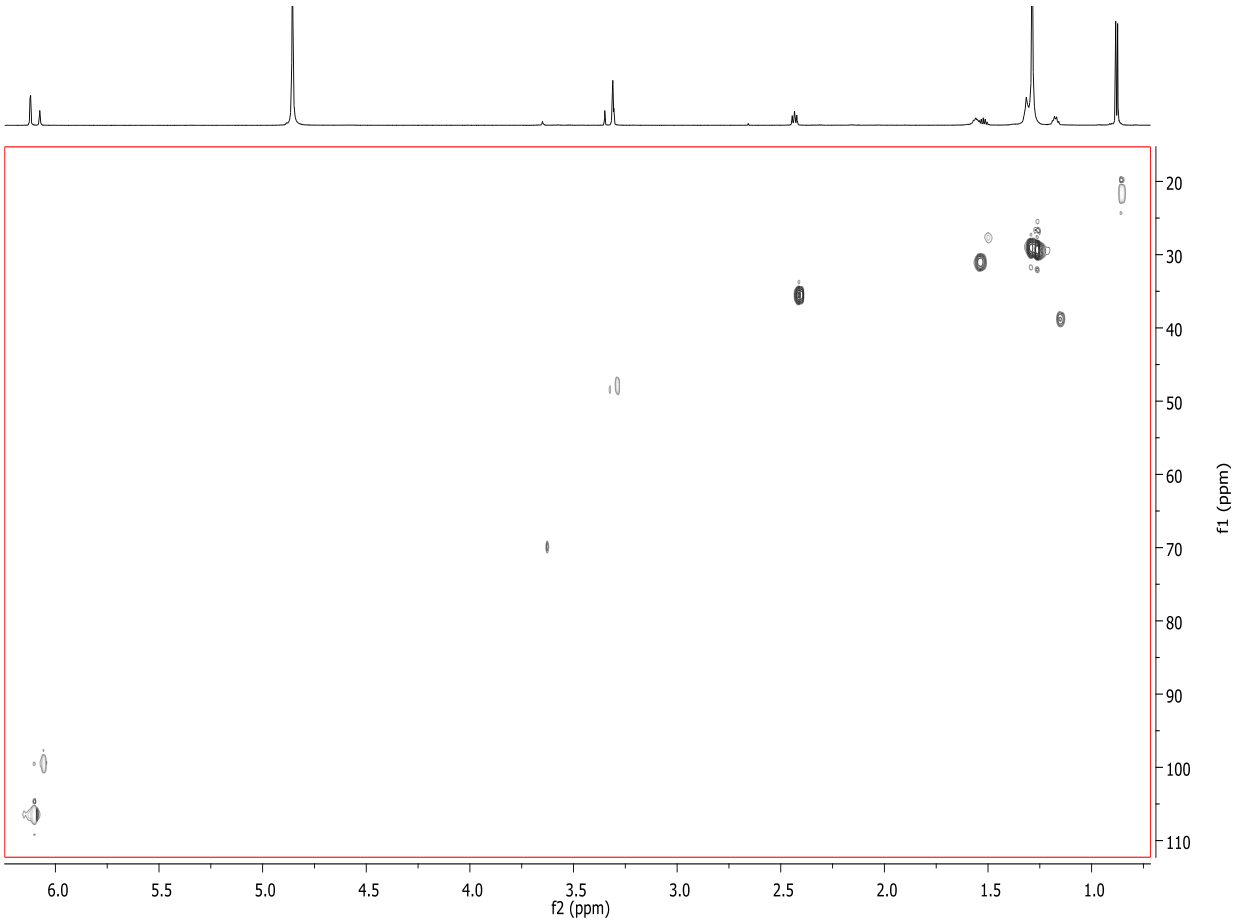
SMILES: OC1=CC(O)=CC(CCCCCCCCCCCCCCC(C)C)=C1



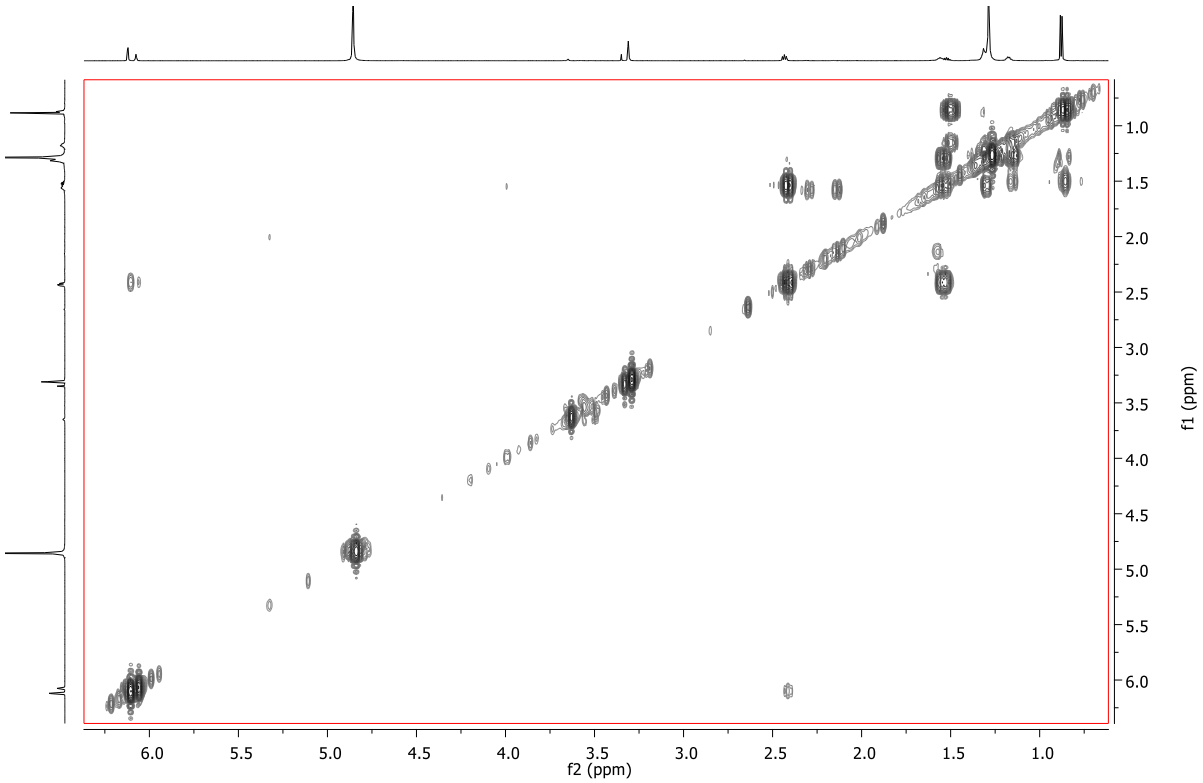
*2.4.23. ^{1}H NMR (600 MHz, CD3OD) spectrum of adipostatin G (**12**).*



*2.4.24. gHSQCAD NMR (600 MHz, CD3OD) spectrum of adipostatin G (**12**).*

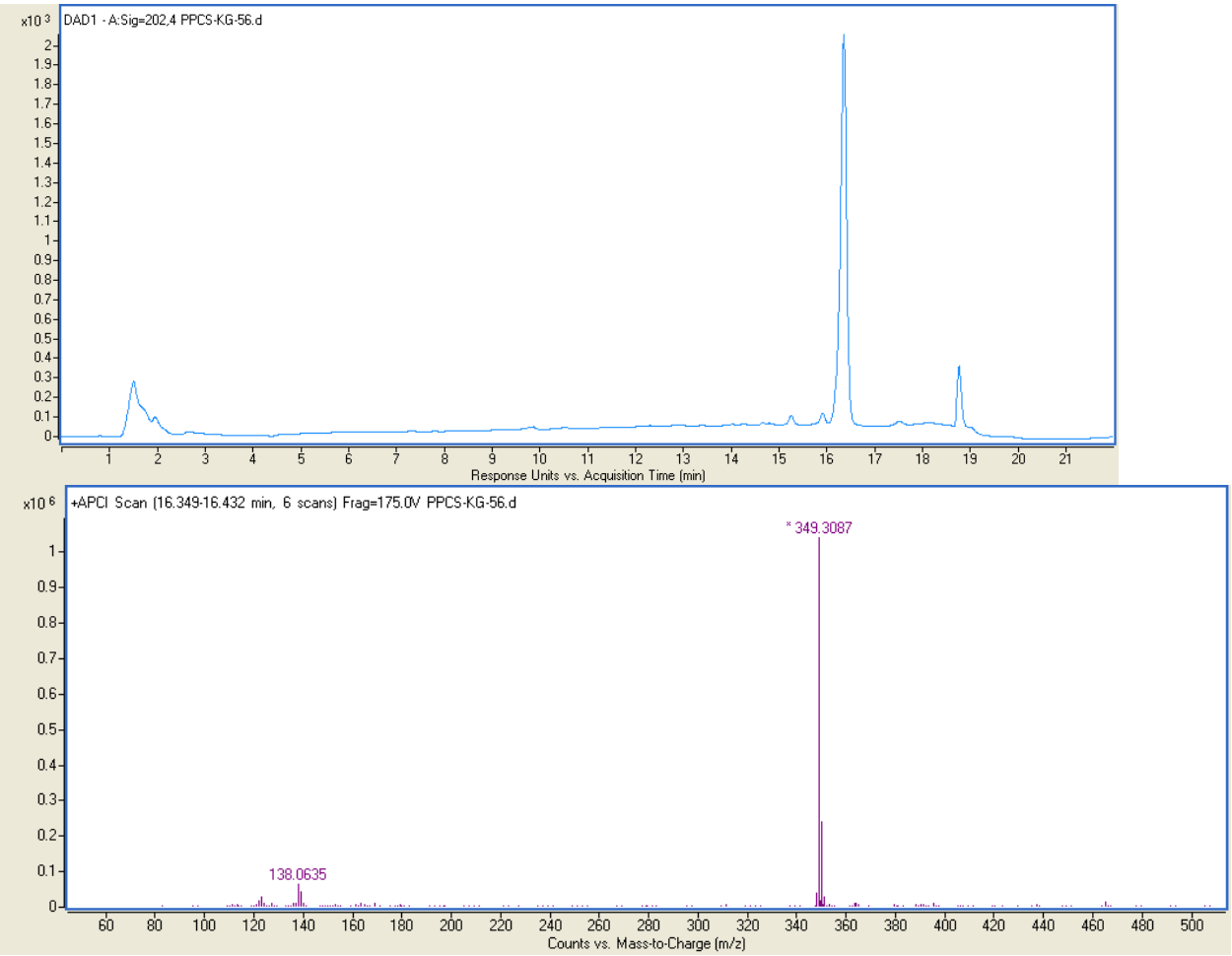


*2.4.25. gCOSY NMR (600 MHz, CD3OD) spectrum of adipostatin G (**12**).*

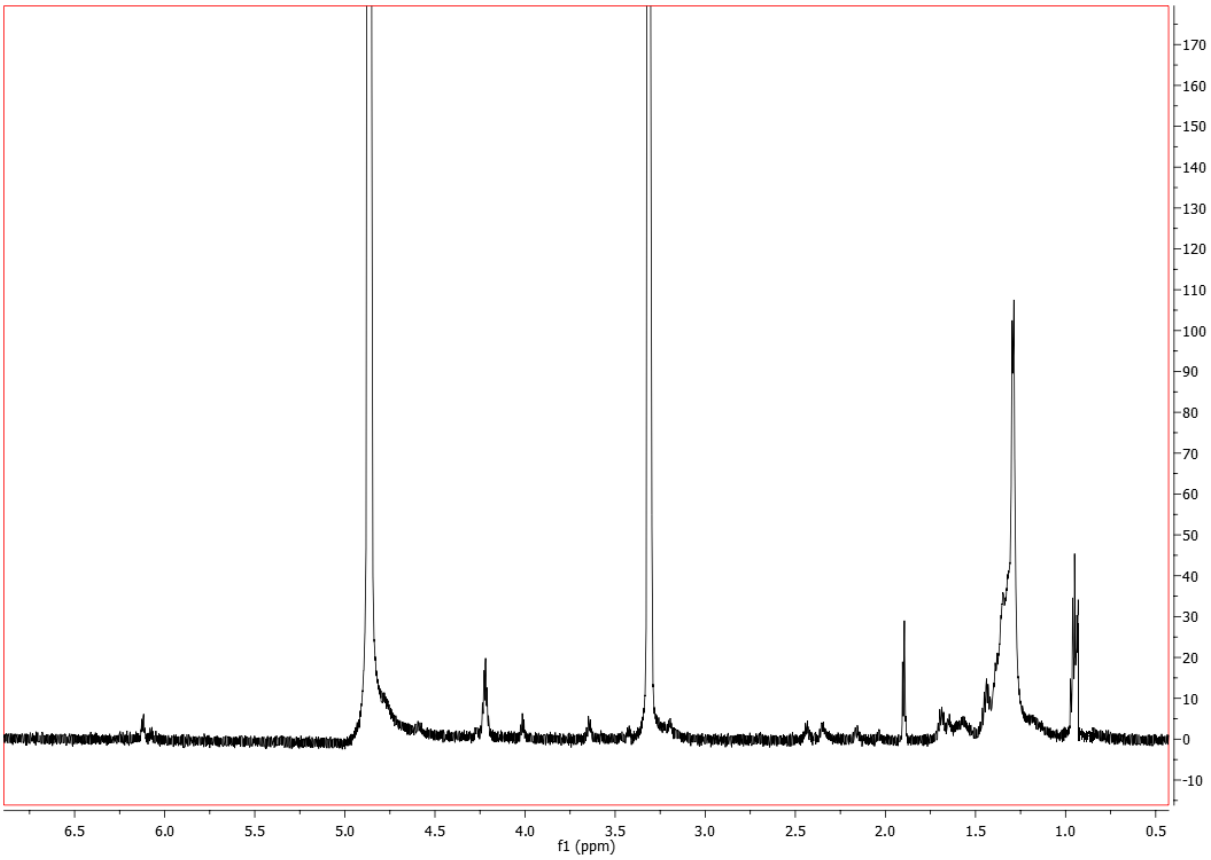


*2.4.26. HR-APCI-MS chromatogram of adipostatins H (**13**).*

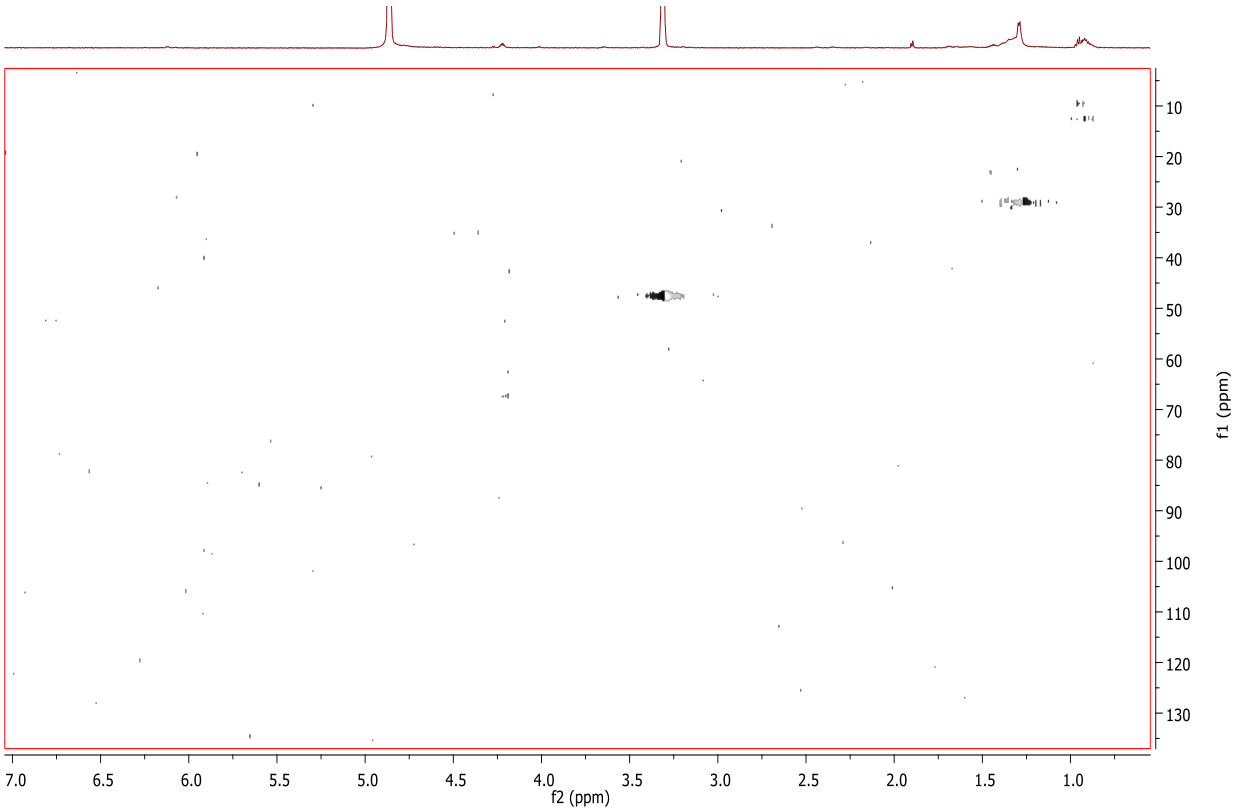
SMILES: OC1=CC(O)=CC(CCCCCCCCCCCCCCCCC)=C1



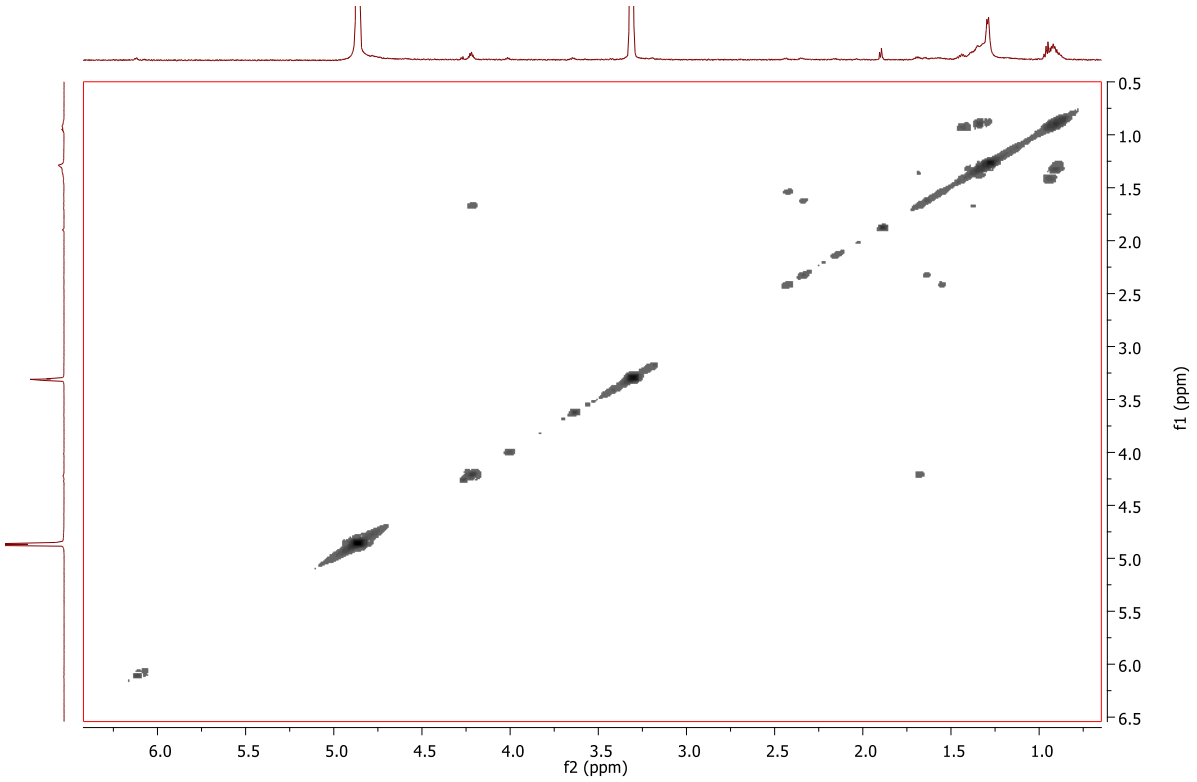
*2.4.27. ^{1}H NMR (600 MHz, CD3OD) spectrum of adipostatin H (**13**).*



*2.4.28. gHSQCAD NMR (600 MHz, CD3OD) spectrum of adipostatin H (**13**).*

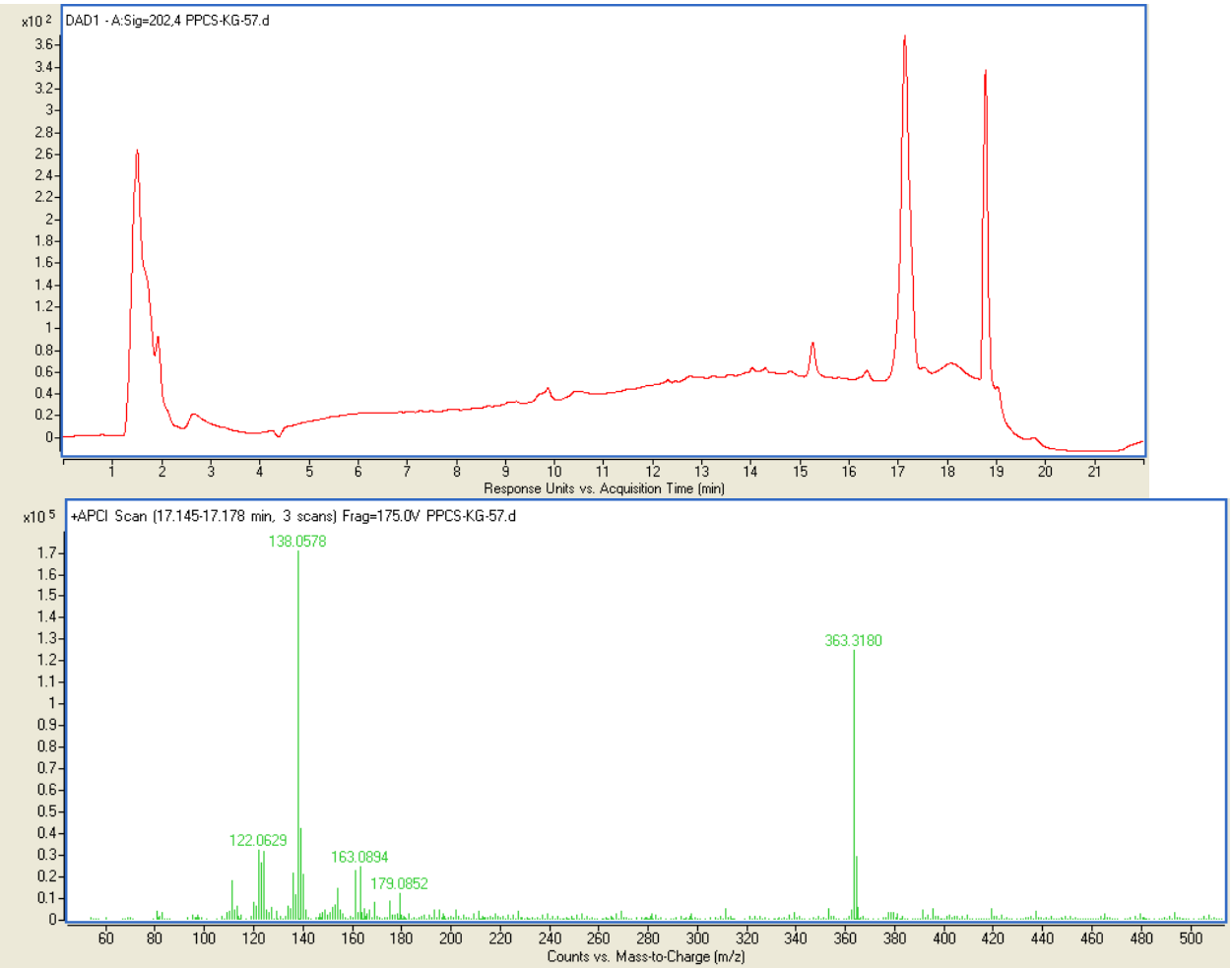


*2.4.29. gCOSY NMR (600 MHz, CD3OD) spectrum of adipostatin H (**13**).*

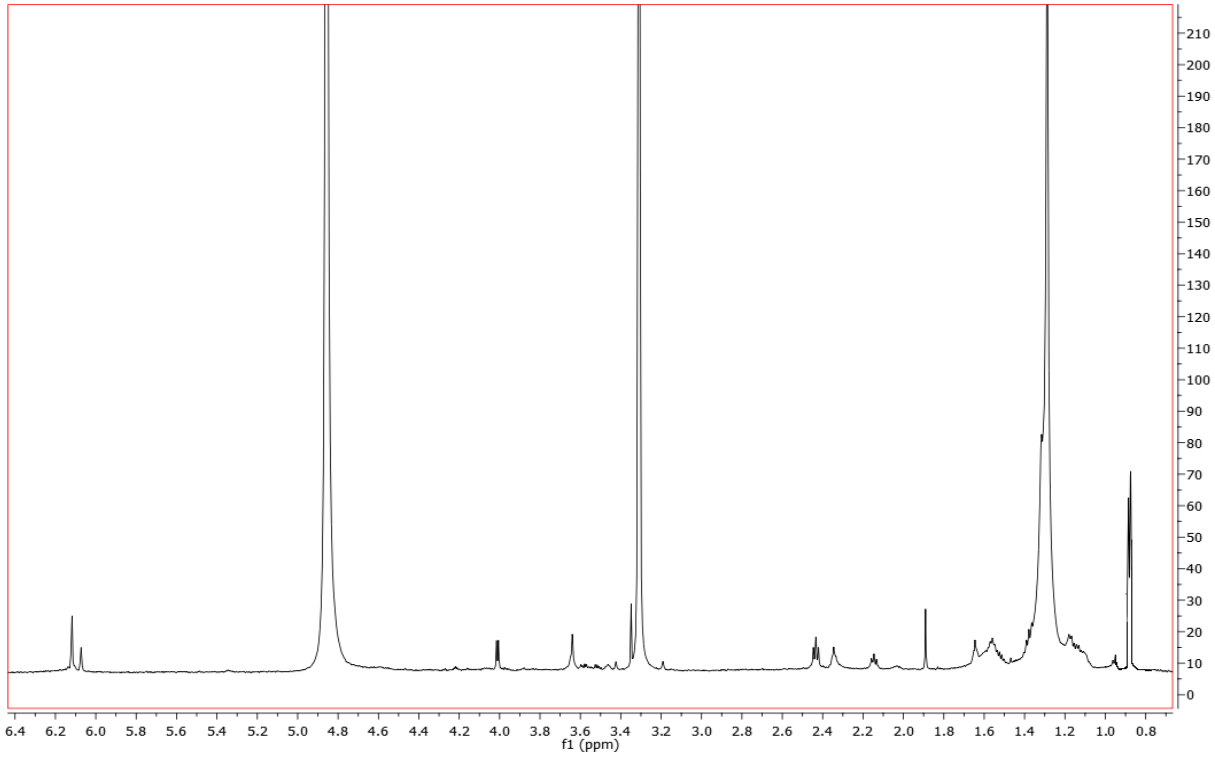


*2.4.30. HR-APCI-MS chromatogram of adipostatins I (**14**).*

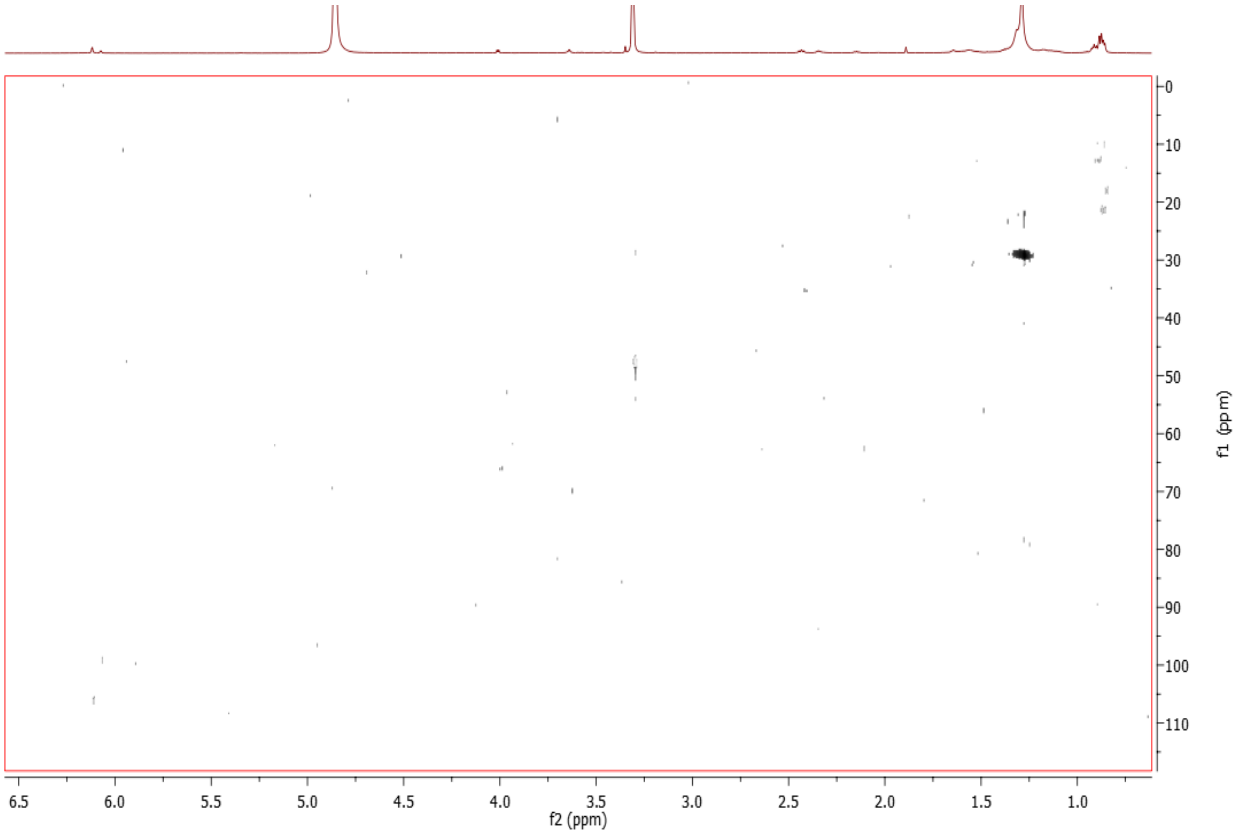
SMILES: OC1=CC(O)=CC(CCCCCCCCCCCCCCCCCCCCC)=C1



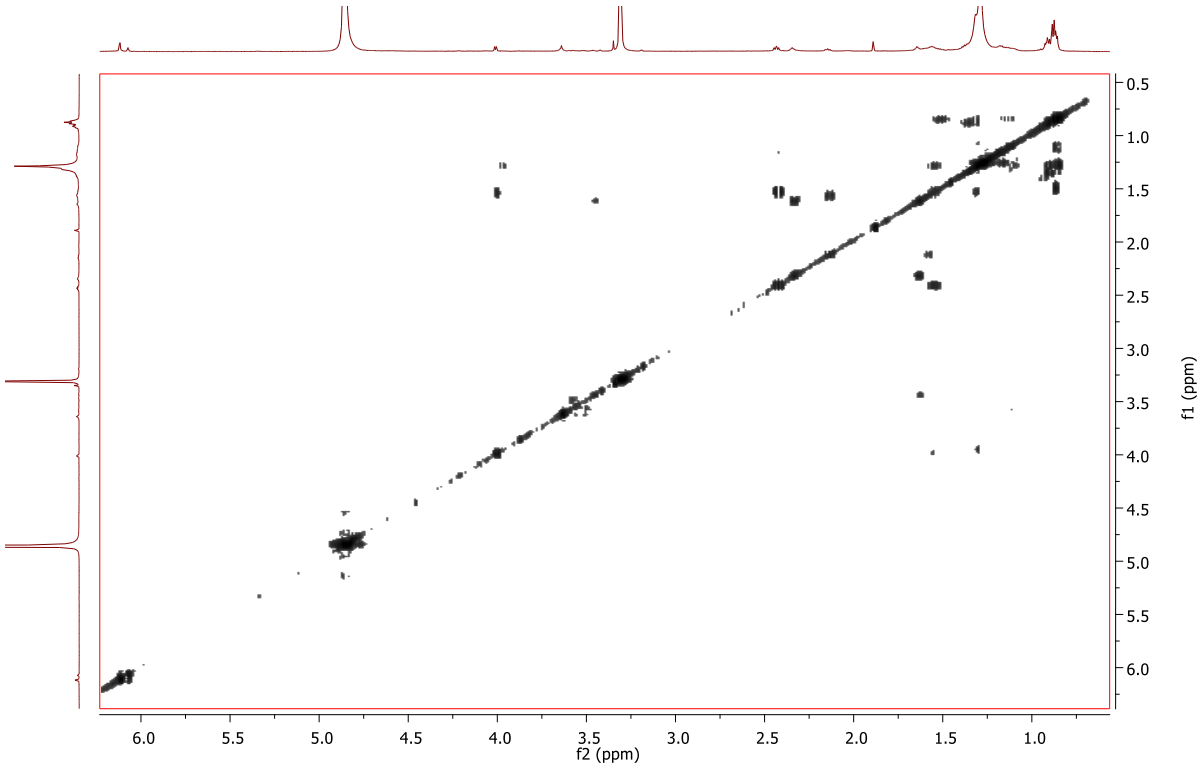
*2.4.31. ^{1}H NMR (600 MHz, CD3OD) spectrum of adipostatin I (**14**).*



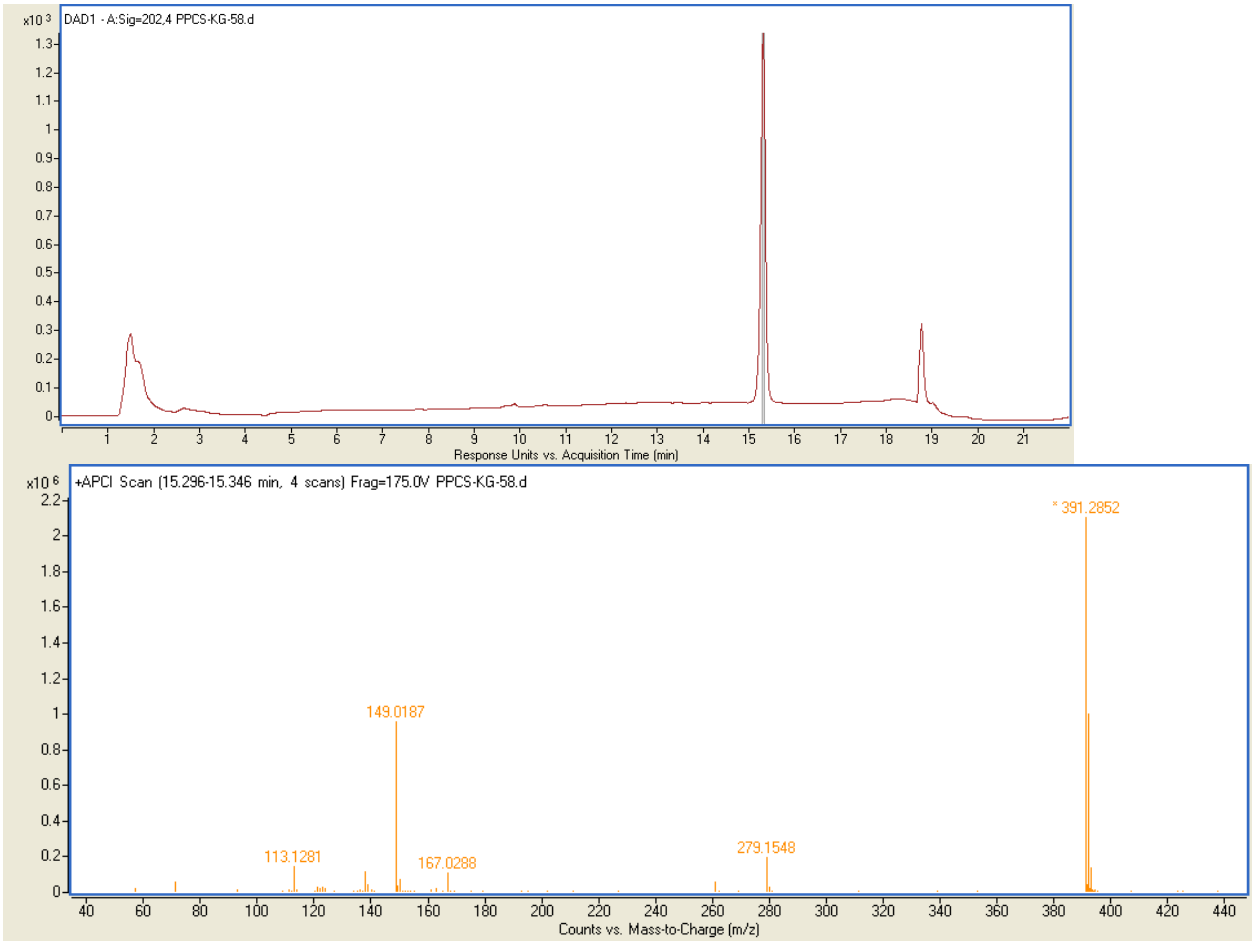
*2.4.32. gHSQCAD NMR (600 MHz, CD3OD) spectrum of adipostatin I (**14**).*



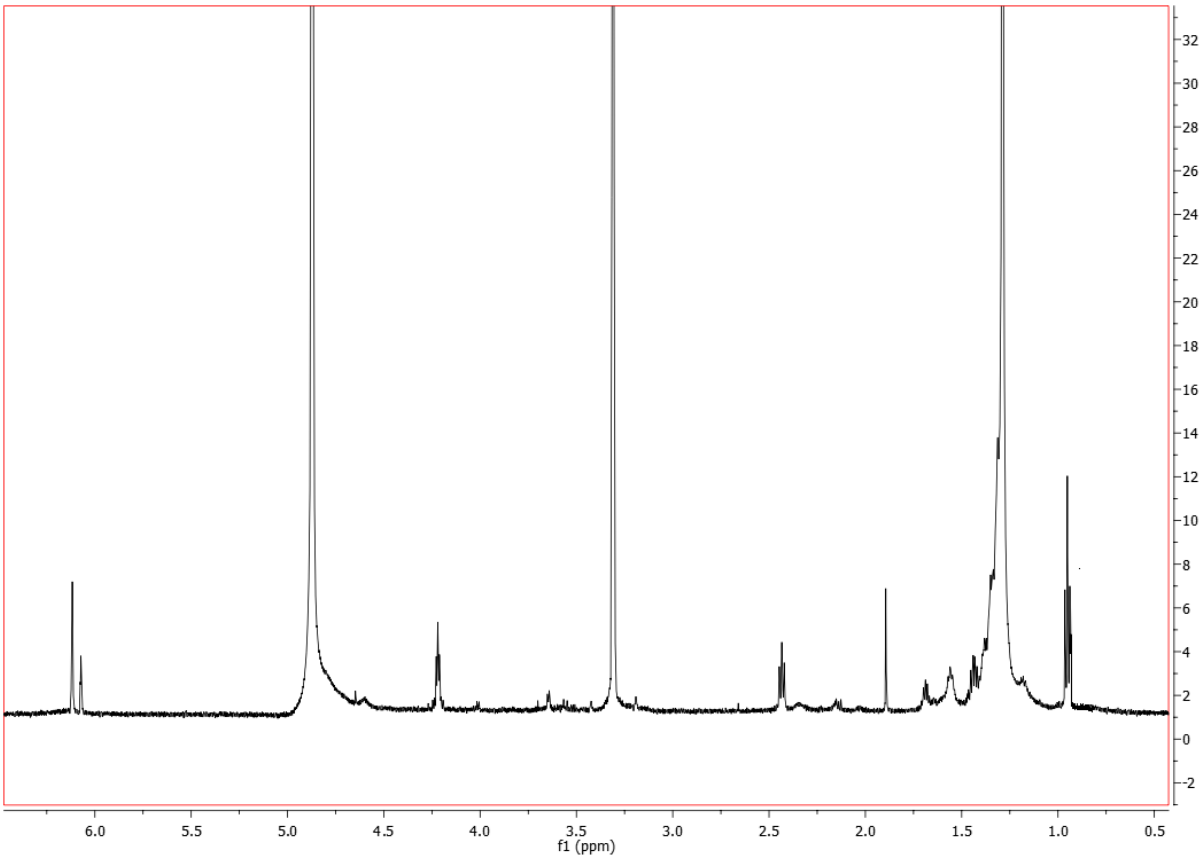
*2.4.33. gCOSY NMR (600 MHz, CD3OD) spectrum of adipostatin I (**14**).*



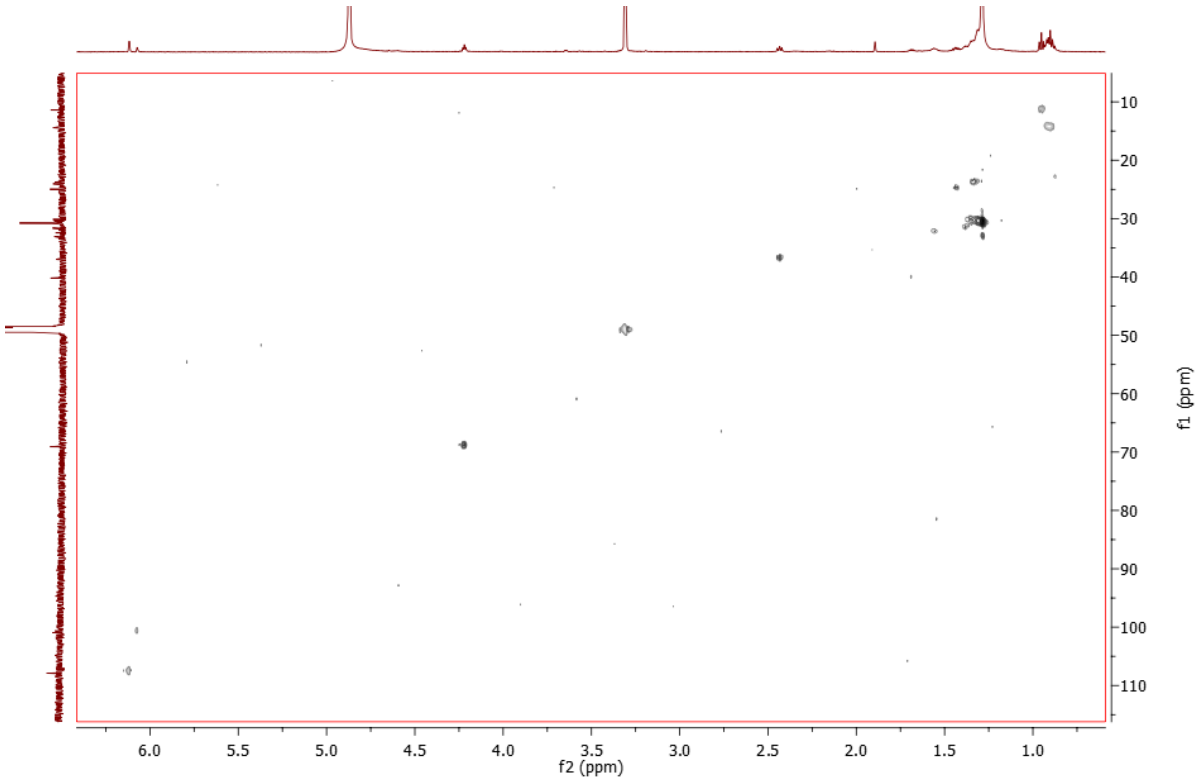
*2.4.34. HR-APCI-MS chromatogram of adipostatins J (**15**).*



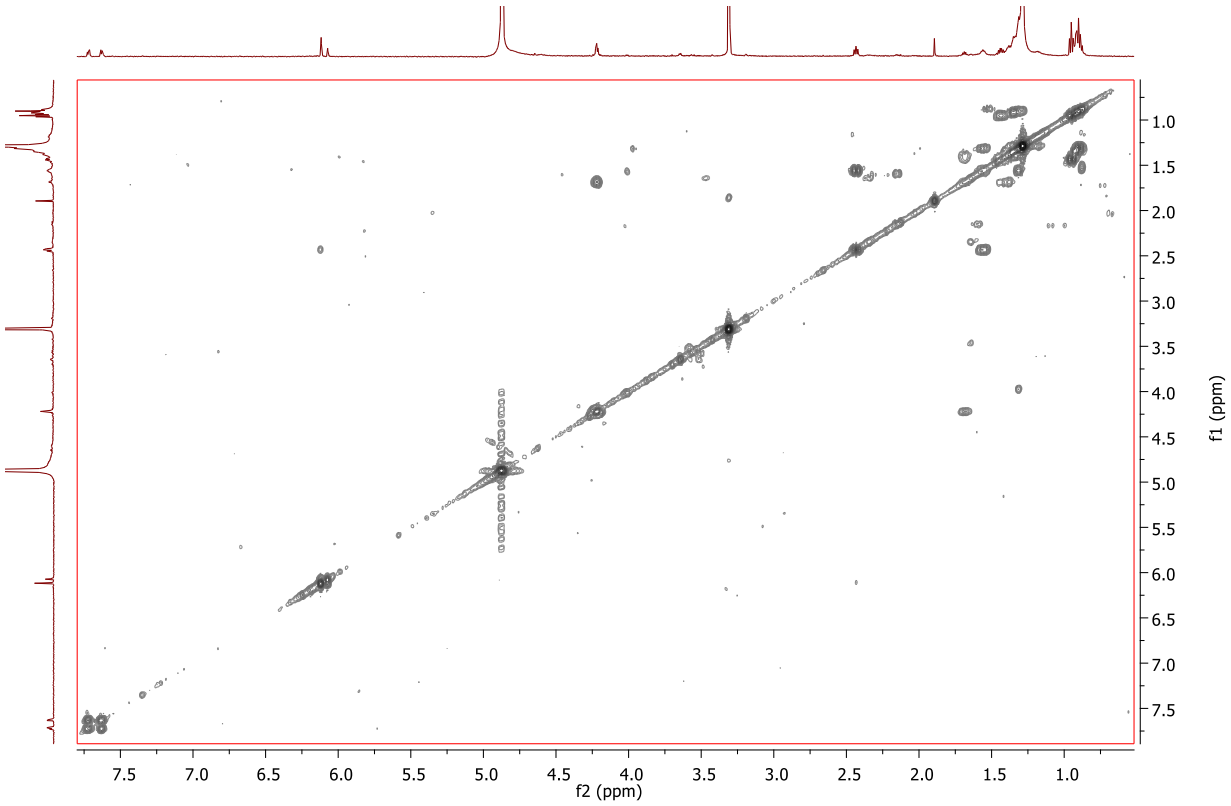
*2.4.35. ^{1}H NMR (600 MHz, CD3OD) spectrum of adipostatin J (**15**).*



*2.4.36. gHSQCAD NMR (600 MHz, CD3OD) spectrum of adipostatin J (**15**).*



*2.4.37. gCOSY NMR (600 MHz, CD3OD) spectrum of adipostatin J (**15**).*



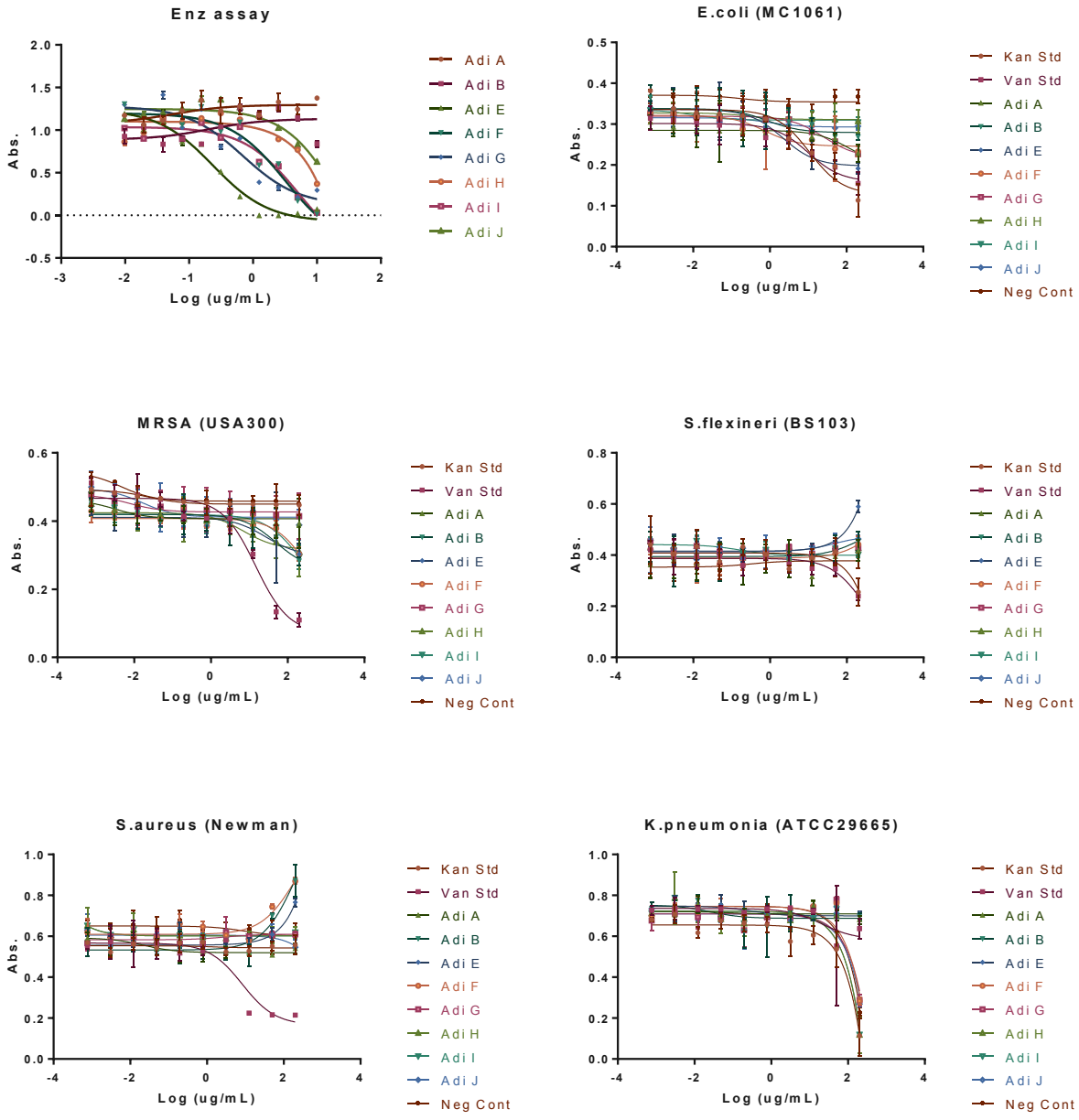
*2.4.38. Table SI 1- In vitro and microbial bioactivity (**µM**) assessment of adipostatins A-B (**6-7**) and E-J (**10-15**) against purified enzyme.*

Adipostatin A (**6**)	>300
Adipostatin B (**7**)	>300
Adipostatin E (**10**)	0.93
Adipostatin F (**11**)	7.1
Adipostatin G (**12**)	4.3
Adipostatin H (**13**)	>300
Adipostatin I (**14**)	6.62
Adipostatin J (**15**)	>300

*2.4.39. Table SI 2- In vitro and microbial bioactivity (**µM**) assessment of adipostatins A-B (**6-7**) and E-J (**10-15**) against pathogenic microbes.*

	E.coli **(MC1061)**	***E. faecalis*** **(ATCC29212)**	***B.subtilis*** **(168)**	**MRSA (USA300)**	***L.monocytogenes*** **(ATCC19115)**	***S.aureus*** **(Newman)**	***B.anthracis*** **(34f2)**	***S.enterica*** **(ATCC14028)**	***S.flexineri*** **(ATCC14028)**	***K.pneumoniae*** **(ATCC29665)**	***S.pneumoniae*** **(D39)**
6	N/A	>200	26.7	N/A	>200	N/A	46.8	N/A	N/A	N/A	>200
7	78.1	81.1	54.6	N/A	N/A	N/A	32.5	N/A	>200	>200	77.3
10	34.3	9.2	3.4	>200	5.9	N/A	15.6	N/A	>200	>200	30.2
11	50.2	13.2	11.4	N/A	34.2	N/A	26.8	N/A	N/A	>200	47.5
12	47.3	16.9	10.2	>200	20.3	N/A	20.5	N/A	N/A	>200	46.3
13	N/A	N/A	N/A	N/A	N/A	N/A	N/A	N/A	N/A	N/A	>200
14	70.2	15.3	14.5	>200	N/A	N/A	>200	N/A	N/A	>200	70
15	>200	N/A	>200	N/A	N/A	N/A	N/A	N/A	N/A	N/A	>200

2.4.40 In vitro enzymatic assay and antimicrobial evaluation of adipostatins against select pathogenic microbes showing no appreciable bioactivity.



2.5 Materials and Methods

2.5.1 General Experimental Procedures

Spectrophotometric assays were performed on Molecular Devices SpectraMax M5 384 variable wavelength spectrometer. All NMR spectra were acquired on a Varian INOVA 500 MHz and a Varian INOVA 700 MHz spectrometer at the NMR Facility, Department of Chemistry, University of Michigan. High-resolution APCIMS spectra were measured at the University of Michigan core facility in the Department of Chemistry using an Agilent 6520 QTOF mass spectrometer equipped with an Agilent 1290 HPLC system. RP-HPLC was performed using Luna 5 µm Phenyl-Hexyl 250 x 10 mm column in a solvent system of ACN and H2O. The LCMS analysis of HPLC fractions was performed on a Shimadzu 2010 EV APCI spectrometer using ZORBAX Extend 80Å C18, 4.6 x 100 mm, 3.5 µm HPLC column.

2.5.2 Biological Material

Streptomyces blancoensis (Strain # 20733-1) was isolated from marine sediments collected near Cabo Blanco, Costa Rica (collection permit R-CM-INBio-30- 2007). The procedure for the isolation of actinomycetes from these samples was previously described by Magarvey et al.[23] Maintenance and propagation of cultures were performed using standard media and protocols where 500 mg of wet sediment was diluted in 10 mL of sterile water and vortexed for 10 min. Then, 1 mL of this suspension was applied directly to the top of the discontinuous sucrose gradient and centrifuged for 30 minutes at 300 x g. 500 µL of the 20%, 30%, and 40% layers were then plated to HVA agar supplemented with 10 µg/mL chlortetracycline, 25 µg/mL cyclohexamide, and 25 µg/mL of nalidixic acid. The plates were then incubated at 28 °C for one month. The colony was picked off the plate and streaked onto ISP2 agar until pure. Seed cultures were grown in 17 mL dual position cap tubes containing 2 mL of ISP2 and grown for 4 days on a rotary shaker at 200 rpm. The seed culture was then poured into a 250 mL baffled flask containing 100 mL of ISP2 and grown for 18 days on a rotary shaker at 200 rpm. The culture was centrifuged at 4000 rpm for 10 min to remove the cells and 2 g of XAD16 resin (Sigma-Aldrich, St. Louis, Mo.) contained within a polypropylene mesh bag was added to the broth and incubated overnight on the rotary shaker. The resin bag was removed and placed into 10 ml of MeOH followed by 10 ml of acetone and 10 ml of ethyl acetate. Each of the three fractions was dried *in vacuo* and reconstituted to a final concentration of 15 mg/mL in DMSO.

2.5.3 Culture Maintenance and Fermentation

Seed cultures of 100 mL (×5) of ISP2 media (1% malt extract, 0.4% yeast extract, 0.4% dextrose, 3% NaCl) were inoculated with a loopful of vegetative cells from an oatmeal plate (6% oat meal, 1.25% agar, 3% NaCl) culture of *Streptomyces blancoensis* and incubated with shaking (200 rpm) at 28 ^{o}C for 5 days. A 25 mL portion of the seed cultures were transferred to a 2.8 L Fernbach flask containing 1.5L of the ISP2 medium, and the 30L fermentation was carried out on a rotary shaker (200 rpm) at 28 °C for 11 days. After 11 days of growth, the cultures were harvested by centrifugation. The resulting cell free broth was subjected to solid phase extraction using 15 g of Amberlite XAD-16. The resin was then separated by filtration and subjected to organic extraction using MeOH:EtOAc (1:1).

2.5.4 Isolation and Purification of Adipostatin E-J (10-15)

The organic extracts concentrated under vacuum to afford the crude extracts (~9 g) obtained from 20 L culture. The crude extracts were dissolved in 100 mL of H2O and were subjected to a C18-silica gel column (20 × 2.6 cm, YMC Gel ODS-A, 12 nm, S-150 μm). The C18 column was eluted with a stepwise gradient of H_2O/ACN (100:0 → 0:100) to give eight fractions (Fr.1−Fr.8), which were then concentrated in vacuo. All eight fractions were assayed in the developed in vitro enzymatic assay at 10 and 1.0 ppm. The bio-active Fr.6 was further purified by RP-HPLC on isocratic conditions of 71% ACN for 50 minutes at a flow rate of 3 mL/min. This was followed by UV/vis photodiode array detection at 210 nm to yield pure compounds **6** (2.8 mg), **7** (2.5 mg), **10** (1.8 mg), **11** (0.7 mg), **12** (0.5 mg), **13** (0.6 mg), **14** (1.3 mg) and **15** (0.6 mg).

2.5.5 Gene Cloning, Expression, and Purification of Streptococcus pneumoniae PPCS [25]

Using PCR, the coaB gene was amplified from *S. pneumoniae* TIGR4 genomic DNA. The forward primer CATATGAAAATTTTAGTTACATC and the reverse primer CTCGAGAGAATGATAGGCTTGAATTTTTTC were utilized to introduce NdeI site before and XhoI site after the gene. The product from PCR amplification was digested with NdeI and XhoI, and afterwards ligated into pET23a(+) (Novagen), also digested with NdeI and XhoI. To confirm the coaB gene was inserted the DNA was sequenced and the plasmid was designated pUMJY140h. Because the reverse primer was designed to exclude the stop codon of the gene, the linker and hexa-histidine tag encoded by the pET23a(+) vector is expressed with the gene to generate the C-terminal hexa-histidine tagged PPCS.

E. coli strain BL21 AI was transformed with the pUMJY140h plasmid and later incubated in four 1 L flasks containing 250 mL each of LB-ampicillin media at 37ºC and 250 rpm until reaching an OD600 of 0.6-0.8. The culture was then cooled to 16ºC and induced with L-arabinose (0.065% w/v final concentration); culture was incubated at 16ºC and 250 rpm shaking was continued for 16 hours. Cells were harvested from 1 L of culture via centrifugation at 6,000 x g, washed with 20 mM HEPES pH 8.0, and resuspended in 60 mL of 20 mM HEPES pH 8.0. The harvested cells were lysed via French Press, and the lysed mixture was centrifuged at 20,000 x g for 30 minutes to spin down the cellular debris as the pellet.

The resulting supernatant was shaken gently with Ni-NTA resin (4 mL per 1 L culture) in a solution of 10 mM imidazole and 20 mM HEPES pH 8.0 for 10 minutes. Afterwards, the mixture was poured into a 20 mL column and the resin was washed with 5 column volumes of 50 mM imidazole, 20 mM HEPES pH 8.0, followed by 5 column volumes of 50 mM imidazole, 500 mM NaCl, 20 mM HEPES pH 8.0. The column was pre-equilibrated prior to elution by flowing through 2 column volumes of 50 mM imidazole, 20 mM HEPES pH 8.0, and then eluted with 250 mM imidazole, 20 mM HEPES pH 8.0 solution. The elution was collected as 1 mL fractions, until proteins were no longer eluted. The fractions containing protein were collected, diluted 4 fold with 20 mM HEPES pH 8.0, and chromotographed on a Mono Q 5/50 GL column pre-equilibrated with 20 mM HEPES pH 8.0 buffer. The column was eluted over a 10 column volume linear gradient of 0 – 0.5 M NaCl buffered with 20 mM HEPES pH 8.0. Approximately 30 mg of *S. pneumoniae* PPCS was purified per liter of culture.

2.5.6 Natural Product Extract Library

At the time of screening, the natural product extract (NPE) library at the University of Michigan Center for Chemical Genomics contained ~20,000 extracts. Each extract in the library is derived from marine samples collected from all over the world, including Costa Rica, Panama, and Papua New Guinea. Some of these samples are from isolated microbes (n=19055) while others were derived from field-collected biomass samples ("macrosamples," n=800). Previous work describes in detail how these extracts are prepared for the library.[39]

2.5.7 Assay Development and High-Throughput Screening

High-throughput assays were performed in 384-well polystyrene NBS plates. All components of the assay were dispensed with a Thermo Scientific Multidrop dispenser. First, 30 µL of the enzyme mix, consisting of inorganic pyrophosphatase (PP_iase), *S. pneumoniae* PPCS,

and $MgCl_2$ buffered in 100 mM HEPES pH 8.0, was added to each well. In the next step, natural product extracts from the library, kept at 5 mM in DMSO solution, were added into the plates to a final concentration of ca. 15 μM with a BioMek FX automation working with a high-density replication pintool. Finally, the enzymatic reaction was started with the addition of 10 μL substrate mix, consisting of CTP, cysteine, phosphopantothenate (PPA), and DTT also buffered in 100 mM HEPES pH 8.0, to each well. Different amounts of reaction components were used for the development of the assay, but the final concentration of the 40 μL enzyme reaction used in our high throughput screen was 12.5 nM PPCS, 0.1 U/mL PP_iase, 2 mM $MgCl_2$, 250 μM CTP, 250 μM DTT, 150 μM cysteine, and 150 μM PPA.

The reaction was stopped by quenching the 40 μL reaction with 40 μL of malachite green after 25 minutes. This mixture was incubated at room temperature for 5 min, and the absorbance at 600 nm was recorded on a PHERAstar microplate reader (BMG Labtech) to determine the amount of phosphate produced. In order to avoid phosphate contamination, the substrate mix was made fresh and kept on ice until used to minimize the hydrolysis of CTP and PPA. In each plate, the 32 wells of the left two columns were run as positive inhibition controls (no PPCS enzyme) while another 32 wells of the right two columns were run as negative inhibition controls (no compounds, 0.5% DMSO).

2.5.8 Confirmation and Counterscreen Assay

Hits selected from the primary screen were confirmed by repeating the assay with the hit extracts in triplicate. Because extracts that inhibit inorganic pyrophosphatase would also show as positives in our screen, all hits were evaluated for inorganic pyrophosphatase inhibition in a counterscreen. This was done in the same 40 μL, 384- well format, where a final concentration of 250 μM PP_i was added to a solution of 10 μU/mL PP_iase, 1 mM $MgCl_2$, and the extracts in 100 mM HEPES, pH 8.0 buffer. The reaction was incubated for 20 minutes, and subsequently quenched with malachite green reagent for absorbance measurement at 600 nm. Hits that showed inhibition against PP_iase or failed the confirmation screen were not pursued further.

2.5.9 Dose-Response Assays Against Purified Enzymes

The PPCS reaction was observed in the forward reaction via an enzyme coupled assay.[18] The coupled assay measured production of pyrophosphate from *S. pneumoniae* PPCS activity via the oxidation of NADH, which could be monitored as a disappearance of absorption at 340 nm. For each mole of pyrophosphate produced, two moles of NADH are oxidized. The commercially

available Pyrophosphate Reagent (PR) from Sigma-Aldrich was used as the pyrophosphate detection system. Assays were performed on a SpectraMax M5 (Molecular Devices) microplate reader using 96-well half-area plates (Costar UV), with a final assay volume of 100 µL. The pre-incubation mixture consisted of 30 µL PR, 1U additional PP_i-PFK, 10 mM DTT, and varying concentrations (from 2 µg/mL to 200 µg/mL final concentration) of inhibitor (dissolved in 10% methanol/ 90% water) in a total volume of 70 µL buffered in 50 mM Tris-HCl and pH 7.6. All assay mixes contained $MgCl_2$ in 1:1 molar stoichiometry with nucleotide triphosphate in addition to the 2 mM $MgCl_2$ already present from the PR. The assay mix and the enzyme solution (275 nM PPCS in 50 mM Tris-HCl pH 7.6) were incubated at 37˚C for 15 min before the assay. Reactions were initiated by adding 30 µL of enzyme solution to the assay mix. The oxidation of NADH, monitored by a decreasing UV absorbance at 340 nm (ε = 6.22 mM^{-1} cm^{-1}), was measured over the course of the assay and the activity of the enzyme was calculated by adjusting for pathlength (0.5 cm) and taking into account that each mole of pyrophosphate produced leads to the oxidation of 2 moles of NADH. Assays were run in duplicates, with the average velocities reported. As a control, pre-incubation of the PR (in the absence of PPCS) with the highest concentrations of inhibitors (1000 nM) showed no inhibition of the coupling enzymes when assayed as above with the addition of magnessium pyrophosphate (0.1 mM).

2.5.10 Dose-Response Assays Against Microbial Cell Cultures

Compounds were diluted in DMSO (concentrations ranging from 100 µM to 0.8 nM; three fold dilutions down plate). Kanamycin and vancomycin dissolved in DMSO (at same concentrations) were used as positive control while an equal volume of DMSO was used as negative control. Strains were grown in LB-Miller medium (*B. subtilis* 168, *E. coli* MC1061, *S. enterica* ATCC14028, *S. flexneri* BS103 and *B. anthracis* 34F2 strains), BHI medium (*E. faecalis* ATCC29212, *S. aureus* (Newman), *L. monocytogenes* ATCC19115, *MRSA* (USA 300) and *K. pneumoniae* ATCC29665 strains) and THY medium (*S. pneumoniae* D39 strain). After overnight growth of strains (200 rpm; 37^o), cultures were diluted and grown to mid log phase (0.4 < OD600 < 0.6). For dose response analysis, optical densities after 8 hours were taken to determine the highest OD (OD_H) and the lowest OD (OD_L) of inhibitor-treated cultures and were fit to the following equation using GraphPad Prism software:

$$OD = OD_L + \frac{OD_H - OD_L}{1 + 10^{[\mathrm{I}] - \log(IC_{50})}}$$

2.5.11 16S rDNA PCR Amplification, Cloning, and Sequencing

The genomic DNA of *Streptomyces blancoensis* was extracted from 1 mL of culture using the Wizard® Genomic DNA Purification Kit (Promega A1120) per the manufacturer's protocol. The 16S rDNA was amplified from the isolated genomic DNA by PCR using the universal primers FC27 (52- AGAGTTTGATCCTGGCTCAG-32) and RC1492 (52- TACGGCTACCTTGTTACGACTT- 32).[40] The PCR reaction mixtures were prepared according to the standard protocol described by GoTaq® Green Master Mix (Promega M7122). A Bio-Rad iCycler thermocycler was used for template amplification with the following PCR cycle conditions: an initial denaturation step at 98°C for 30 s, followed by 30 cycles of 95°C for 30 s, 50°C for 30 s, 72°C for 90 s, and a final extension of 72°C for 7 min. The PCR products were purified using the Wizard® SV Gel DNA Recovery Kit (Promega A9282). The purified PCR fragments were modified to add a 3' A overhang using Taq DNA polymerase. Ligation of the modified product into pGEM®-T Easy vector (Promega) was completed with T4 DNA Ligase (NEB M0202) according to the manufacturer's standard protocol. The resulting pGEM-16S rDNA construct was transformed into chemically competent E. coli DH-5α cells. The transformation reactions were mixed with 40 µL of X-gal (20 mg/mL in DMSO) and 40 µL IPTG (100 mM in sterile H2O) before plating on LB agar plates containing ampicillin (250 µg/mL). Plates were incubated overnight at 37°C for α-complementation. After incubation, single white colonies were used to inoculate LB media in sterile culture tubes (×6). All the tubes were incubated at 37°C, 250 rpm for overnight growth. Plasmid DNA was isolated from pelleted cells using the Wizard® SV Miniprep Kit (Promega A1460) and sequenced using T7 and SP6 primers. The 16S sequence for *S. blancoencis* has been given the GenBank accession number KT359354.

2.6 References

1. Davies, J.; Davies, D. Origins and Evolution of Antibiotic Resistance. *Microbiol Mol Biol Rev* **2010,** *74*, 417-433.
2. Ferri, M.; Ranucci, E.; Romagnoli, P.; Giaccone, V. Antimicrobial resistance: A global emerging threat to public health systems. *Crit Rev Food Sci Nutr* **2017,** *57*, 2857-2876.
3. Boucher, H. W.; Talbot, G. H.; Bradley, J. S.; Edwards, J. E.; Gilbert, D.; Rice, L. B.; Scheld, M.; Spellberg, B.; Bartlett, J. Bad bugs, no drugs: no ESKAPE! An update from the Infectious Diseases Society of America. *Clin. Infect. Dis.* **2009,** *48* (1), 1-12.
4. Centers for Disease Control and Prevention. Methicillin-resistant Staphylococcus aureus (MRSA) in healthcare settings (2019). https://www.cdc.gov/mrsa (accessed July 20).

5. Lowy, F. D. Antimicrobial resistance: the example of Staphylococcus aureus. *J Clin Invest* **2003,** *111*, 1265-1273.
6. Chambers, H. F. The Changing Epidemiology of Staphylococcus aureus? *Emerg Infect Dis* **2001,** *7*, 178-182.
7. Fuda, C. C. S.; Fisher, J. F.; Mobashery, S. Beta-Lactam resistance in Staphylococcus aureus: the adaptive resistance of a plastic genome *Cell Mol Life Sci* **2005,** *62*, 2617-2633.
8. Livermore, D. M. Discovery research: the scientific challenge of finding new antibiotics. *J. Antimicrob. Chemother.* **2011,** *66* (9), 1941-4.
9. Fischbach, M. A.; Walsh, C. T. Antibiotics for emerging pathogens. *Science* **2009,** *325* (5944), 1089-93.
10. Newman, D. J.; Cragg, G. M. Natural Products as Sources of New Drugs from 1981 to 2014. *J. Nat. Prod.* **2016,** *79*, 629-661.
11. Tripathi, A.; Schofield, M. M.; Chlipala, G. E.; Schultz, P. J.; Yim, I.; Newmister, S. A.; Nusca, T. D.; Scaglione, J. B.; Hanna, P. C.; Tamayo-Castillo, G.; Sherman, D. H. Baulamycins A and B, Broad-Spectrum Antibiotics Identified as Inhibitors of Siderophore Biosynthesis in Staphylococcus aureus and Bacillus anthracis. *JACS* **2014,** *136*, 1579-1586.
12. Spry, C.; Kirk, K.; Saliba, K. J. Coenzyme A biosynthesis: an antimicrobial drug target. *FEMS Microbiol Rev.* **2008,** *32*, 56-106.
13. Leonardi, R.; Zhang, Y. M.; Rock, C. O.; Jackowski, S. Coenzyme A: back in action. *Prog Lipid Res* **2005,** *44*, 125-153.
14. Bosveld, F.; Rana, A.; Lemstra, W.; Kampinga, H. H.; Sibon, O. C. Drosophila phosphopantothenoylcysteine synthetase is required for tissue morphogenesis during oogenesis. *BMC Res. Notes* **2008,** *1* (75), 1-10.
15. Kupke, T. Molecular Characterization of the 4′-Phosphopantothenoylcysteine Synthetase Domain of Bacterial Dfp Flavoproteins. *J. Biol. Chem.* **2002,** *277* (39), 36137-36145.
16. Strauss, E.; Kinsland, C.; Ge, Y.; McLafferty, F. W.; Begley, T. P. Phosphopantothenoylcysteine synthetase from Escherichia coli. Identification and characterization of the last unidentified coenzyme A biosynthetic enzyme in bacteria. *J. Biol. Chem.* **2001,** *276* (17), 13513-13516.
17. Manoj, N.; Strauss, E.; Begley, T. P.; Ealick, S. E. Structure of Human Phosphopantothenoylcysteine Synthetase at 2.3 Å Resolution. *Structure* **2003,** *11* (8), 927-936.
18. Yao, J.; Patrone, J. D.; Dotson, G. D. Characterization and kinetics of phosphopantothenoylcysteine synthetase from enterococcus faecalis. *Biochem.* **2009,** *48* (12), 2799-2806.
19. Stanitzek, S.; Augustin, M. A.; Huber, R.; Kupke, T.; Steinbacher, S. Structural basis of CTP-dependent peptide bond formation in coenzyme A biosynthesis catalyzed by Escherichia coli PPC synthetase. *Structure* **2004,** *12*, 1977-1988.
20. Park, S. R.; Tripathi, A.; Wu, J.; Schultz, P. J.; Yim, I.; McQuade, T. J.; Yu, F.; Arevang, C.-J.; Mensah, A. Y.; Tamayo-Castillo, G.; Xi, C.; Sherman, D. H. Discovery of Cahuitamycins A-E, Potent Biofilm Inhibitors Derived from a Bifurcated Biosynthetic Pathway. *Nat. Commun.* **2016,** *7*, 1-11.
21. Mike, L. A.; Tripathi, A.; Blankenship, C. M.; Saluk, A.; Schultz, P. J.; Tamayo-Castillo, G.; Sherman, D. H.; Mobley, H. L. Discovery of Nicoyamycin A, an Inhibitor of Uropathogenic Escherichia coli Growth in Low Iron Environments. *Chemical Communications* **2017,** *53* (95), 12778-12781.

22. Tripathi, A.; Park, S. R.; Sikkema, A.; Cho, H. J.; Wu, J.; Lee, B.; Xi, C.; Smith, J. L.; Sherman, D. H. A Defined and Flexible Pocket Explains Aryl Substrate Promiscuity by the Cahuitamycin Starter Unit Activating Enzyme CahJ. *ChemBioChem* **2018,** *19* (15), 1595-1600.
23. Magarvey, N. A.; Keller, J. M.; Bernan, V.; Dworkin, M.; Sherman, D. H. Isolation and characterization of novel marine-derived actinomycete taxa rich in bioactive metabolites. *Appl. Environ. Microbiol.* **2004,** *70* (12), 7520-7529.
24. Montaser, R.; Luesch, H. Marine natural products : a new wave of drugs ? *Future Med. Chem.* **2012,** *3*, 1475-1489.
25. Patrone, J. D.; Yao, J.; Scott, N. E.; Dotson, G. D. Selective Inhibitors of Bacterial Phosphopantothenoylcysteine Synthetase. *J Am Chem Soc.* **2009,** *131* (45), 16340-16341.
26. Tsuge, N.; Mizokami, M.; Imai, S.; Shimazu, A.; Seto, H. Adipostatins A and B, New Inhibitors of Glycerol-3-Phosphate Dehydrogenase. *J. Antibiot.* **1992,** *45* (6), 886-891.
27. Rateb, M. E.; Yang, D.; Vodanovic-Jankovic, S.; Yu, Z.; Kron, M. A.; Shen, B. Adipostatins A–D from Streptomyces sp. 4875 inhibiting Brugia malayi asparaginyl-tRNA synthetase and killing adult Brugia malayi parasites. *J. Antibiot.* **2015,** *68* (8), 540-542.
28. Matsumori, N.; Kaneno, D.; Murata, M.; Nakamura, H.; Tachibana, K. Stereochemical Determination of Acyclic Structures Based on Carbon-Proton Spin-Coupling Constants. A Method of Configuration Analysis for Natural Products. *J. Org. Chem.* **1999,** *64* (3), 866-876.
29. Ping Geng, J. M. H., Pei Chen. Differentiation of Whole Grain from Refined Wheat (T. aestivum) Flour Using Lipid Profile of Wheat Bran, Germ, and Endosperm with UHPLC-HRAM Mass Spectrometry. *J. Agric. Food. Chem.* **2015,** *63* (27), 6189–6211.
30. Roemer, T.; Xu, D.; Singh, S. B.; Parish, C. a.; Harris, G.; Wang, H.; Davies, J. E.; Bills, G. F. Confronting the challenges of natural product-based antifungal discovery. *Chem. Biol.* **2011,** *18* (2), 148-164.
31. Kardar, M.; Zhang, T.; Coxon, G.; Watson, D.; Fearnley, J.; Seidel, V. Characterisation of triterpenes and new phenolic lipids in Cameroonian propolis. *Phytochemistry* **2014,** *106*, 156-163.
32. Rejman, J.; Kozubek, A. Long-chain orcinol homologs from cereal bran are effective inhibitors of glycerophosphate dehydrogenase. *Cellular and Molecular Biology Letters* **1997,** *4* (02), 411-419.
33. Kozubek, A.; Tyman, J. H. Resorcinolic lipids, the natural non-isoprenoid phenolic amphiphiles and their biological activity. *Chemical Reviews* **1999,** *99* (1), 1-26.
34. Westhuyzen, R. V. D.; Hammons, J. C.; Meier, J. L.; Dahesh, S.; Moolman, W. J. A.; Pelly, S. C.; Nizet, V.; Burkart, M. D.; Strauss, E. The antibiotic CJ-15,801 is an antimetabolite that hijacks and then inhibits CoA biosynthesis. *Chem. Biol.* **2012,** *19* (5), 559-571.
35. Chohnan, S.; Murase, M.; Kurikawa, K.; Higashi, K.; Ogata, Y. Antimicrobial Activity of Pantothenol against Staphylococci Possessing a Prokaryotic Type II Pantothenate Kinase. *Microbes. Environ.* **2014,** *29* (2), 224-226.
36. Thomas, J.; Cronan, J. E. Antibacterial Activity of N-Pentylpantothenamide Is Due to Inhibition of Coenzyme A Synthesis. *Antimicrob. Agents Chemother.* **2010,** *54* (3), 1374-1377.
37. Strauss, E.; Begley, T. P. The Antibiotic Activity of N-Pentylpantothenamide Results from Its Conversion to Ethyldethia-Coenzyme A, a Coenzyme A Antimetabolite. *J. Biol. Chem.* **2002,** *277* (50), 48205-48209.
38. Velaparthi, S.; Brunsteiner, M.; Uddin, R.; Wan, B.; Franzblau, S. G.; Petukhov, P. A. 5-tert-Butyl-N-pyrazol-4-yl-4,5,6,7-tetrahydrobenzo[d]isoxazole-3-carboxamide Derivatives as

Novel Potent Inhibitors of Mycobacterium tuberculosis Pantothenate Synthetase: Initiating a Quest for New Antitubercular Drugs. *J. Med. Chem.* **2008,** *51* (7), 1999-2002.
39. Cruz, P. G.; Auld, D. S.; Schultz, P. J.; Lovell, S.; Battaile, K. P.; Macarthur, R.; Shen, M.; Tamayo-Castillo, G.; Inglese, J.; Sherman, D. H. Titration-based screening for evaluation of natural product extracts: identification of an aspulvinone family of luciferase inhibitors. *Chem. Biol.* **2011,** *18* (11), 1442-1452.
40. Rainey, F. A.; Ward-Rainey, N.; Kroppenstedt, R. M.; Stackebrandt, E. The genus Nocardiopsis represents a phylogenetically coherent taxon and a distinct actinomycete lineage: proposal of Nocardiopsaceae fam. nov. *Int. J. Syst. Bacteriol.* **1996,** *46* (4), 1088-1092.

Chapter 3

Isolation, Characterization and Structural Elucidation of HIV Nef Inhibitors

3.1 Introduction

3.1.1 Viral Proliferation

The human immunodeficiency virus (HIV) is a life-threatening virus that spreads through contact with bodily fluids of an infected patient. Once inside, the virus will utilize its own reverse transcriptase to convert the viral single stranded RNA into a double stranded DNA and integrate it into the host's chromosome.[1-2] After this, it will use the cell's own machinery to replicate and resume infection. HIV mainly infects cells that form part of the immune system, namely $CD4^+$ T cells.[3-4] When untreated, the $CD4^+$ T cell count in the host will be reduced to very low levels, giving way to the development of acquired immunodeficiency syndrome (AIDS).[5] Once the disease progresses to this stage, many opportunistic infections and certain cancers exploit the compromised immune system leaving the body unable to defend itself and ultimately cause the patient to die.

3.1.2 HIV is a Global Threat

As of 2017, UNAIDS estimates 36.9 million people in the world are currently infected with HIV, 4.9% of these being children under 15 years of age.[6] Although the majority of these patients reside in low and middle income countries (53% being from Eastern and Southern Africa), there are an astounding 4% of patients living in North America. According to the Centers for Disease Control (CDC), about 1.1 million of the infected patients reside in the US, with a yearly infection rate of 38,700 new cases per year.[7] Among these, gay and bisexual men, particularly those from disadvantageous backgrounds, have the highest rates among all the group division statistics (Fig 3.1). Even though many advances have been achieved in lowering the risk of transmission and enhancing the success of available treatments, HIV remains a pandemic and a cause for concern in many countries around the globe.

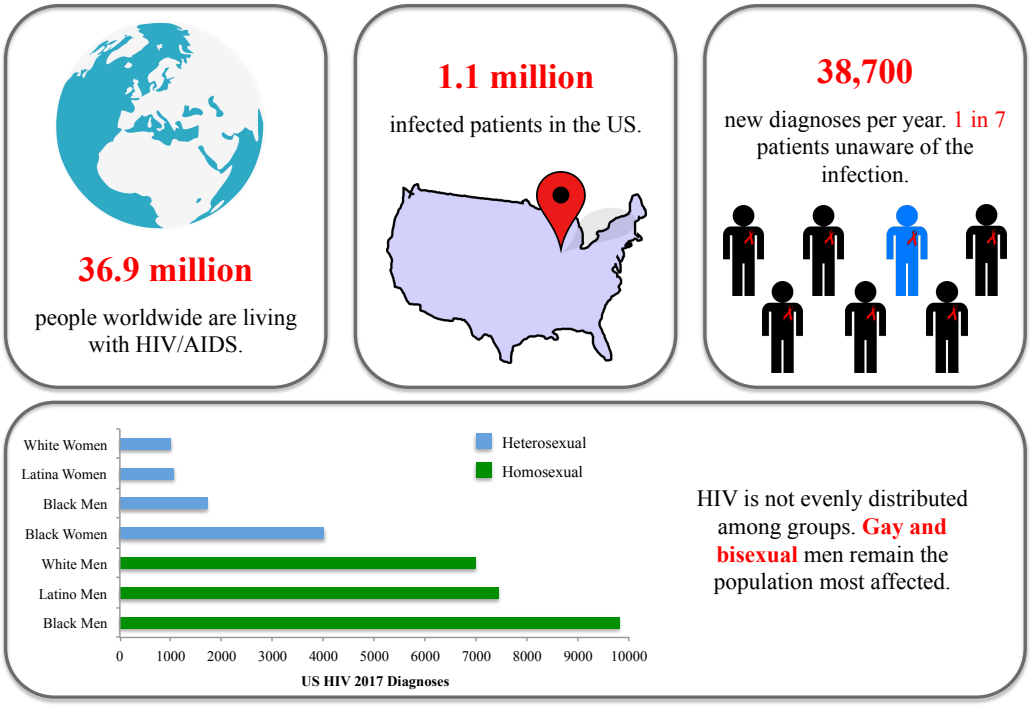


Figure 3.1. *CDC HIV-1 infection statistics*. From the estimated 36.9 million patients living with HIV around the world, 1.1 million reside in the US; over 150,000 of these are not aware they are infected. The biggest spread occurs through male homosexual contacts (figure adapted from UNAIDS, 2018).

3.1.3 Current Available Treatments

Although much research and efforts have been focused on finding ways to eradicate the virus, scientists have yet to identify a cure for HIV. Current treatment, known as antiretroviral therapy (ART), consists on the everyday consumption of three HIV drugs from two or more classes of inhibitors.[8] This regimen targets different areas of HIV proliferation, such as inhibition of reverse transcriptase, protease, integrase and viral fusion into the cell (Fig 3.2).[9-10] Since blocking these targets is not enough to eradicate the virus completely, the main goal of ART is to prevent the virus from creating more copies of itself to reduce the viral load within the host.[8] Preventing the progression to AIDS gives the advantage of permitting the immune system to recuperate some of its fighting abilities to defeat additional infections, which in turn lowers tremendously the risk of transmitting HIV.

A huge hurdle to overcome when combating retroviruses like HIV is their propensity towards drug resistance.[11-12] When the virus creates a replicate, there is a higher chance for mutations to occur which creates modified versions of the ART targets. Some of these might possess the ability to evade interaction with the drugs in the regimen and are, therefore, unable to

be treated with available medicine. Another reason ART is not successful at eradicating the virus from the body is the presence of latent HIV reservoirs.[13-15] These reservoirs exist in HIV infected cells that reach a resting phase, where no HIV is replicated. This creates an absence of HIV proteins that are used as target for inhibition, meaning ART is essentially ineffectual against them. Although it is not completely known how it occurs, these reservoirs are able to reactivate eventually and begin creating fresh virions, making ART regimen a life long daily commitment.

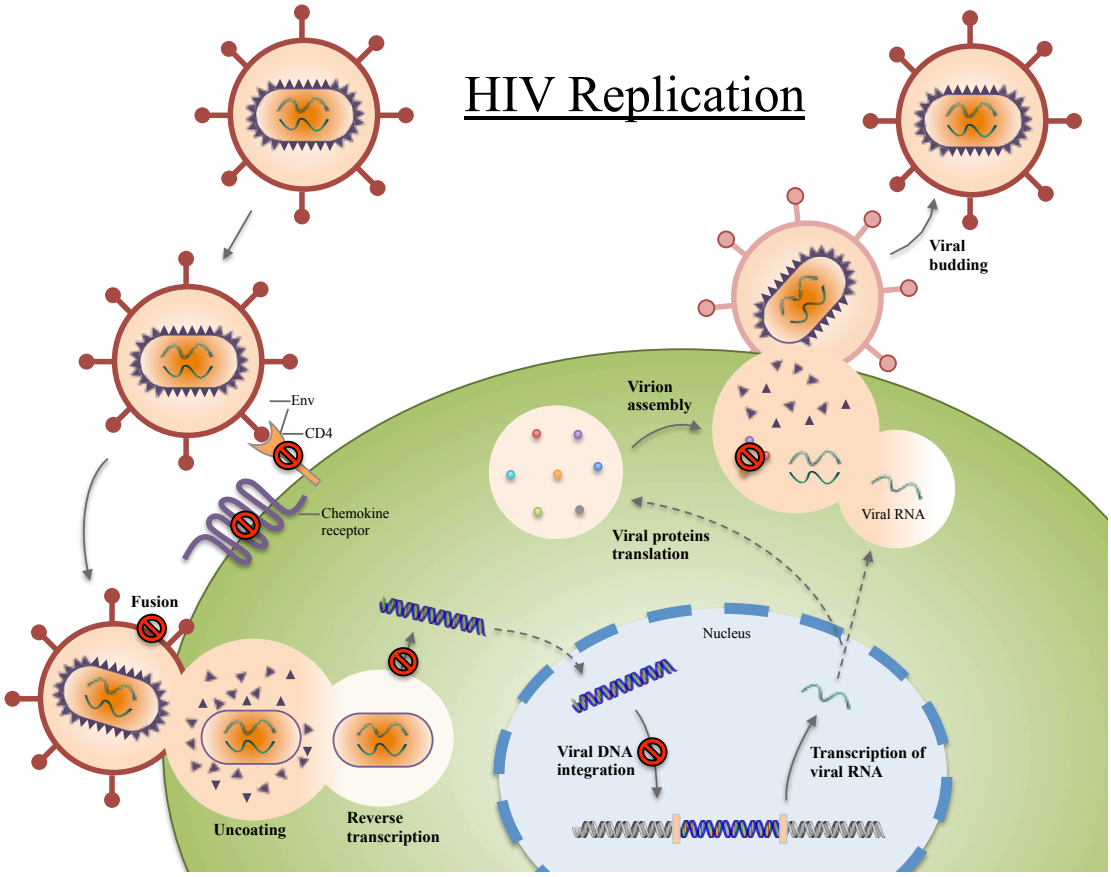


Figure 3.2. *Areas targeted by ART during HIV-1 replication*. The different types of anti-HIV drugs currently being used as part of the combination therapy inhibit the reverse transcriptase, protease, integrase as well as entry into the host cell (figure adapted from Wynn & Santos, 2015).[16]

3.1.4 HIV-1 Nef As a Drug Target

Like many other viruses, HIV-1 has developed several strategies to avoid detection and destruction by the host cells. A particular strategy is the unique ability to encode four accessory proteins in addition to its regulatory proteins and classical structural and enzymatic factors lentiviruses are known to produce.[17-20] These accessory proteins (Vif, Vpu, Vpr and Nef) each

have their own unique role in maintaining virus proliferation and have been widely studied. Although both regulatory proteins and accessory proteins are critical for viral replication, accessory proteins play important roles in immunoevasion and pathogenesis, and are therefore an attractive area to target to stop viral replication and propagation.[21-23]

The Nef protein is relatively small (~27 kDa) and can be divided into three main domains: the N-terminal anchor, the core domain and the C-terminal regions. As implied, Nef contains an addition moiety at its N-terminus that aids in the attachment of the protein to the membrane. The myristoyl group helps Nef perform many of its functions such as altering intracellular trafficking.[24] Although it is one of the first proteins HIV-1 expresses after infection, Nef appears to lack enzymatic activity and functions instead through protein-protein interactions with other host proteins, such as the major histocompatibility complex I (MHC-I) molecules and adaptor protein (AP) complex.[25-27] One of the functions of MHC-I in the cell is to present foreign antigens on the surface to warn cytotoxic T lymphocytes (CTLs) of infection, which leads to an immune response that causes cell death. The Nef/MHC-I interaction is particularly important for the virus proliferation because it leads to the down-modulation of MHC-I, and subsequent evasion of CTLs.[28]

The model for how Nef orchestrates MHC-I down-modulation begins with the binding to the cytoplasmic tail of MHC-I while it is in the trans-Golgi network (TGN) (Fig 3.3).[29] Of the four AP complexes present in mammalian cells, AP-1 heterotetramer is involved in clathrin mediated trafficking of protein cargo across the trans-Golgi membrane by recognizing a YXXΦ or (D/E)XXXLL peptide signal.[30-31] Once Nef binds to MHC-I, it will stabilize the otherwise weak interactions between AP-1 and the YXXXAXXD signal from MHC-I by providing additional contact regions. True to its nature, once AP-1 interacts with MHC-I it will transport it through clathrin-coated pits from the TGN to the endo-lysosomal pathway where degradation will occur. Because of this, MHC-I molecules are unable to present the foreign antigens on the cell surface and pathogens are able to evade CTL recognition, resulting in viral proliferation.[32] Therefore, we hypothesize that identifying novel Nef inhibitors will lay the groundwork for future developments of an improved HIV drug that increases the recognition of infected cells and leads to an immune system response.

Previous studies in mice and simian models, along with *in vitro* data, support the Nef protein as a dominant player in HIV pathogenesis. Using transgenic mice, researchers were able

to obtain an AIDS-like phenotype through induction of HIV-1 Nef, while other accessory proteins were found to not be necessary.[33] During another study, viral load in rhesus monkeys infected with a version of the simian immunodeficiency virus (SIV) that lacks the Nef gene was lowered 100 fold when compared with wild type virus.[34] In addition, *in vitro* studies have found that cells infected with HIV-1 lacking a functional *nef* gene maintained their surface MHC-I molecules levels and about 90% of cells were recognized by CTLs. Meanwhile, maintaining a functional *nef* gene showed resistance to CTLs and a reduction of surface MHC-I molecules.[32] It has also been reported that patients infected with a mutated HIV lacking Nef manifested consistent low viral levels and had a delay in the progression towards AIDS.[35-37] Furthermore, it was reported earlier in the year a correlation between maximal Nef activity and the early establishment of HIV reservoirs in latent cells.[38]

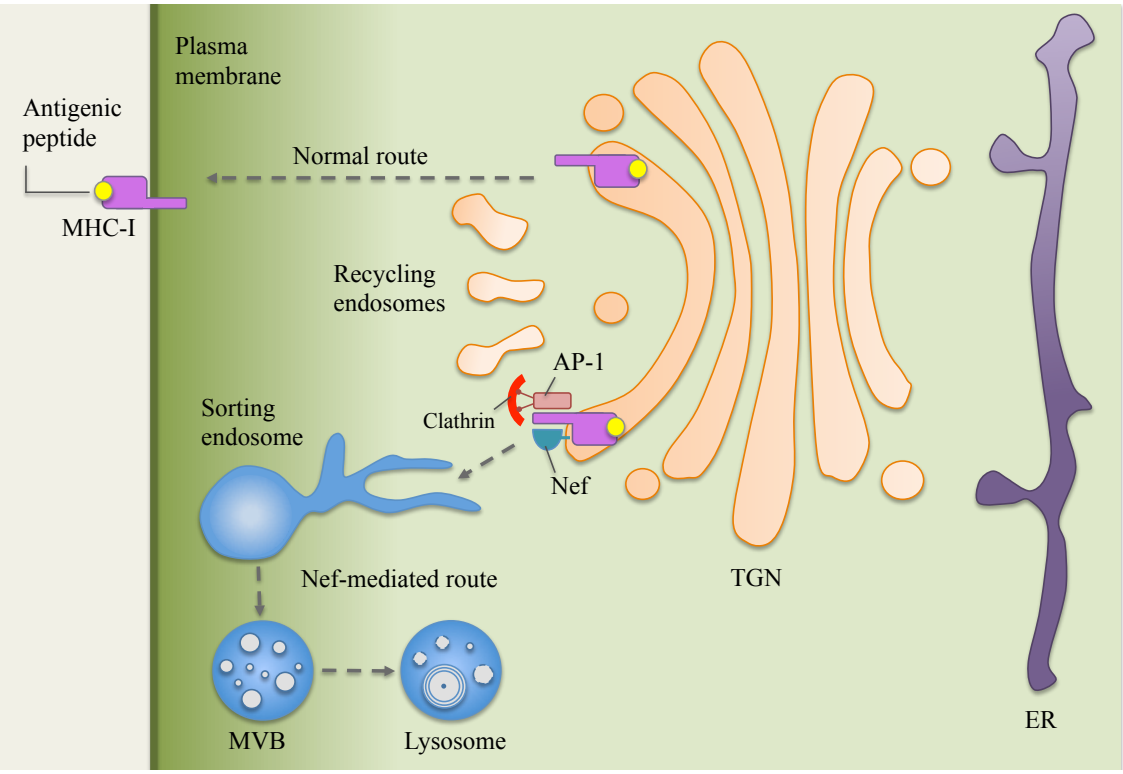


Figure 3.3. *Mechanism of MHC-I degradation by HIV-1 Nef.* Nef accessory protein deters MHC-I from reaching the cell surface and presenting foreign antigens by diverting it to the lysosome through AP-1 directed clathrin-coated pits, where it will eventually get degraded (figure adapted from Hurley & Bonifacino, 2012).[15]

Numerous studies have been done in the search for Nef small molecule antagonists. A single domain antibody-SH3 fusion protein and the use of a technique consisting of covering

several Nef interaction surfaces, termed "wrapping Nef", have been successful in blocking many of the Nef effects including MHC-I down-modulation.[39-40] Previously, a small molecule named DLC27 (Fig 3.4), which consisted of a *t*-butyl-phenyl group attached to a phenyl carboxylic acid through a modified carbamate linker, was found to bind Nef and enhance its sensitivity to proteolysis.[41-42] Further testing proved to be difficult due to its poor solubility and high toxicity, which led to the compound being dropped from further development. Another molecule called B9 (Fig 3.4) claiming to inhibit HIV replication only in the presence of Nef was reported and identified as a Nef dimerization inhibitor.[43] Many studies have suggested that Nef dimerization at the TGN is necessary for down-regulation activities and viral replication to occur.[44-47] Finally, an area that has also been studied is the blocking of Nef from associating and creating a signaling multi-kinase complex, which has been suggested to prevent MHC-I reaching the cell surface.[48] From this study a secondary metabolite derivative called 2C (Fig 3.4) was found to disrupt Nef-Src family kinase.[48] Although none of these molecules were able to go through any further development, the studies served as a proof-of-concept towards the effectiveness of Nef inhibition in the ongoing quest to eradicate the virus.

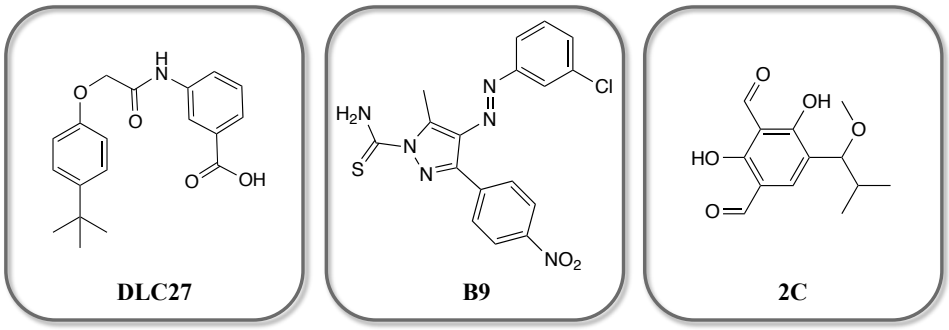


Figure 3.4. *Published Nef Inhibitors*. Molecules from several studies identified as Nef inhibitors.[41-43,48]

3.2 Results and Discussion

3.2.1 High-Throughput Screening

Fueled by the need to discover novel Nef inhibitors, Dr. Kathleen Collins laboratory developed a high-throughput flow cytometry based assay to test the natural product extracts (NPEs) library available at the CCG. The extracts are primarily derived from marine microorganisms collected from places around the globe such as Costa Rica, Papua New Guinea and Antarctica. The assay consisted on transducing an adenoviral vector that expresses Nef through the control of the elongation factor 1 alpha promoter (EF1α).[49] After two days, infected

cells were treated with the NPEs and harvested 24 hours later for HLA-A2, a type of human MHC-I, cell surface expression analysis. A negative counter screen followed directly, where a cell line that does not express HLA-A2 was used for the assay. The two rounds of screening queried over 26,000 NPEs, and yielded 37 strains with greater than 30% inhibition of Nef mediated MHC-I down-modulation (Fig 3.5). A third validation assay was performed by using HIV-1 ΔGPE, a mutated version of the virus that lacks the genes responsible for the structural proteins, further narrowed the list to eleven hit strains.

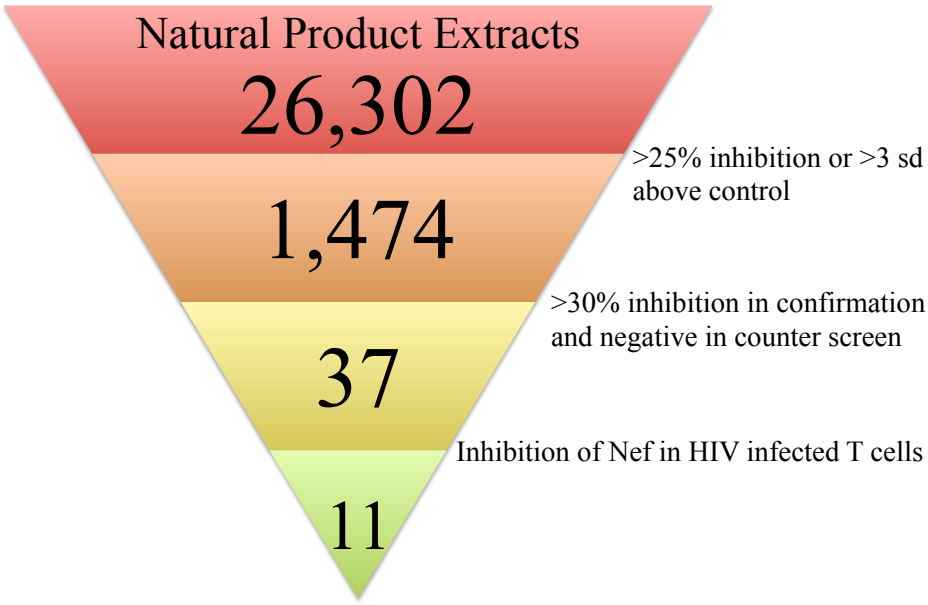


Figure 3.5. *Flowchart for the identification of Nef inhibiting strains*. Over 26,000 NPEs available at the CCG were tested for Nef inhibitory activity, yielding 37 potential extracts after confirmation and a counter screen assay using a cell line that did not express HLA-A2. This number was further lowered to 11 when testing against the mutated HIV-1 ΔGPE, which lacks the gag, pol and env structural proteins. Assay performed by members of the Collins lab.

3.2.2 Isolation and Structural Elucidation of Active Natural Products

Among the active extracts, strains 34893-N3I and 39098-H2N were of particular interest because of their anti-Nef activity and reproducibility. Both strains were originally isolated from marine sediments collected in Costa Rica near Playa Langosta. Repeated bioactive-guided C18 fractionation of 34893-N3I and following RP-18 HPLC purification led to the identification of a peak (**LG-6**) responsible for the anti-Nef activity (Fig. SI-3.4.1). High-resolution mass spectrometry (HR-MS) provided a $[M+H+Na]^+$ ion peak of 645.3988 m/z (Fig. SI-3.4.2).

To probe the structural diversity of the secondary metabolites produced by this strain, the crude extract was submitted through targeted MS/MS fragmentation. This data was used to

create a molecular network that displays fragment similarities between each of the molecules detected using the Global Natural Products Social Molecular Networking (GNPS) (Fig 3.6.A).[50] The mass of interest was located within the molecular network to assess its similarity to other secondary metabolites produced by the strain. Although it is not connected to any other node, based on its fractionation patter the GNPS library was able to predict a structure belonging to Bafilomycin A_1 (Baf-A_1) (Fig 3.6.B). Aided by 1D and 2D NMR data along with a Baf-A_1 standard, we confirmed the **LG-6** active peak was in fact Baf-A_1.

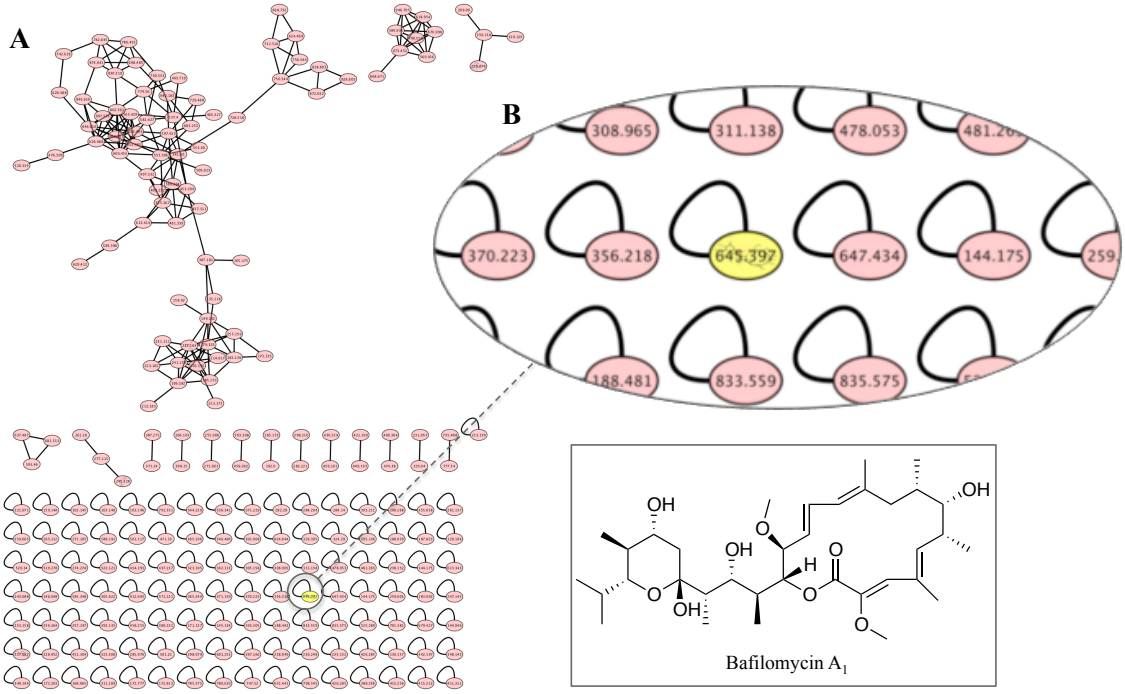


Figure 3.6. *LC-MS/MS generated molecular network of 34893-N3I.* **A**. Molecular network of all the masses present in the extract. Links between each show structural similarities based on the MS/MS fractionation pattern. **B**. Mass from the identified bioactive metabolite does not show correlation to other extract component, however it does give a predicted structure from the GNPS NPs library belonging to Bafilomycin A_1.

Following a similar workflow, two active peaks were identified from strain 39098-H2N, each with $[M-H]^-$ of 719.4053 m/z and 814.4405 m/z. These also showed similar MS/MS fractions to Baf-A_1, and were confirmed to be Bafilomycin C_1 (Baf-C_1) and Bafilomycin B_1 (Baf-B_1) respectively.

Bafilomycins belong to the family of plecomacrolides antibiotics, distinguished by their 16 membered macrolactone ring with a hemiacetal side chain, with the exception of Baf-D (Fig 3.7).[51-52] Although they are known for having an array of biological activities, such as anti-

fungal, anti-parasitic and anti-osteoporotic, they are most famously known for being vacuolar ATPase (V-ATPase) inhibitors.[53] Among the many proteins Nef has been shown to interact with in the cell, subunit H of the V-ATPase has been identified in several studies.[54] These reports have found this interaction responsible for the internalization of another Nef downmodulation target, CD4.

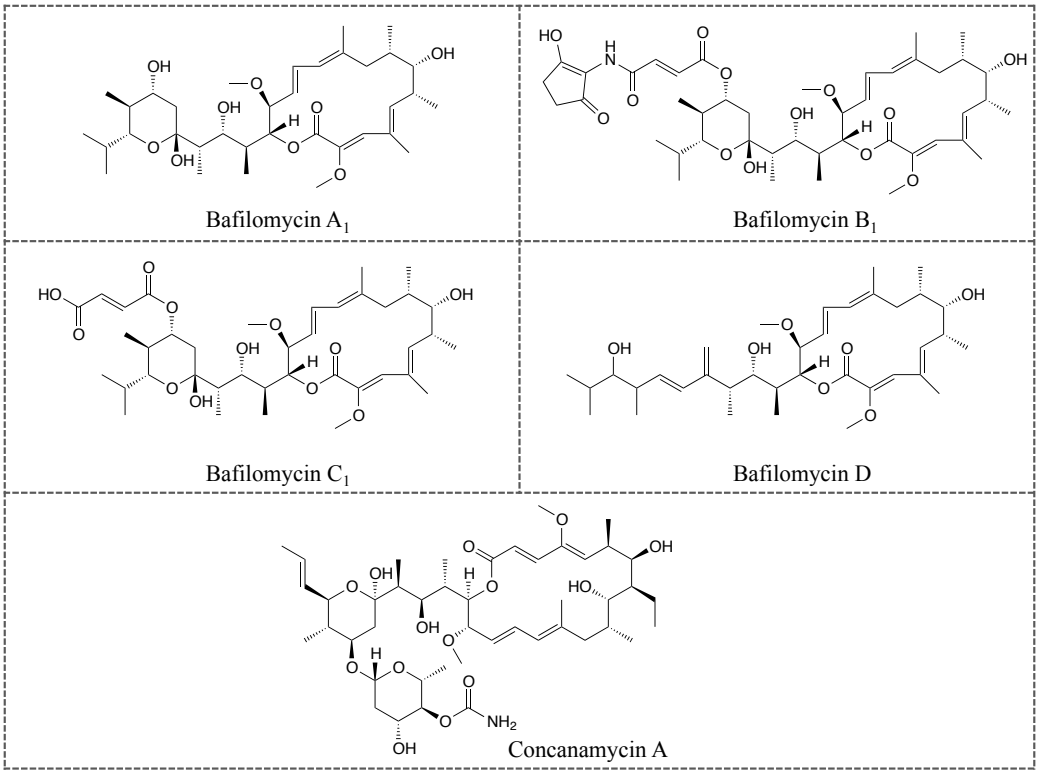


Figure 3.7. *Plecomacrolides known to posses V-ATPase inhibitory activity*.

3.2.3 Biological Testing

To test the bafilomycins ability to inhibit HLA-A2 downmodulation, four of the commercially available plecomacrolides were tested over a range of concentrations against infected peripheral blood mononuclear cells (PBMCs). As seen in figure 3.8, Baf-C_1 (blue) undeniably shows the highest inhibition out of the four bafilomycins tested. Baf-B_1 and Baf-A_1 followed in the potency profile, while Baf-D seemed to be an outlier with markedly lower inhibition. These results are important to establish structure activity relationships (SAR) for any future modifications on the bafilomycin molecules. Firstly, Baf-D lacks the hemiacetal side chain at C18, holding instead a ring-opened version. Although this version provides higher stability,

the activity suffers immensely as can be see in the IC_{50} drop to the μM area. While Baf-A_1 and Baf-B_1 are close in potency, a clear window can be seen showing the A version to be less active. Baf-A_1 has no substitution in the hemiacetal ring alcohol at C21, indicating this is an important area that can be targeted in future studies for improvement. The identity of this substitution is also important as Baf-C_1 has a higher activity with a fumarate substitute over Baf-B_1 with the 2-amino-3-hydroxycyclopent-2-enone.

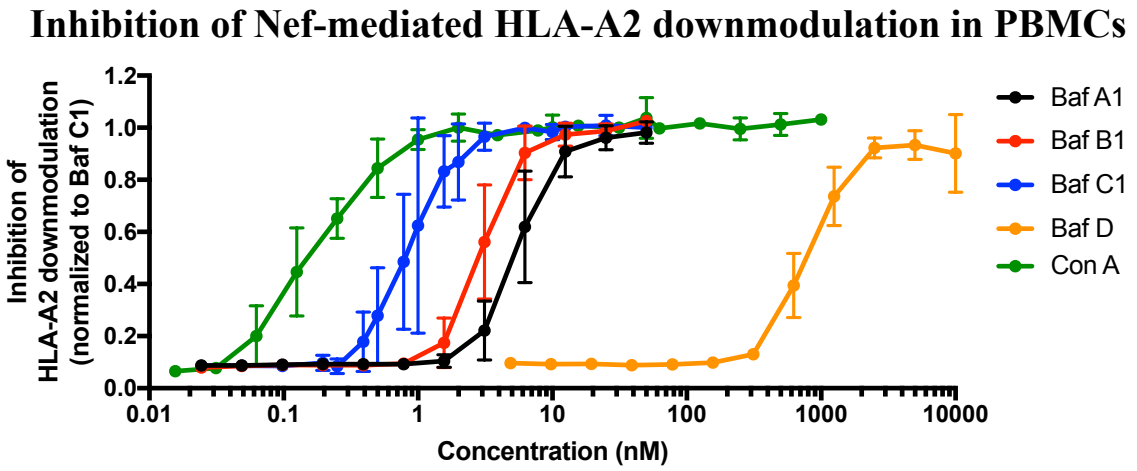


Figure 3.8. *Plecomacrolides activity profile for MHC-I cell surface restoration*. The plecomacrolides family of molecules [Baf-A_1 (black), Baf-B_1 (red), Baf-C_1 (blue), Baf-D (yellow), ConA (green)] were able to restore surface expression of MHC-I HLA-A2 over six different concentrations. ConA had the highest potency with activity in the pM range, while Baf-D had significantly lower potency. Assays were run on biological triplicates. Experiment completed by Mark Painter, Gretchen Zimmerman and Madeline Merlino from Dr. Collins Lab.

The success of these known V-ATPase inhibitors led to the identification and testing of another plecomacrolide, concanamycin A (ConA).[53] Although similar, some key structural differences between ConA and bafilomycins are the extended 18 membered lactone ring and an additional sugar moiety at the hemiacetal ring alcohol. Compared to bafilomycins, ConA surprisingly exceeded the HLA-A2 downmodulation inhibition activity with an IC_{50} in the picomolar range. Given we had obtained restoration of HLA-A2 to the cell surface, the next step was to determine if these levels would be enough for CTLs to recognize and kill infected cells. For this purpose, the Collin's lab developed a CTL killing assay infecting primary T cells with an HIV-PLAP reporter virus system. As seen in figure 3.9, using a low dose of ConA, the killing of infected cells is enhanced to a similar degree as in the absence of Nef.

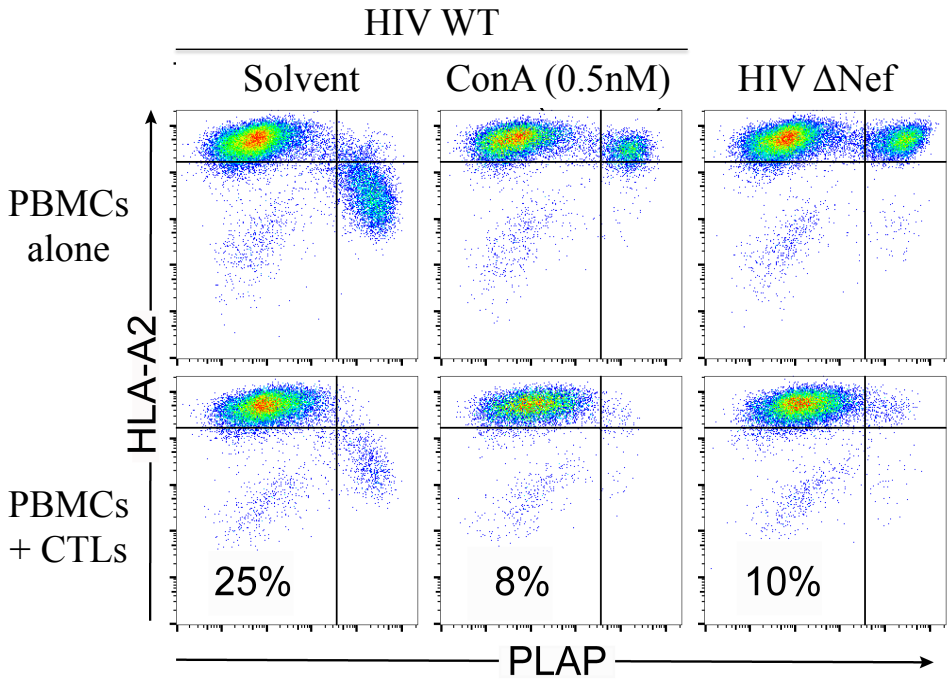


Figure 3.9. *ConA is able to restore HLA-A2 expression and increases killing by CTLs*. Using a low dose of ConA there is a clear shift to higher HLA-A2 surface expression in the infected cell population to levels comparable to uninfected PBMCs (upper panel). We also see the disappearance of the infected cell population in the presence of CTLs when incubating these with ConA, while the CTLs were not as successful when no plecomacrolide was added (lower panel). Experiment completed by Mark Painter with assistance from Val Terry from Dr. Collins lab using anti-HIV CTLs provided by Alicja Trocha from Dr. Walkers lab at the Ragon Institute.

An issue that has usually followed plecomacrolides, and the reason they have mostly failed during clinical trials, is their unfortunate toxicity profile.[55] This is caused by the disruption of organelles acidification by inhibition of the V-ATPase, which leads to the accumulation of undigested autophagosomes in the lysosome. To test the correlation between ConA V-ATPase inhibition and anti-Nef activity, a LysoTracker assay to follow lysosome acidification at varying ConA concentrations was employed. When plotted next to each other (Fig 3.10) the concentration needed for inhibition of Nef mediated MHC-I downmodulation is about ten times lower than the needed for lysosome deacidification events. This significant therapeutic window between both occurrences suggests the deacidification and anti-Nef events are independent of each other. The toxicity separation was further confirmed by cell viability analysis upon treatment with the plecomacrolides. Although Baf-A_1 and Baf-C_1 have a clear separation, ConA has the widest concentration gap between anti-Nef activity and toxicity (Fig SI-3.4.9).

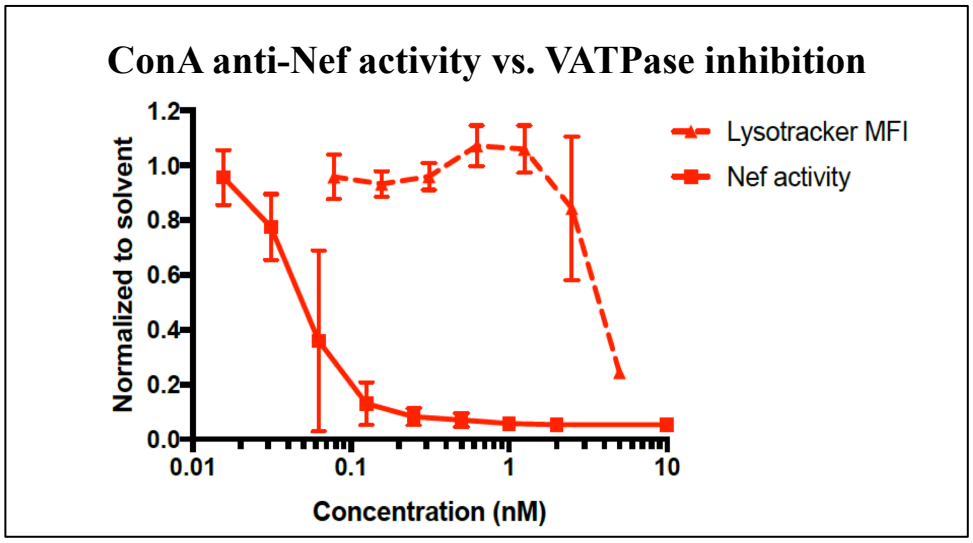


Figure 3.10. *Lysosome acidification analysis through LysoTracker*. ConA V-ATPase inhibition (triangles) occurs at higher concentrations than the needed for Nef dependent MHC-I downmodulation (squares) creating a clear window between both activities. Each assay was run on triplicate. Experiment completed by Mark Painter and Gretchen Zimmerman from Dr. Collins Lab.

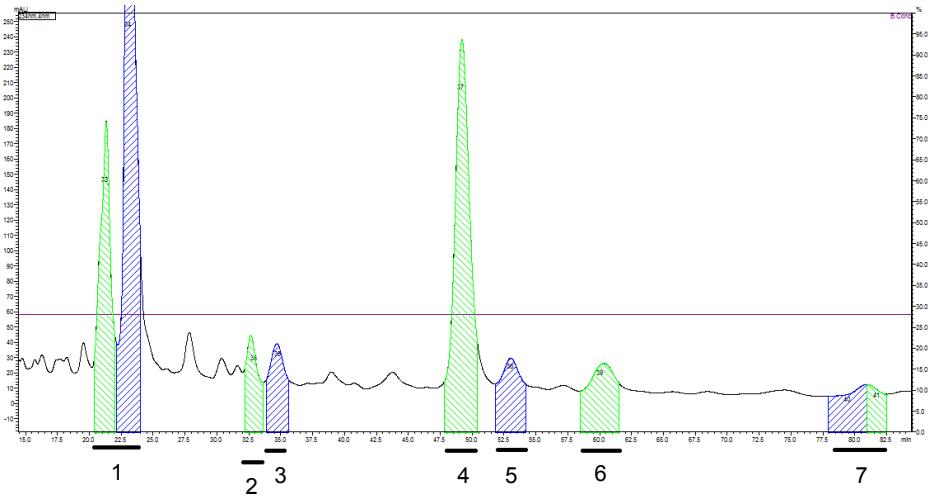
3.3 Conclusion

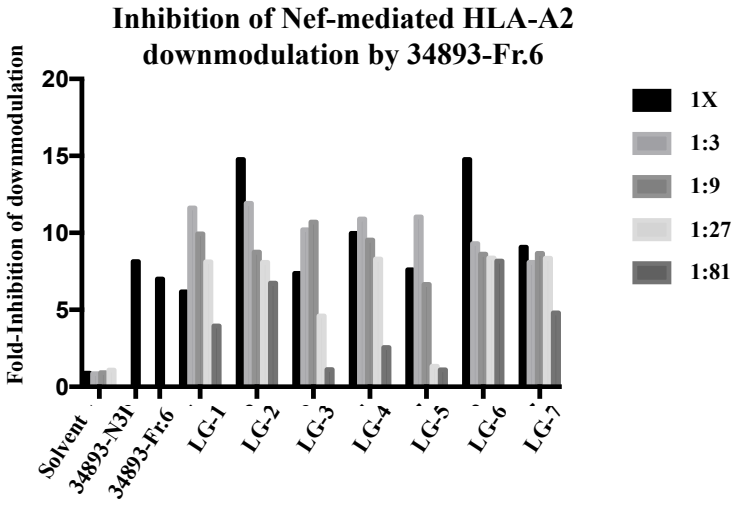
Aided by molecular networking we were able to identify a known family of compounds that show promising anti-Nef activity from a marine microbial-derived NPE library. Bafilomycins A_1, B_1 and C_1 demonstrated to restore surface expression of HLA-A2 at low nM concentrations in primary T cells. Even more pivotal, ConA demonstrated to be the most potent out of all the plecomacrolides at concentrations extending to picomolar levels and displayed the ability to restore killing by CTLs. These results show far more potency than any currently published Nef inhibitor.

Although the bafilomycins and ConA natural products have been shown to have a wide array of bioactivity, the plecomacrolides have not endured further in clinical trials due to their toxicity caused by V-ATPase inhibition.[53] Despite the fact that we showed there is a clear distinction between the modes of action between restoration of HLA-A2 to the surface and V-ATPase inhibition, the exact mechanism through which these molecules are performing the former is unknown. Additionally, improvements on the selectivity and molecule stability can be made on these lead structures using semi-synthetic approaches that could further lower the IC_{50} for the anti-Nef activity.

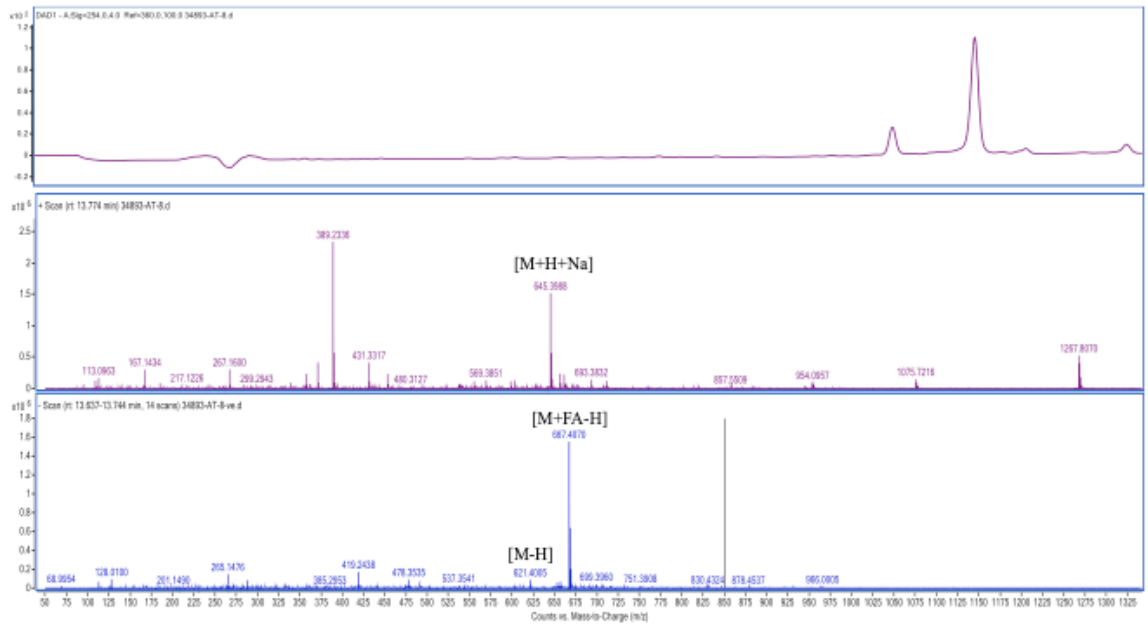
3.4 Supplemental Information (SI)

3.4.1 Bioassay-guided purification of LG-6 (Bafilomycin A_1) from 34893-N3I. Assay completed by Mark Painter and Gretchen Zimmerman from Dr. Collins lab.

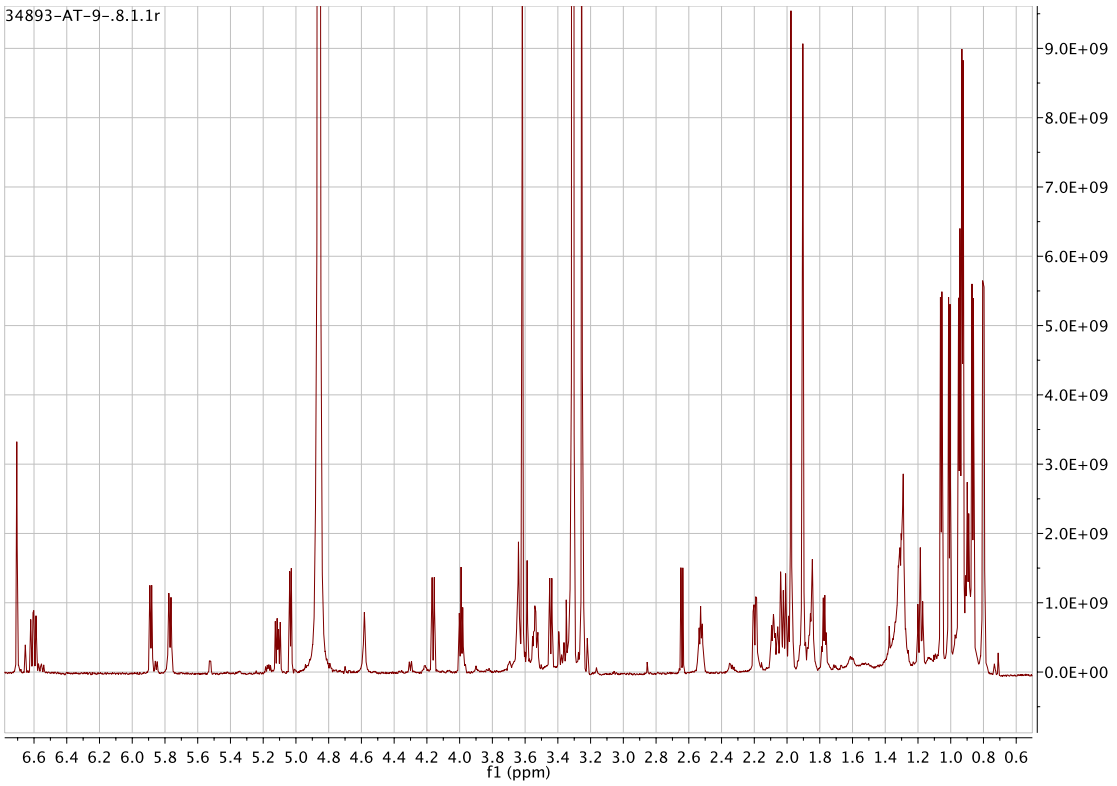




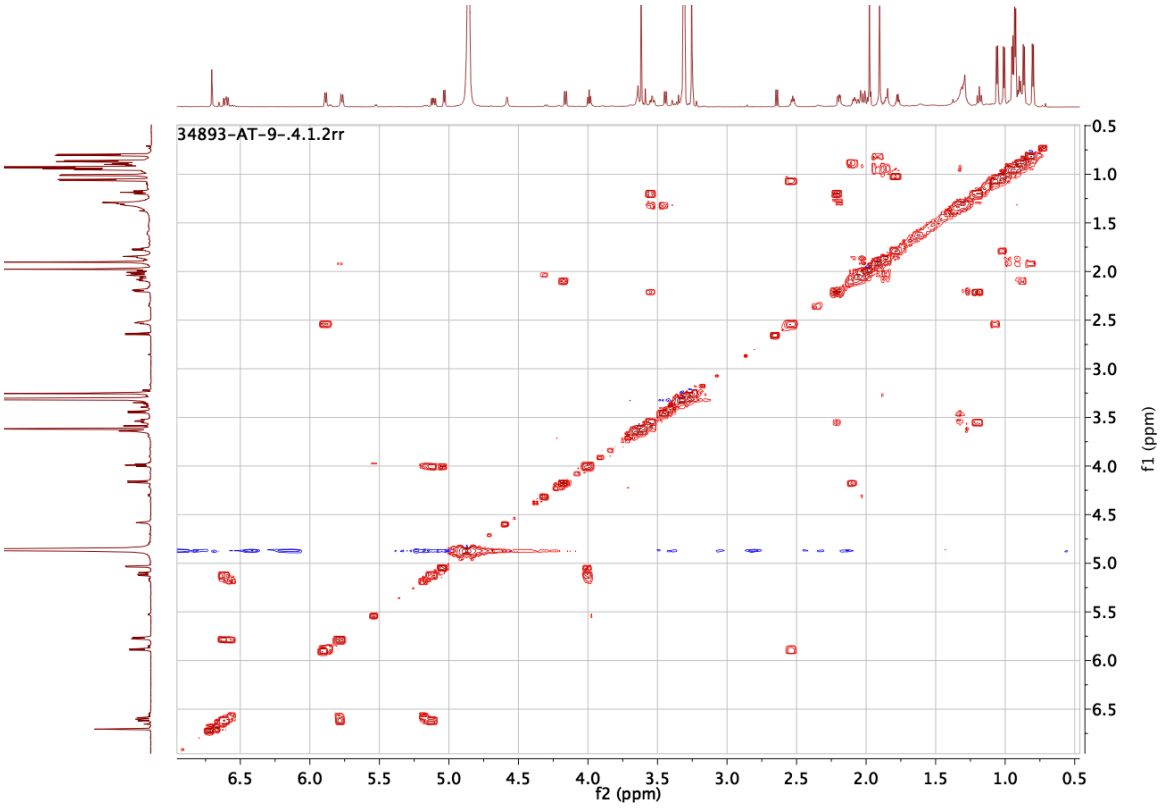
3.4.2 HR-MS chromatogram of LG-6 (Bafilomycin A_1).



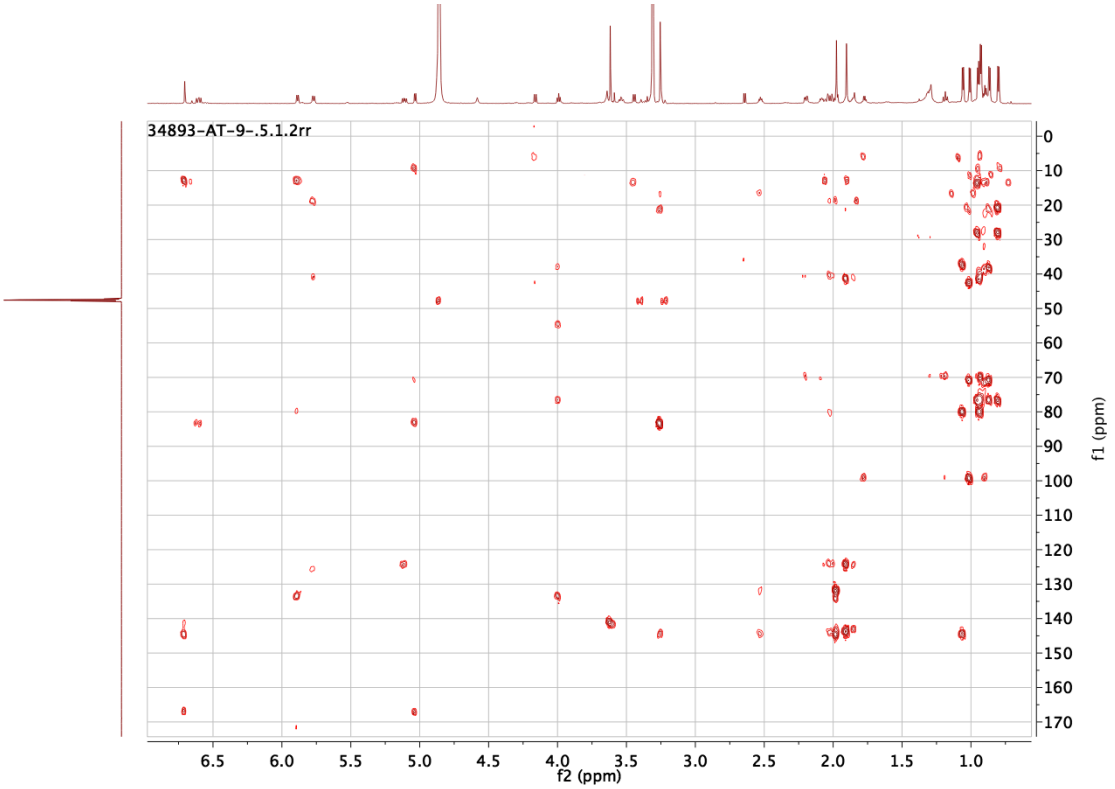
3.4.3 ^{1}H NMR (600 MHz, CD3OD) spectrum of LG-6 (Bafilomycin A_1).



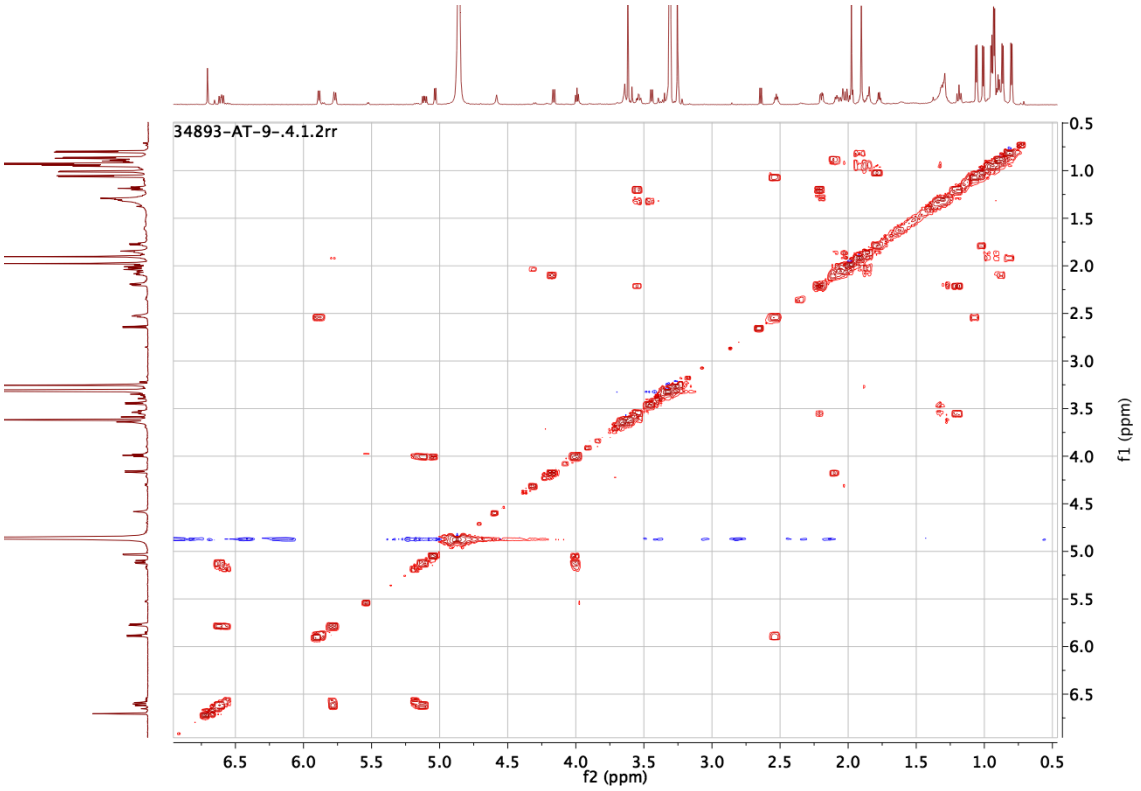
3.4.4 gCOSY NMR (600 MHz, CD3OD) spectrum of LG-6 (Bafilomycin A_1).



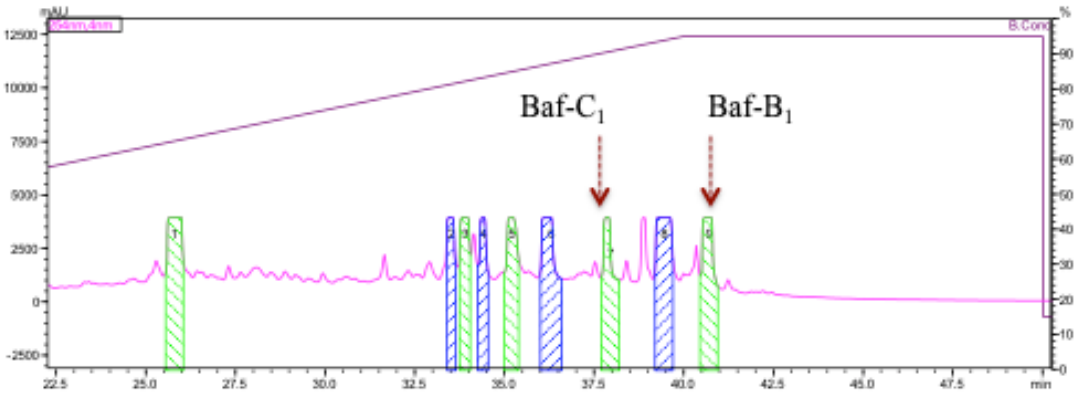
3.4.5 gHMBCAD NMR (600 MHz, CD3OD) spectrum of LG-6 (Bafilomycin A_1).



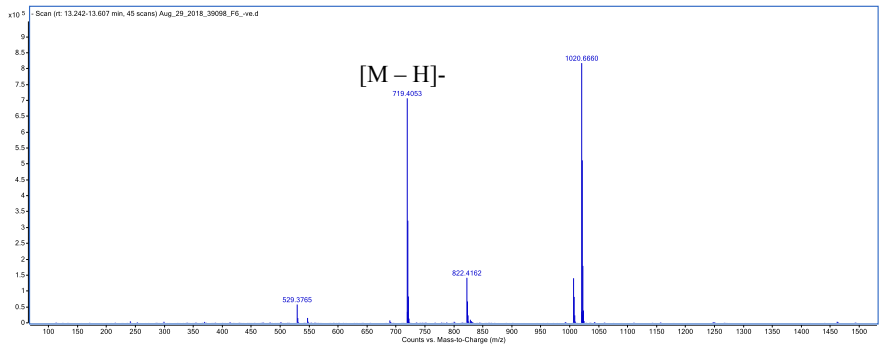
3.4.6. dqfCOSY NMR (600 MHz, CD3OD) spectrum of LG-6 (Bafilomycin A_1).



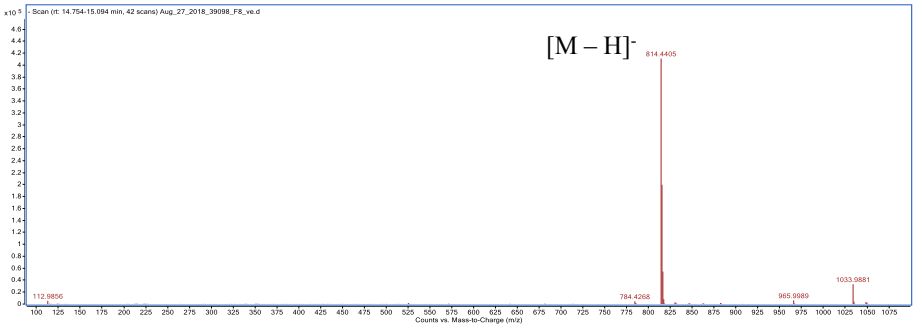
3.4.6 Purification of Bafilomycin B_1 and Bafilomycin C_1 from 39098-H2N.



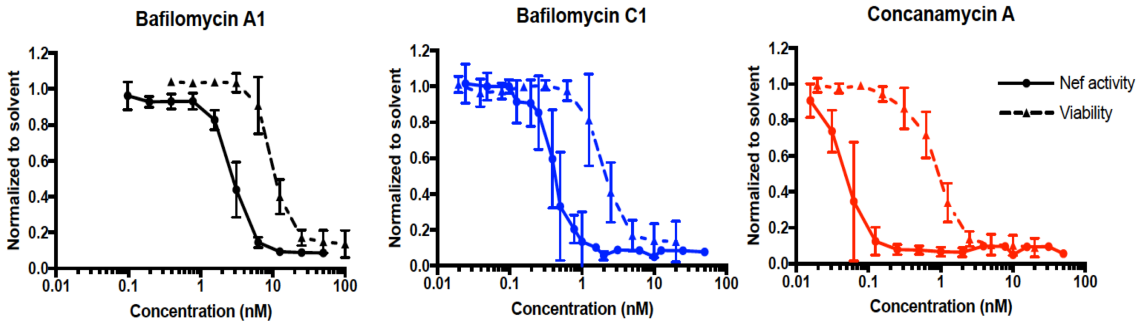
3.4.7. HR-MS chromatogram of Bafilomycin C_1.



3.4.8. HR-MS chromatogram of Bafilomycin B_1.



3.4.9. Cell viability assay (Collin's Lab). Assay completed by Mark Painter, Gretchen Zimmerman and Madeline Merlino from Dr. Collins lab.



3.5 Materials and Methods

3.5.1 General Experimental Procedures

Spectrophotometric assays were performed on Molecular Devices SpectraMax M5 384 variable wavelength spectrometer. All NMR spectra were acquired on a Varian INOVA 600 MHz spectrometer at the NMR Facility, Life Sciences Institute, University of Michigan. High-resolution APCIMS spectra were measured at the University of Michigan core facility in the Department of Chemistry using an Agilent 6520 QTOF mass spectrometer equipped with an Agilent 1290 HPLC system. RP-HPLC was performed using Luna 5 µm Phenyl-Hexyl 250 x 10 mm column in a solvent system of ACN and H2O. The LCMS analysis of HPLC fractions was performed on a Shimadzu 2010 EV APCI spectrometer using ZORBAX Extend 80Å C18, 4.6 x 100 mm, 3.5 µm HPLC column.

3.5.2 Biological Material

Strain 34893-N3I and 39898-H2N were isolated from marine sediments collected near Cabo Blanco, Costa Rica (collection permit R-CM-INBio-30- 2007). The procedure for the isolation of actinomycetes from these samples was previously described by Magarvey et al.[56] Maintenance and propagation of cultures were performed using standard media and protocols where 500 mg of wet sediment was diluted in 10 mL of sterile water and vortexed for 10 min. Then, 1 mL of this suspension was applied directly to the top of the discontinuous sucrose

gradient and centrifuged for 30 minutes at 300 x g. 500 µL of the 20%, 30%, and 40% layers were then plated to HVA agar supplemented with 10 µg/mL chlortetracycline, 25 µg/mL cyclohexamide, and 25 µg/mL of nalidixic acid. The plates were then incubated at 28 °C for one month. The colony was picked off the plate and streaked onto ISP2 agar until pure. Seed cultures were grown in 17 mL dual position cap tubes containing 2 mL of ISP2 and grown for 4 days on a rotary shaker at 200 rpm. The seed culture was then poured into a 250 mL baffled flask containing 100 mL of ISP2 and grown for 18 days on a rotary shaker at 200 rpm. The culture was centrifuged at 4000 rpm for 10 min to remove the cells and 2 g of XAD16 resin (Sigma-Aldrich, St. Louis, Mo.) contained within a polypropylene mesh bag was added to the broth and incubated overnight on the rotary shaker. The resin bag was removed and placed into 10 ml of MeOH followed by 10 ml of acetone and 10 ml of ethyl acetate. Each of the three fractions was dried *in vacuo* and reconstituted to a final concentration of 15 mg/mL in DMSO.

3.5.3 Culture Maintenance and Fermentation

Seed cultures of 100 mL (×5) of ISP2 media (1% malt extract, 0.4% yeast extract, 0.4% dextrose, 3% NaCl) were inoculated with a loopful of vegetative cells from an oatmeal plate (6% oat meal, 1.25% agar, 3% NaCl) culture of *Streptomyces blancoensis* and incubated with shaking (200 rpm) at 28 ^{o}C for 5 days. A 25 mL portion of the seed cultures were transferred to a 2.8 L Fernbach flask containing 1.5L of the ISP2 medium, and the 30L fermentation was carried out on a rotary shaker (200 rpm) at 28 °C for 9 days. After 9 days of growth, the cultures were harvested by centrifugation. The resulting cell free broth was subjected to solid phase extraction using 15 g of Amberlite XAD-16. The resin was then separated by filtration and subjected to organic extraction using MeOH:EtOAc (1:1).

3.5.4 Isolation and Purification of Bafilomycin A_1, B_1 and C_1.

The organic extracts concentrated under vacuum to afford the crude extracts (~9 g) obtained from 20 L culture of strain 34893-N3I. The crude extracts were dissolved in 100 mL of H2O and were subjected to a C18-silica gel column (20 × 2.6 cm, YMC Gel ODS-A, 12 nm, S-150 µm). The C18 column was eluted with a stepwise gradient of H_2O/ACN (100:0 → 0:100) to give eight fractions (Fr.1−Fr.8), which were then concentrated in vacuo. All eight fractions were assayed in the developed cell-based assay. The bio-active Fr.6 was further purified by RP-HPLC on isocratic conditions of 62% ACN for 85 minutes at a flow rate of 3 mL/min. This was followed by UV/vis photodiode array detection at 210 nm to yield bafilomycin A_1 (0.8 mg).

In addition, 20L culture of strain 39098-H2N was extracted and concentrated under vacuum to afford the crude extracts (~3 g). This was dissolved in 100 mL of H2O and were subjected to a C18-silica gel column (20 × 2.6 cm, YMC Gel ODS-A, 12 nm, S-150 μm). The C18 column was eluted with a stepwise gradient of H_2O/ACN (100:0 → 0:100) to give eight fractions (Fr.1−Fr.8), which were then concentrated in vacuo. All eight fractions were assayed in the developed cell-based assay. The bio-active Fr.6 was further purified by RP-HPLC following a 60-95% ACN gradient conditions for 50 minutes at a flow rate of 3 mL/min. This was followed by UV/vis photodiode array detection at 210 nm to yield bafilomycin B_1 (0.3 mg) and bafilomycin C_1 (0.5 mg).

3.5.5 Natural Product Extract Library

At the time of screening, the NPE library at the University of Michigan CCG contained ~26,000 extracts. Each extract in the library is derived from marine samples collected from all over the world, including Costa Rica, Panama, and Papua New Guinea. Some of these samples are from isolated microbes (n=19055) while others were derived from field-collected biomass samples ("macrosamples," n=800). Previous work describes in detail how these extracts are prepared for the library.[57]

3.5.6 Assay Development and High-Throughput Screening

The Collins lab developed a high-throughput "mix and measure" flow cytometric assay for Nef-dependent MHC-I downmodulation using a high throughput Accuri flow cytometer available to at the Center for Chemical Genomics, Life Sciences Institute, University of Michigan. For this assay, a CEM T cell line that expresses MHC-I HLA-A2 (CEM-A2) was transiently transduced with an adenoviral vector that expresses Nef under the control of an EF1α promoter.[58] Two days after transduction, the Nef-expressing T cells were treated with the unique library of >26,000 pre-fractionated marine microbial-derived NPEs in 384 well plates, which yielded 37 confirmed hits. Positive hit strains were re-grown to reproduce the NPEs for confirmation. The tertiary validation was done using CEM-A2 cells infected with HIV-1 ΔGPE, which narrowed this list down to 11 promising NPEs that inhibited Nef in the context of HIV-1 infection.

3.5.7 Lysosome Acidity

LysoTracker® works by accumulating inside the lysosome as the fluorophore is protonated under acidic conditions. The Collins lab used this system to assess lysosome activity

when infected PBMCs are treated with varying concentrations of ConA for 24 hours. These were then incubated in PBS with 100nM LysoTracker® Red DND-99 (Fisher L7528) at a density of 1 million cells/mL for 1 hour at 37˚ C, at which point they were washed twice and fixed in 2% PFA for 20 minutes at room temperature before flow cytometric analysis.

3.6 References

1. Kirchhoff, F. HIV Life Cycle: Overview. In *Encyclopedia of AIDS*, Springer-Verlag New York: New York, NY, 2018.
2. Moir, S.; Chun, T. W.; Fauci, A. S. Pathogenic Mechanisms of HIV Disease. *Annu Rev Pathol-Mech* **2010,** *6*, 223-248.
3. Doitsh, G.; Cavrois, M.; Lassen, K. G.; Zepeda, O.; Yang, Z.; Santiago, M. L.; Hebbeler, A. M.; Greene, W. C. Abortive HIV Infection Mediates CD4 T Cell Depletion and Inflammation in Human Lymphoid Tissue. *Cell* **2010,** *143*, 789-801.
4. Galloway, N. L. K.; Doitsh, G.; Monroe, K. M.; Yang, Z.; Muñoz-Arias, I.; Levy, D. N.; Greene, W. C. Cell-to-Cell Transmission of HIV-1 Is Required to Trigger Pyroptotic Death of Lymphoid-Tissue-Derived CD4 T Cells. *Cell Rep* **2015,** *12*, 1555-1563.
5. Douek, D. C.; Brenchley, J. M.; Betts, M. R.; Ambrozak, D. R.; Hill, B. J.; Okamoto, Y.; Casazza, J. P.; Kuruppu, J.; Kunstman, K.; Wolinsky, S.; Grossman, Z.; Dybul, M.; Oxenius, A.; Price, D. A.; Connors, M.; Koup, R. A. HIV preferentially infects HIV-specific CD4+ T cells. *Nature* **2002,** *417*, 95-98.
6. UNAIDS. *Fact sheet—latest global and regional statistics on the status of the AIDS epidemic*. UNAIDS: Geneva, 2018.
7. Centers for Disease Control and Prevention. Estimated HIV incidence in the United States, 2007-2010. HIV Surveillance Supplemental Report 2012;17(No. 4). http://www.cdc.gov/hiv/topics/surveillance/resources/reports/ - supplemental. Published December 2012. Accessed July 20, 2015.
8. Arts, E. J.; Hazuda, D. J. HIV-1 Antiretroviral Drug Therapy. *Cold Spring Harb Perspect Med* **2012,** *2*, 1-23.
9. Archin, N. M.; Liberty, A. L.; Kashuba, A. D.; Choudhary, S. K.; Kuruc, J. D.; Crooks, A. M.; Parker, D. C.; Anderson, E. M.; Kearney, M. F.; Strain, M. C.; Richman, D. D.; Hudgens, M. G.; Bosch, R. J.; Coffin, J. M.; Eron, J. J.; Hazuda, D. J.; Margolis, D. M. Administration of vorinostat disrupts HIV-1 latency in patients on antiretroviral therapy. *Nature* **2012,** *487*, 1-12.
10. Lehrman, G.; Hogue, I. B.; Palmer, S.; Jennings, C.; Spina, C. A.; Wiegand, A.; Landay, A. L.; Coombs, R. W.; Richman, D. D.; Mellors, J. W.; Coffin, J. M.; Bosch, R. J.; Margolis, D. M. Depletion of latent HIV-1 infection in vivo: a proof-of-concept study. *Lancet* **2005,** *366*, 549-555.
11. Clutter, D. S.; Jordan, M. R.; Bertagnolio, S.; Shafer, R. W. HIV-1 drug resistance and resistance testing. *Infect Genet Evol* **2016,** *46*, 292-307.
12. Iyidogan, P.; Anderson, K. S. Current Perspectives on HIV-1 Antiretroviral Drug Resistance. *Viruses* **2014,** *6*, 4095-4139.
13. Sengupta, S.; Siliciano, R. F. Targeting the Latent Reservoir for HIV-1. *Immunity* **2018,** *48*, 872-895.
14. Elsheikh, M. M.; Tang, Y.; Li, D.; Jiang, G. Deep latency: A new insight into a functional HIV cure. *EBioMedicine* **2019,** *45*, 624-629.

15. Hurley, J. H.; Bonifacino, J. S. Nef-arious goings-on at the Golgi. *Nature* **2012,** *19*, 661-662.
16. Wynn, J. E.; Santos, W. L. HIV-1 drug discovery: targeting folded RNA structures with branched peptides. *Org. Biomol. Chem.* **2015,** *13*, 5848-5858.
17. Schindler, M.; Münch, J.; Kutsch, O.; Li, H.; Santiago, M. L.; Bibollet-Ruche, F.; Müller-Trutwin, M. C.; Novembre, F. J.; Peeters, M.; Courgnaud, V.; Bailes, E.; Roques, P.; Sodora, D. L.; Silvestri, G.; Sharp, P. M.; Hahn, B. H.; Kirchhoff, F. Nef-mediated suppression of T cell activation was lost in a lentiviral lineage that gave rise to HIV-1. *Cell* **2006,** *125*, 1055-1067.
18. Margottin, F.; Bour, S. P.; Durand, H.; Selig, L.; Benichou, S.; Richard, V.; Thomas, D.; Strebel, K.; Benarous, R. A novel human WD protein, h-beta TrCp, that interacts with HIV-1 Vpu connects CD4 to the ER degradation pathway through an F-box motif. *Mol. Cell* **1998,** *1*, 565-574.
19. Sheehy, A. M.; Gaddis, N. C.; Choi, J. D.; Malim, M. H. Isolation of a human gene that inhibits HIV-1 infection and is suppressed by the viral Vif protein. *Nature* **2002,** *418*, 646-650.
20. Andersen, J. L.; DeHart, J. L.; Zimmerman, E. S.; Ardon, O.; Kim, B.; Jacquot, G.; Benichou, S.; Planelles, V. HIV-1 Vpr-induced apoptosis is cell cycle dependent and requires Bax but not ANT. *PLoS Pathog.* **2006,** *2*, 1106-1119.
21. Witkowski, W.; Verhasselt, B. Contributions of HIV-1 Nef to immune dysregulation in HIV-infected patients: a therapeutic target? *Expert Opin. Ther. Targets* **2013,** *17*, 1345-1356.
22. Win, N. N.; Ngwe, H.; Abe, I.; Morita, H. Naturally occurring Vpr inhibitors from medicinal plants of Myanmar. *J. Nat. Med.* **2017,** *71*, 579-589.
23. Le Noury, D. A.; Mosebi, S.; Papathanasopoulos, M. A.; Hewer, R. Functional roles of HIV-1 Vpu and CD74: Details and implications of the Vpu-CD74 interaction. *Cell Immunol.* **2015,** *298*, 25-32.
24. Bentham, M.; Mazaleyrat, S.; Harris, M. Role of myristoylation and N-terminal basic residues in membrane association of the human immunodeficiency virus type 1 Nef protein. *J. Gen. Virol.* **2006,** *87*, 563-571.
25. Kammula, E. C.; Mötter, J.; Gorgels, A.; Jonas, E.; Hoffmann, S.; Willbold, D. Brain Transcriptome-Wide Screen for HIV-1 Nef Protein Interaction Partners Reveals Various Membrane-Associated Proteins. *PLoS One* **2012,** *7*, 1-12.
26. Bresnahan, P. A.; Yonemoto, W.; Ferrell, S.; Williams-Herman, D.; Geleziunas, R.; Greene, W. C. A dileucine motif in HIV-1 Nef acts as an internalization signal for CD4 downregulation and binds the AP-1 clathrin adaptor. *Curr. Biol.* **1998,** *8*, 1235-1238.
27. Swann, S. A.; Williams, M.; Story, C. M.; Bobbitt, K. R.; Fleis, R.; Collins, K. L. HIV-1 Nef blocks transport of MHC class I molecules to the cell surface via a PI 3-kinase-dependent pathway. *Virology* **2001,** *282*, 267-277.
28. Schwartz, O.; Maréchal, V.; Le Gall, S.; Lemonnier, F.; Heard, J. M. Endocytosis of major histocompatibility complex class I molecules is induced by the HIV-1 Nef protein. *Nat. Med.* **1996,** *2*, 338-342.
29. Roeth, J. F.; Williams, M.; Kasper, M. R.; Filzen, T. M.; Collins, K. L. HIV-1 Nef disrupts MHC-I trafficking by recruiting AP-1 to the MHC-I cytoplasmic tail. *J. Cell Biol.* **2004,** *167*, 903-913.
30. Wonderlich, E. R.; Williams, M.; Collins, K. L. The tyrosine binding pocket in the adaptor protein 1 (AP-1) mu1 subunit is necessary for Nef to recruit AP-1 to the major histocompatibility complex class I cytoplasmic tail. *J. Biol. Chem.* **2008,** *283*, 3011-3022.

31. Jia, X.; Singh, R.; Homann, S.; Yang, H.; Guatelli, J.; Xiong, Y. Structural basis of evasion of cellular adaptive immunity by HIV-1 Nef. *Nat. Struct. Mol. Biol.* **2012,** *19*, 701-706.
32. Collins, K. L.; Chen, B. K.; Kalams, S. A.; Walker, B. D.; Baltimore, D. HIV-1 Nef protein protects infected primary cells against killing by cytotoxic T lymphocytes. *Nature* **1998,** *391*, 397-401.
33. Hanna, Z.; Kay, D. G.; Rebai, N.; Guimond, A.; Jothy, S.; Jolicoeur, P. Nef Harbors a Major Determinant of Pathogenicity for an AIDS-like Disease Induced by HIV-1 in Transgenic Mice. *Cell* **1998,** *95*, 163-175.
34. Kestier III, H. W.; Ringler, D. J.; Mori, K.; Panicali, D. L.; Sehgal, P. K.; Daniel, M. D.; Desrosiers, R. C. Importance of the nef gene for maintenance of high virus loads and for development of AIDS. *Cell* **1991,** *65*, 651-662.
35. Kirchhoff, F.; Greenough, T. C.; Brettler, D. B.; Sullivan, J. L.; Desrosiers, R. C. Brief report: absence of intact nef sequences in a long-term survivor with nonprogressive HIV-1 infection. *N. Engl. J. Med.* **1995,** *332*, 228-232.
36. Kondo, M.; Shima, T.; Nishizawa, M.; Sudo, K.; Iwamuro, S.; Okabe, T.; Takebe, Y.; Imai, M. Identification of attenuated variants of HIV-1 circulating recombinant form 01_AE that are associated with slow disease progression due to gross genetic alterations in the nef/long terminal repeat sequences. *J. Infect. Dis.* **2005,** *192*, 56-61.
37. Salvi, R.; Garbuglia, A. R.; Di Caro, A.; Pulciani, S.; Montella, F.; Benedetto, A. Grossly defective nef gene sequences in a human immunodeficiency virus type 1-seropositive long-term nonprogressor. *J. Virol.* **1998,** *72*, 3646-3657.
38. Omondi, F. H.; Chandrarathna, S.; Mujib, S.; Brumme, C. J.; Jin, S. W.; Sudderuddin, H.; Miller, R. L.; Rahimi, A.; Laeyendecker, O.; Bonner, P.; Yue, F. Y.; Benko, E.; Kovacs, C. M.; Brockman, M. A.; Ostrowski, M.; Brumme, Z. L. HIV Subtype and Nef-Mediated Immune Evasion Function Correlate with Viral Reservoir Size in Early-Treated Individuals. *J. Virol.* **2018,** *93*, 1-19.
39. Bouchet, J.; Hérate, C.; Guenzel, C. A.; Vérollet, C.; Järviluoma, A.; Mazzolini, J.; Rafie, S.; Chames, P.; Baty, D.; Saksela, K.; Niedergang, F.; Maridonneau-Parini, I.; Benichou, S. Single-Domain Antibody-SH3 Fusions for Efficient Neutralization of HIV-1 Nef Functions. *J. Virol.* **2012,** *86*, 4856–4867.
40. Breuer, S.; Schievink, S. I.; Schulte, A.; Blankenfeldt, W.; Fackler, O. T.; Geyer, M. Molecular Design, Functional Characterization and Structural Basis of a Protein Inhibitor Against the HIV-1 Pathogenicity Factor Nef. *PLoS One* **2011,** *6*, 1-15.
41. Lugari, A.; Breuer, S.; Coursindel, T.; Opi, S.; Restouin, A.; Shi, X.; Nazabal, A.; Torbett, B. E.; Martinez, J.; Collette, Y.; Parrot, I.; Arold, S. T.; Morelli, X. A specific protein disorder catalyzer of HIV-1 Nef. *Bioorg. Med. Chem.* **2011,** *19*, 7401-7406.
42. Betzi, S.; Restouin, A.; Opi, S.; Arold, S. T.; Parrot, I.; Guerlesquin, F.; Morelli, X.; Collette, Y. Protein–protein interaction inhibition (2P2I) combining high throughput and virtual screening: Application to the HIV-1 Nef protein. *Proc. Natl. Acad. Sci. U.S.A.* **2007,** *104*, 19256-19261.
43. Emert-Sedlak, L. A.; Narute, P.; Shu, S. T.; Poe, J. A.; Shi, H.; Yanamala, N.; Alvarado, J. J.; Lazo, J. S.; Yeh, J. I.; Johnston, P. A.; Smithgall, T. E. Effector kinase coupling enables high-throughput screens for direct HIV-1 Nef antagonists with antiretroviral activity. *Chem. Biol.* **2013,** *20*, 82-91.

44. Walk, S. F.; Alexander, M.; Maier, B.; Hammarskjold, M. L.; Rekosh, D. M.; Ravichandran, K. S. Design and use of an inducibly activated human immunodeficiency virus type 1 Nef to study immune modulation. *J. Virol.* **2001,** *75*, 834-843.
45. Ye, H.; Choi, H. J.; Poe, J.; Smithgall, T. E. Oligomerization is required for HIV-1 Nef-induced activation of the Src family protein-tyrosine kinase, Hck. *Biochemistry* **2004,** *43*, 15775-15784.
46. Liu, L. X.; Heveker, N.; Fackler, O. T.; Arold, S.; Le Gall, S.; Janvier, K.; Peterlin, B. M.; Dumas, C.; Schwartz, O.; Benichou, S.; Benarous, R. Mutation of a conserved residue (D123) required for oligomerization of human immunodeficiency virus type 1 Nef protein abolishes interaction with human thioesterase and results in impairment of Nef biological functions. *J. Virol.* **2000,** *74*, 5310-5319.
47. Poe, J. A.; Smithgall, T. E. HIV-1 Nef dimerization is required for Nef-mediated receptor downregulation and viral replication. *J. Mol. Biol.* **2009,** *394*, 329-342.
48. Dikeakos, J. D.; Atkins, K. M.; Thomas, L.; Emert-Sedlak, L.; Byeon, I. L.; Jung, J.; Ahn, J.; Wortman, M. D.; Kukull, B.; Saito, M.; Koizumi, H.; Williamson, D. M.; Hiyoshi, M.; Barklis, E.; Takiguchi, M.; Suzu, S.; Gronenborn, A. M.; Smithgall, T. E.; Thomas, G. Small Molecule Inhibition of HIV-1–Induced MHC-I Down-Regulation Identifies a Temporally Regulated Switch in Nef Action. *Mol. Biol. Cell* **2010,** *21*, 3279-3292.
49. Kasper, M. R.; Roeth, J. F.; Williams, M.; Filzen, T. M.; Fleis, R. I.; Collins, K. L. HIV-1 Nef Disrupts Antigen Presentation Early in the Secretory Pathway. *J. Biol. Chem.* **2005,** *280*, 12840-12848.
50. Wang, M.; Carver, J. J.; Phelan, V. V.; Sanchez, L. M.; Garg, N.; Peng, Y.; Nguyen, D. D.; Watrous, J.; Kapono, C. A.; Luzzatto-Knaan, T.; Porto, C.; Bouslimani, A.; Melnik, A. V.; Meehan, M. J.; Liu, W.; Crüsemann, M.; Boudreau, P. D.; Esquenazi, E.; Sandoval-Calderón, M.; Kersten, R. D.; Pace, L. A.; Quinn, R. A.; Duncan, K. R.; Hsu, C. C.; Floros, D. J.; Gavilan, R. G.; Kleigrewe, K.; Northen, T.; Dutton, R. J.; Parrot, D.; Carlson, E. E.; Aigle, B.; Michelsen, C. F.; Jelsbak, L.; Sohlenkamp, C.; Pevzner, P.; Edlund, A.; McLean, J.; Piel, J.; Murphy, B. T.; Gerwick, L.; Liaw, C. C.; Yang, Y. L.; Humpf, H. U.; Maansson, M.; Keyzers, R. A.; Sims, A. C.; Johnson, A. R.; Sidebottom, A. M.; Sedio, B. E.; Klitgaard, A.; Larson, C. B.; Boya, C. A.; Torres-Mendoza, D.; Gonzalez, D. J.; Silva, D. B.; Marques, L. M.; Demarque, D. P.; Pociute, E.; O'Neill, E. C.; Briand, E.; Helfrich, E. J. N.; Granatosky, E. A.; Glukhov, E.; Ryffel, F.; Houson, H.; Mohimani, H.; Kharbush, J. J.; Zeng, Y.; Vorholt, J. A.; Kurita, K. L.; Charusanti, P.; McPhail, K. L.; Nielsen, K. F.; Vuong, L.; Elfeki, M.; Traxler, M. F.; Engene, N.; Koyama, N.; Vining, O. B.; Baric, R.; Silva, R. R.; Mascuch, S. J.; Tomasi, S.; Jenkins, S.; Macherla, V.; Hoffman, T.; Agarwal, V.; Williams, P. G.; Dai, J.; Neupane, R.; Gurr, J.; Rodríguez, A. M. C.; Lamsa, A.; Zhang, C.; Dorrestein, K.; Duggan, B. M.; Almaliti, J.; Allard, P. M.; Phapale, P.; Nothias, L. F.; Alexandrov, T.; Litaudon, M.; Wolfender, J. L.; Kyle, J. E.; Metz, T. O.; Peryea, T.; Nguyen, D. T.; VanLeer, D.; Shinn, P.; Jadhav, A.; Müller, R.; Waters, K. M.; Shi, W.; Liu, X.; Zhang, L.; Knight, R.; Jensen, P. R.; Palsson, B. Ø.; Pogliano, K.; Linington, R. G.; Gutiérrez, M.; Lopes, N. P.; Gerwick, W. H.; Moore, B. S.; Dorrestein, P. C.; Bandeira, N. Sharing and community curation of mass spectrometry data with Global Natural Products Social Molecular Networking. *Nat. Biotechnol.* **2016,** *34*, 828-837.
51. Werner, G.; Hagenmaier, H.; Drautz, H.; Baumgartner, A.; Zähner, H. Metabolic products of microorganisms. 224. Bafilomycins, a new group of macrolide antibiotics. Production, isolation, chemical structure and biological activity. *J. Antibiot.* **1984,** *37*, 110-117.

52. Bowman, E. J.; Siebers, A.; Altendorf, K. Bafilomycins: a class of inhibitors of membrane ATPases from microorganisms, animal cells, and plant cells. *Proc. Natl. Acad. Sci. USA* **1988,** *85*, 7972-7976.
53. Dröse, S.; Altendorf, K. Bafilomycins and concanamycins as inhibitors of V-ATPases and P-ATPases. *J. Exp. Biol.* **1997,** *200*, 1-8.
54. Geyer, M.; Yu, H.; Mandic, R.; Linnemann, T.; Zheng, Y. H.; Fackler, O. T.; Peterlin, B. M. Subunit H of the V-ATPase Binds to the Medium Chain of Adaptor Protein Complex 2 and Connects Nef to the Endocytic Machinery. *J. Biol. Chem.* **2002,** *277*, 28521-28529.
55. Kinashi, H.; Someno, K.; Sakaguchi, K. Isolation and characterization of concanamycins A, B and C. *J. Antibiot.* **1984,** *37*, 1333-1343.
56. Magarvey, N. A.; Keller, J. M.; Bernan, V.; Dworkin, M.; Sherman, D. H. Isolation and characterization of novel marine-derived actinomycete taxa rich in bioactive metabolites. *Appl. Environ. Microbiol.* **2004,** *70* (12), 7520-7529.
57. Cruz, P. G.; Auld, D. S.; Schultz, P. J.; Lovell, S.; Battaile, K. P.; Macarthur, R.; Shen, M.; Tamayo-Castillo, G.; Inglese, J.; Sherman, D. H. Titration-based screening for evaluation of natural product extracts: identification of an aspulvinone family of luciferase inhibitors. *Chem. Biol.* **2011,** *18* (11), 1442-1452.
58. Kasper, M. R.; Roeth, J. F.; Williams, M.; Filzen, T. M.; Fleis, R. I.; Collins, K. L. HIV-1 Nef disrupts antigen presentation early in the secretory pathway. *The Journal of biological chemistry* **2005,** *280* (13), 12840-8.

Chapter 4
Discussion and Future Directions

4.1 Thesis Overview

In the ongoing war on drug resistance from many pathogens, it is crucial to continue identifying new areas to target for their successful eradication from the host. Microbial natural products have shown time and time again their potential as powerful antibiotics, antiviral and antifungal agents.[1-3] Given the structural diversity of these secondary metabolites it is not uncommon for one to have several biological activities associated with it. Throughout this dissertation we showed how previously identified natural products, particularly adipostatins, bafilomycins and concanamycin A, showed promising activity against pathogenic bacteria and HIV-1 targets, in addition to their previously known roles.

In chapter two we focused on inhibiting PPCS as it holds considerable potential as a drug target for developing new antimicrobials.[4] This synthetase is responsible for installing a cysteamine group within phosphopantetheine, a key structural element in biological acyl transfer reactions found embedded within CoA.[5-6] With an adapted malachite green assay specific for bacterial PPCS we screened for inhibitors of CoA biosynthesis against a library of marine microbial derived NPEs. Analysis of the NPE derived from *Streptomyces blancoensis* led to the isolation of novel antibiotics (**10-12**, and **14**) from the adipostatin class of molecules. The most potent molecule (**10**) displayed *in vitro* activity with IC_{50}= 0.93 μM, against *S. pneumoniae* PPCS. In addition, using a whole cell antimicrobial assay against isolated molecules we demonstrated their ability to penetrate bacterial cells and inhibit clinically relevant pathogenic strains.

For the following chapter we discussed how HIV-1 has developed the unique ability to produce accessory proteins that aid in evading recognition by CTLs and spreading the virus efficiently through the host cell.[7-10] The Nef accessory protein mediates the mislocalization to the endo-lysosomal pathway and subsequent degradation of the antigen-presenting MHC-I

molecules.[11-13] We hypothesized that targeting the Nef protein for inhibition could potentially reverse its effects on infected cells and reduce the viral load significantly when combined with current ART regimen. In collaboration with Dr. Collins lab, a high-throughput cell-based assay was developed to test a wide array of microbial derived NPEs for inhibitors of Nef-mediated MHC-I downregulation. From several of the top hit strains we identified the bafilomycins and ConA as the active secondary metabolites. Upon testing commercially available bafilomycin analogs (A-D) and ConA in human primary T cells, Baf C_1 and ConA showed encouraging potencies against Nef activities in the pM to nM range. During this chapter we will discuss the ongoing and future work that will be executed by our group in collaboration with Dr. Collins lab with the goal of eradicating the virus from the host.

4.2 HIV-1 Nef Inhibitors Future Directions

4.2.1 Derivatization of Bafilomycins and Concanamycin A

Having identified ConA and the bafilomycin family of NPs to be effective against Nef mediated MHC-I downmodulation activity, we now hope to further increase the concentration window between toxicity and anti-Nef events. Modifications to the core of our lead compounds, Baf-C_1 and ConA, might be able to achieve this, as well as provide stronger chemical properties, such as increased solubility and stability.[14-15] To accomplish this we can use to our advantage the SAR information provided during the testing of the four bafilomycin analogs against infected PBMCs, such as the important presence of a fumarate at the C21 position.

In the past, the Sherman lab has successfully created analogs that have exhibited higher activity through substrate analog feeding studies upon discovery of the biosynthetic pathway.[16] Thankfully, the type I PKS biosynthetic pathway of the bafilomycin molecules was previously elucidated in the lab from S. lohii.[17-18] As seen in figure 4.1, Baf C_1 is created from Baf A_1 after the latter is released from the PKS and interacts with a fumaryl transferase. Preliminary studies have also identified Baf A_1 production to be at its peak at 6 days after the culture growth start (Fig 4.2). Because of this, we will be adding numerous fumarate analogs to the cell cultures during the 4-8 days of growth window to study the flexibility of the fumaryl transferase to take these analogs (Fig 4.1) and place them into Baf-A_1. This small library will contain Baf-C_1 analogs that posses some clinically relevant moieties at the end of C21 that could potentially create a more stable and less toxic compound.

Furthermore, the Dröse and Ingenhorst groups previously discovered that a reduction at the hemiacetal ring at C21, giving way to a deoxy form of ConA, showed little effects on the V-ATPase activity while providing higher structural stability.[14-15] Based on these findings, we set out to create a deoxy-Baf-A_1 analog and found its anti-Nef activity to be comparable with the naturally produced Baf-A_1. Further semi-synthetic derivatizations and future preclinical tests of bafilomycins will be performed with these analogs as they provide a tremendous improvement in the stability of the compounds. We are also currently working on optimizing ConA production to develop the corresponding deoxy analog.

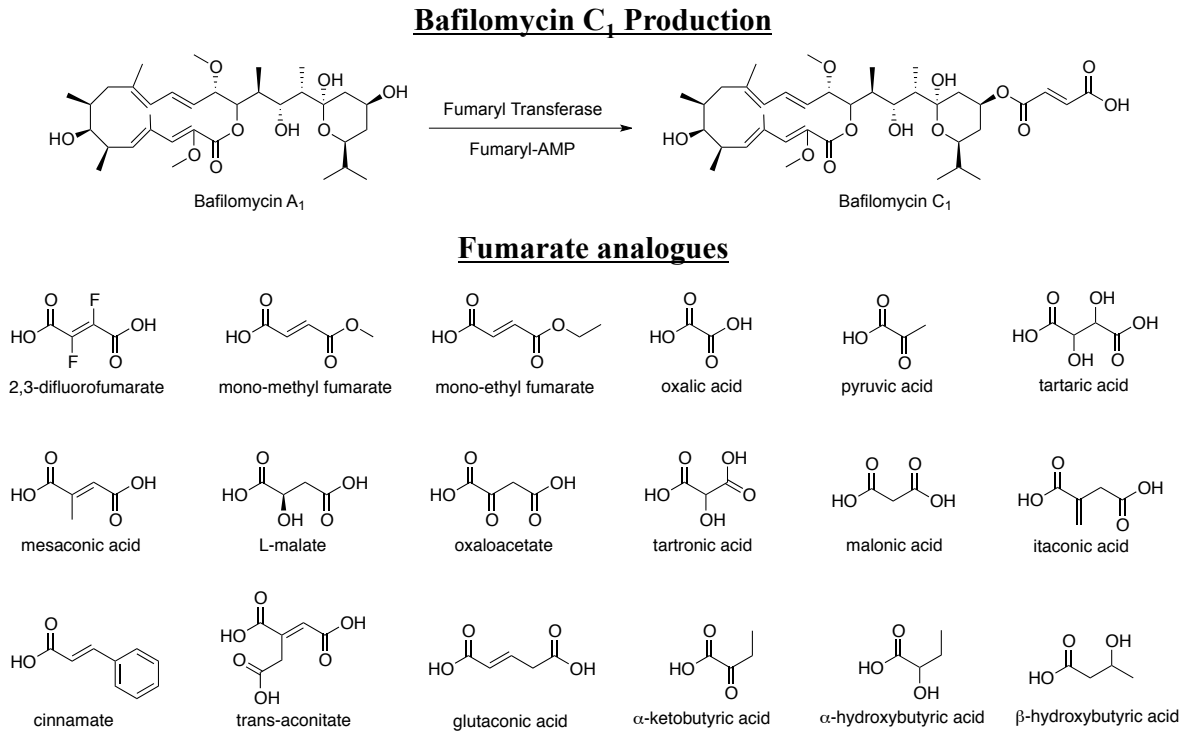


Figure 4.1. *Potential fumarate analogues to study fumaryl transferase substrate flexibility*. Using an array of commercially available fumarate analogs, we will study the ability of the fumaryl transferase to incorporate these into Baf-A_1 to create a small library of Baf-C_1 analogs.

Both Baf-A_1 and ConA have easily accessible hydroxyl groups that can be taken advantage of via medicinal chemistry. Commercially available anhydrates will be used to produce ester analogs of Baf-A_1 and Con A at their previously shown most reactive alcohols, C7/C21 and C9/C23, respectively (Fig 4.3).[14-15, 19] These reactions can be executed at small scale, given the little amount needed for testing, and will be scaled up as needed. This study will

provide us with the necessary knowledge of what area of the molecule contains the pharmacophore, which are more prone for modifications and how additional O-acyl groups affect activity and toxicity.

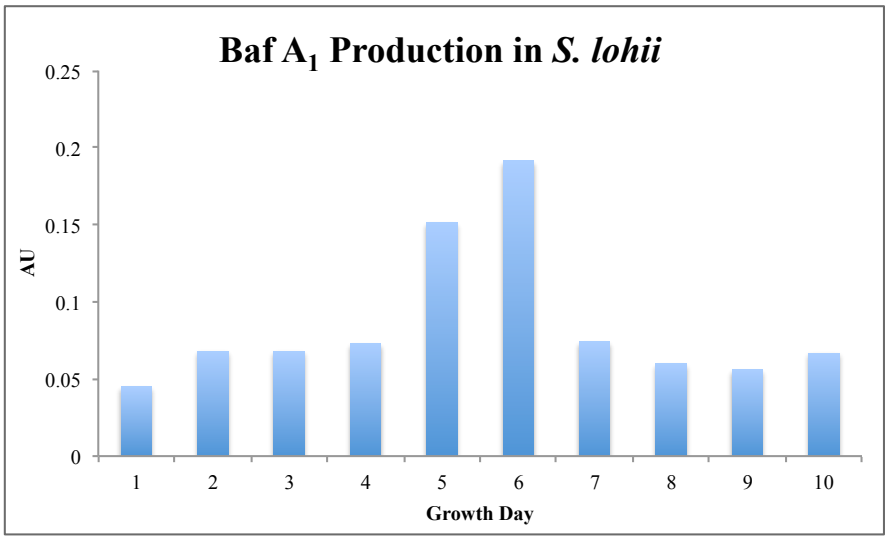


Figure 4.2. *Baf-A_1 production in* S. lohii *peaks around day 6*. Although it seems to be present from the first culture day, Baf-A_1 production is most abundant between 5-6 days after *S. lohii* growth start. The decline on the amount of Baf-A_1 after day 6 could be due to Baf-C_1 production.

Finally, given we have shown ConA has a higher anti-Nef activity among all the plecomacrolides tested, we can manipulate some of the structural differences between this molecule and the bafilomycins to study how these might affect the activity. One key difference is the presence of a sugar moiety at the C23 position missing in the corresponding Baf-A_1 C21. Glycosilation of small molecules has gained interest seeing as these sugar additions or substitutions have shown increase in bioactivity, such as the increase in solubility by the double glycosylation of vancomycin, [20-22] as was the case with thiazoles decrease in off-target interactions that led to toxicity.[23-24] To asses whether the sugar substitution is key for the increased activity we plan to add the 2-deoxy-β-D-rhamnose present in ConA to the equivalent C21 alcohol in Baf-A_1. In addition to this, we will add other sugar moieties found in successful and easily accessible natural products, such as mycaminose and desosamine.

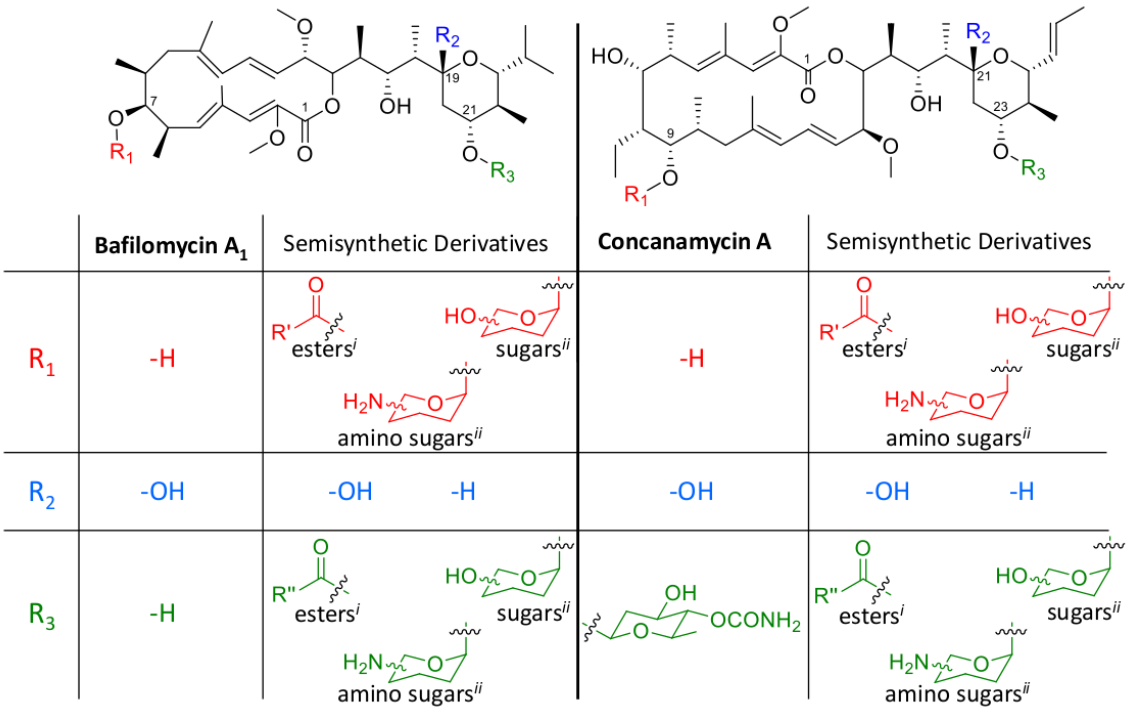


Figure 4.3. *Proposed derivatization sites for Baf-A$_1$ and ConA*. For *i*. R_1 and R_3 ester linkages will be introduced using commercially available anhydrides and R′ will be any sidechain. During *ii*. there will be a sugar addition *via* regiodivergent glycodiversification and R″ represents any sugar. Scheme done in collaboration with Dr. Andrew Roberson.

4.2.2 Elucidation of ConA Nef Inhibition Mechanism

Although the plecomacrolides have shown a promising activity profile against Nef effects, their mechanism of action is not completely understood. Given the Collin's lab showed that the concentrations needed for ConA to act as a Nef-activity inhibitor are lower than what is needed for deacidification of the lysosome, we can hypothesize that disruption of MHC-I downmodulation occurs by rerouting these to follow their normal trafficking pathway towards the cell surface. Understanding the specific mechanism, knowing the target proteins, identifying the binding sites and characterizing their interactions will facilitate the development of a plecomacrolide analog that has minimum toxicity and higher efficacy. From the knowledge we have of the Nef MHC-I degradation mechanism we can theorize about possible areas the plecomacrolides might be targeting. The Collin's lab has developed several assays to study the direct effects ConA has on the known proteins involved in the Nef-mediated MHC-I degradation mechanism. Some of the areas they will be exploring are changes in the intracellular localization

of the key proteins, such as Nef, MHC-I and AP-1, whether ConA disrupts AP-1 sorting to endosomes at the TGN and whether it deters Nef from stabilizing interactions between MHC-I and AP-1 at the TGN.

These experiments are undoubtedly important and will provide necessary knowledge for the development of an ideal plecomacrolide, however these approaches are biased towards the already known players in the Nef-mediated MHC-I downmodulation pathway. It is possible additional proteins in primary T cells are involved in this disruption of MHC-I degradation. To identify any proteins that interact with ConA we will work with the Collin's lab to treat PBMCs lysates with a ConA analog that possesses both a chemical handle and a photoafinity tag at positions C9 and C23 (Fig 4.4).[14-15] The photoafinity tag will ensure covalent linkage between the proteins and ConA upon UV irradiation, while the chemical handle will couple the complex to an activated biotin to yield the protein-ConA-biotin conjugate.[25] This complex will be purified from the lysate through biotin-affinity chromatography for proteomics analysis[26] using the Orbitrap in collaboration with the Mass Spectrometry Core and the Natural Products Discovery Core. As shown in figure 4.4, the label groups can be exchanged as well as alterations to the chain lengths in the reporter tag can be explored to probe for a higher affinity.

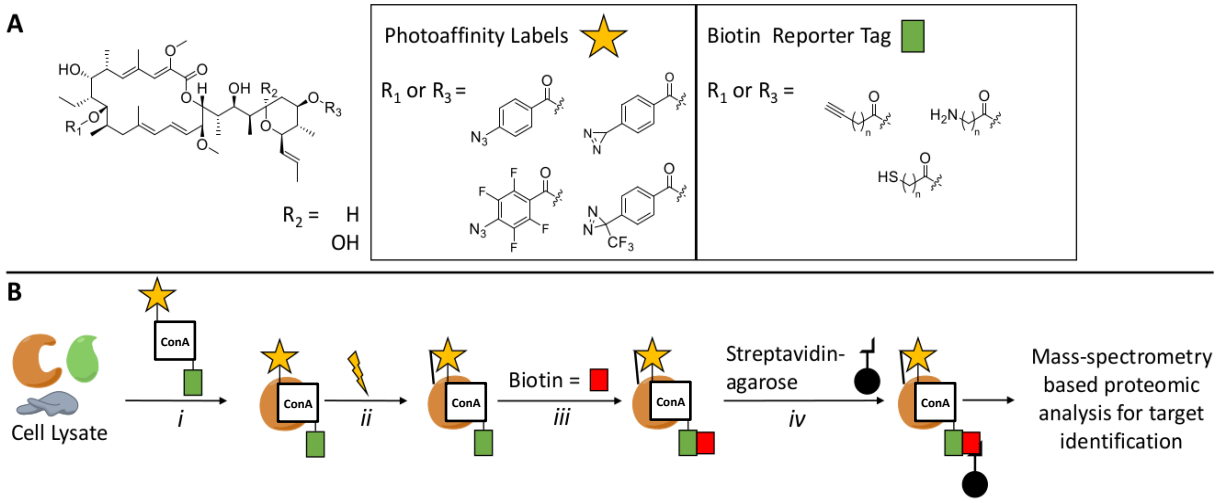


Figure 4.4. *Use of labeled ConA for the identification of target proteins*. **A**. ConA sites proposed for derivatization (R_2) and for the addition of a photoaffinity label and a selective chemical handle for coupling with biotin (R_1 and R_3). **B**. Mass-spectrometry based approach for target protein identification: (*i*) treatment of PBMC lysate with doubly-labeled ConA; (*ii*) UV irradiation of sample for labeled ConA coupling to target proteins; (*iii*) coupling of ConA-protein complex to activated-biotin using reactive biotin reporter tag; (iv) protein-ConA-biotin conjugate capturing through biotin affinity chromatography (figure adapted from Smith et al., 2015).[25] Scheme done in collaboration with Dr. Andrew Roberson.

4.3 Contributions

The structural diversity of secondary metabolites from culturable microbes has been exploited for decades by researchers for potential drug leads.[27] The use of a bioassay-guided workflow when seeking to block novel targets has been successfully employed by our lab before and currently led us to discover additional biological activity of previously known natural products.[28-33] First, we presented new adipostatin analogs with promising activity against bacterial PPCS. In addition, their ability to kill pathogenic bacterial cultures provides further proof of the advantage in using PPCS as a drugable target. Just as critical, we identified new biological activity associated with well-established V-ATPase inhibitors, Baf-C_1 and ConA. These plecomacrolides posses the ability to hinder Nef-mediated MHC-I downmodulation in primary T cells and restore CTLs recognition. The discovery of the antimicrobial activity of adipostatins and antiviral activity from plecomacrolides could provide a foundation for future medicinal chemistry approaches towards drug development in the antibiotics and antiretroviral therapy areas, in addition to bringing numerous benefits to the public health.

4.4 References

1. Rossiter, S. E.; Fletcher, M. H.; Wuest, W. M. Natural Products as Platforms To Overcome Antibiotic Resistance. *Chem. Rev.* **2017,** *117*, 12415-12474.
2. Harvey, A. L.; Edrada-Ebel, R.; Quinn, R. J. The re-emergence of natural products for drug discovery in the genomics era. *Nat. Rev. Drug Discov.* **2015,** *14*, 111-129.
3. Rodrigues, T.; Reker, P.; Schneider, G. Counting on natural products for drug design. *Nat. Chem.* **2016,** *8*, 531-541.
4. Yao, J.; Patrone, J. D.; Dotson, G. D. Characterization and kinetics of phosphopantothenoylcysteine synthetase from enterococcus faecalis. *Biochem.* **2009,** *48* (12), 2799-2806.
5. Kupke, T. Molecular Characterization of the 4′-Phosphopantothenoylcysteine Synthetase Domain of Bacterial Dfp Flavoproteins. *J. Biol. Chem.* **2002,** *277* (39), 36137-36145.
6. Strauss, E.; Kinsland, C.; Ge, Y.; McLafferty, F. W.; Begley, T. P. Phosphopantothenoylcysteine synthetase from Escherichia coli. Identification and characterization of the last unidentified coenzyme A biosynthetic enzyme in bacteria. *J. Biol. Chem.* **2001,** *276* (17), 13513-13516.
7. Schindler, M.; Münch, J.; Kutsch, O.; Li, H.; Santiago, M. L.; Bibollet-Ruche, F.; Müller-Trutwin, M. C.; Novembre, F. J.; Peeters, M.; Courgnaud, V.; Bailes, E.; Roques, P.; Sodora, D. L.; Silvestri, G.; Sharp, P. M.; Hahn, B. H.; Kirchhoff, F. Nef-mediated suppression of T cell activation was lost in a lentiviral lineage that gave rise to HIV-1. *Cell* **2006,** *125*, 1055-1067.
8. Margottin, F.; Bour, S. P.; Durand, H.; Selig, L.; Benichou, S.; Richard, V.; Thomas, D.; Strebel, K.; Benarous, R. A novel human WD protein, h-beta TrCp, that interacts with HIV-1

Vpu connects CD4 to the ER degradation pathway through an F-box motif. *Mol. Cell* **1998,** *1*, 565-574.
9. Sheehy, A. M.; Gaddis, N. C.; Choi, J. D.; Malim, M. H. Isolation of a human gene that inhibits HIV-1 infection and is suppressed by the viral Vif protein. *Nature* **2002,** *418*, 646-650.
10. Andersen, J. L.; DeHart, J. L.; Zimmerman, E. S.; Ardon, O.; Kim, B.; Jacquot, G.; Benichou, S.; Planelles, V. HIV-1 Vpr-induced apoptosis is cell cycle dependent and requires Bax but not ANT. *PLoS Pathog.* **2006,** *2*, 1106-1119.
11. Kammula, E. C.; Mötter, J.; Gorgels, A.; Jonas, E.; Hoffmann, S.; Willbold, D. Brain Transcriptome-Wide Screen for HIV-1 Nef Protein Interaction Partners Reveals Various Membrane-Associated Proteins. *PLoS One* **2012,** *7*, 1-12.
12. Bresnahan, P. A.; Yonemoto, W.; Ferrell, S.; Williams-Herman, D.; Geleziunas, R.; Greene, W. C. A dileucine motif in HIV-1 Nef acts as an internalization signal for CD4 downregulation and binds the AP-1 clathrin adaptor. *Curr. Biol.* **1998,** *8*, 1235-1238.
13. Swann, S. A.; Williams, M.; Story, C. M.; Bobbitt, K. R.; Fleis, R.; Collins, K. L. HIV-1 Nef blocks transport of MHC class I molecules to the cell surface via a PI 3-kinase-dependent pathway. *Virology* **2001,** *282*, 267-277.
14. Dröse, S.; Boddien, C.; Gassel, M.; Ingenhorst, G.; Zeeck, A.; Altendorf, K. Semisynthetic Derivatives of Concanamycin A and C, as Inhibitors of V- and P-Type ATPases: Structure−Activity Investigations and Developments of Photoaffinity Probes. *Biochemistry* **2001,** *40*, 2816-2825.
15. Ingenhorst, G.; Kai, U.; Bindseil, C.; Boddien, C.; Dröse, S.; Gaßel, M.; Altendorf, K.; Zeeck, A. Synthesis of a Doubly Labelled Concanamycin Derivative for ATPase Binding Studies. *Eur. J. Org. Chem* **2001,** *48*, 12-20.
16. Park, S. R.; Tripathi, A.; Wu, J.; Schultz, P. J.; Yim, I.; McQuade, T. J.; Yu, F.; Arevang, C.-J.; Mensah, A. Y.; Tamayo-Castillo, G.; Xi, C.; Sherman, D. H. Discovery of Cahuitamycins A-E, Potent Biofilm Inhibitors Derived from a Bifurcated Biosynthetic Pathway. *Nat. Commun.* **2016,** *7*, 1-11.
17. Li, Z.; Du, L.; Zhang, W.; Zhang, X.; Jiang, Y.; Liu, K.; Men, P.; Xu, H.; Fortman, J. L.; Sherman, D. H.; Yu, B.; Gao, S.; Li, S. Complete elucidation of the late steps of bafilomycin biosynthesis in Streptomyces lohii. *J. Biol. Chem.* **2017,** *292*, 7095-7104.
18. Zhang, W.; Fortman, J. L.; Carlson, J. C.; Yan, J.; Liu, Y.; Bai, F.; Guan, W.; Jia, J.; Matainaho, T.; Sherman, D. H.; Li, S. Characterization of the Bafilomycin Biosynthetic Gene Cluster from Streptomyces lohii. *ChemBioChem* **2013,** *14*, 301-306.
19. Deeg, M.; Hagenmaier, H.; Kretschmer, A. Chemical modifications of bafilomycin-type 16-membered dienlactone macrolides. *J. Antibiot.* **1987,** *40*, 320-328.
20. Elshahawi, S. I.; Shaaban, K. A.; Kharel, M. K.; Thorson, J. S. A comprehensive review of glycosylated bacterial natural products. *Chem. Soc. Rev.* **2015,** *44*, 7591-7697.
21. Fu, X.; Albermann, C.; Jiang, J.; Liao, J.; Zhan, C.; Thorson, J. S. Antibiotic optimization via in vitro glycorandomization. *Nat. Biotechnol.* **2003,** *21*, 1467.
22. Tay, J.-H.; Argüelles, A. J.; DeMars, M. D.; Zimmerman, P. M.; Sherman, D. H.; Nagorny, P. Regiodivergent Glycosylations of 6-Deoxy-erythronolide B and Oleandomycin-Derived Macrolactones Enabled by Chiral Acid Catalysis. *J. Am. Chem. Soc.* **2017,** *137*, 2299-2306.
23. Chun, M. W.; Kim, M. J.; Shin, J. H.; Jeong, L. S. Synthesis of 3'-deoxy-3'-C-hydroxymethyl analogues of tiazofurin and ribavirin. *Nucleosides Nucleotides Nucleic Acids* **2005,** *24*, 975-977.

24. Abu-Zaied, M. A.; Elgemeie, G. H. Thiazoles in glycosylation reactions: Novel synthesis of thiazole thioglycosides. *Heteroatom Chem* **2017,** *28*, 1-6.
25. Smith, E.; Collins, I. Photoaffinity labeling in target- and binding-site identification. *Future Med. Chem.* **2015,** *7*, 159-183.
26. Rath, C. M.; Janto, B.; Earl, J.; Ahmed, A.; Hu, F. Z.; Hiller, L.; Dahlgren, M.; Kreft, R.; Yu, F.; Wolff, J. J.; Kweon, H. K.; Christiansen, M. A.; Hakansson, K.; Williams, R. M.; Ehrlich, G. D.; Sherman, D. H. Meta-omic characterization of the marine invertebrate microbial consortium that produces the chemotherapeutic natural product ET-743. *ACS Chem. Biol.* **2011,** *6*, 1244-1256.
27. Altmann, K. H. Drugs from the Oceans: Marine Natural Products as Leads for Drug Discovery. *CHIMIA* **2017,** *71*, 646-652.
28. Carlson, J. C.; Li, S.; Burr, D. A.; Sherman, D. H. Isolation and characterization of tirandamycins from a marine-derived Streptomyces sp. *J. Nat. Prod.* **2009,** *72*, 2076-2079.
29. Cruz, P. G.; Auld, D. S.; Schultz, P. J.; Lovell, S.; Battaile, K. P.; Macarthur, R.; Shen, M.; Tamayo-Castillo, G.; Inglese, J.; Sherman, D. H. Titration-based screening for evaluation of natural product extracts: identification of an aspulvinone family of luciferase inhibitors. *Chem. Biol.* **2011,** *18* (11), 1442-1452.
30. Fribley, A. M.; Cruz, P. G.; Miller, J. R.; Callaghan, M. U.; Cai, P.; Narula, N.; Neubig, R. R.; Showalter, H. D.; Larsen, S. D.; Kirchhoff, P. D.; Larsen, M. J.; Burr, D. A.; Schultz, P. J.; Jacobs, R. R.; Tamayo-Castillo, G.; Ron, D.; Sherman, D. H.; Kaufman, R. J. Complementary cell-based high-throughput screens identify novel modulators of the unfolded protein response. *J. Biomol. Screen* **2011,** *21*, 825-835.
31. Mike, L. A.; Tripathi, A.; Blankenship, C. M.; Saluk, A.; Schultz, P. J.; Tamayo-Castillo, G.; Sherman, D. H.; Mobley, H. L. Discovery of Nicoyamycin A, an Inhibitor of Uropathogenic Escherichia coli Growth in Low Iron Environments. *Chemical Communications* **2017,** *53* (95), 12778-12781.
32. Park, S. R.; Tripathi, A. T.; Wu, J.; Schultz, P. J.; Yim, I.; McQuade, T. J.; Yu, F.; Arevang, C. J.; Mensah, A. Y.; Tamayo-Castillo, G.; Xi, C.; Sherman, D. H. Discovery of Cahuitamycins A-E, Potent Biofilm Inhibitors Derived from a Bifurcated Biosynthetic Pathway. *Nat. Commun.* **2016,** *7*, 1-11.
33. Tripathi, A.; Schofield, M. M.; Chlipala, G. E.; Schultz, P. J.; Yim, I.; Newmister, S. A.; Nusca, T. D.; Scaglione, J. B.; Hanna, P. C.; Tamayo-Castillo, G.; Sherman, D. H. Baulamycins A and B, Broad-Spectrum Antibiotics Identified as Inhibitors of Siderophore Biosynthesis in Staphylococcus aureus and Bacillus anthracis. *JACS* **2014,** *136*, 1579-1586.